

THE GEOLOGY OF THE
COBB RESERVOIR AREA,
NORTH WEST NELSON.

A thesis
submitted in partial fulfillment
of the requirements for the degree
of
Master of Science in Geology
in the
University of Canterbury
by
Mike Stewart

University of Canterbury
1988

ABSTRACT

This thesis examines the geology of an 80 km² area of Lower Paleozoic rocks centred on the Cobb Reservoir, N.W. Nelson.

An extensive and detailed field mapping programme has identified three fault bounded slices, of markedly contrasting lithologic and deformational character, from west to east the Balloon, Junction and Mataki Fault Bounded Slices.

The Balloon Slice comprises predominantly a pervasively foliated, east dipping "block in matrix" tectonite, with lenses of chert, limestone, conglomerate and andesite (collectively known as the Balloon Formation). The tectonite has a strong linear fabric plunging down dip parallel to a regional lineation. Hornblende andesites of calc-alkaline arc affinity are restricted to the Balloon Formation. Conglomerates outcropping north of the Reservoir (the Battey Conglomerate) are of uncertain affinity to the Balloon Formation.

The Mataki Slice is poorly exposed and understood. It contains three lithologic units of unknown interrelationship; the Salisbury Conglomerate, the M Creek Formation and the Mataki Basalts. The M Creek Formation comprises laminated siltstones and angular basalt rich mass flow conglomerates. The Mataki Basalts are distinctive high Ti and Mg tholeiitic basalts and have a probable seamount trace element signature. The Mataki Slice is bounded to the west by the Mataki Fault and to the east by the Junction Fault.

The Junction Slice comprises well bedded quartzose sandstones and siltstones (the Junction Formation), folded into irregularly oriented but consistently east plunging asymmetric folds.

Large lateral displacement between the Slices is indicated from the presence of igneous rocks of widely contrasting geotectonic origin.

The timing of juxtaposition predates the imposition of a regional extensional deformation, interpreted to be related to the Devonian or Silurian Tuhuan event.

It is apparent that the structural complexity of the study area is greater than can be fully resolved with the outcrop available. Previous attempts (Grindley 1971, 1980) to establish a regional stratigraphy are not applicable in this area.

There is perhaps no phase of geological science more conjectural than that relating to geological history. It is especially difficult in New Zealand where tectonic changes have been so frequent and of such diversified character. The particular part of the country being discussed in this Bulletin has seen many changes. The extremely complicated topography and geological structure now exposed to the observer render the exact extent and full signification of these events most difficult to interpret. In consequence, the following remarks on the geological history must be considered partly hypothetical.

James.M.Bell. (1907)

(On rocks of the Tasman Mountains)

TABLE OF CONTENTS

	Page
Abstract	i
List of Figures	vi
List of Tables and Maps	vii
 CHAPTER ONE: INTRODUCTION	
REGIONAL GEOLOGY	1
AIM	2
STUDY AREA	2
FIELD WORK AND MAPS	4
SPECIMENS	4
 CHAPTER TWO: REVIEW	
INTRODUCTION	6
BACKGROUND	6
THE NEW MODEL	8
WEAKNESSES IN THE ALLOCHTHONOUS CENTRAL BELT MODEL	13
STRUCTURE	13
STRATIGRAPHY	14
 CHAPTER THREE: GENERAL FIELD RELATIONS	16
 CHAPTER FOUR: BALLOON FAULT BOUNDED SLICE	
INTRODUCTION	18
BATTEY CONGLOMERATE	18
BALLOON FORMATION	
Introduction	20
Reference Section	20
Age of the Balloon Formation	21
General Character of the Balloon Formation	22
Block in Matrix Tectonites	
Introduction	22
Block in Matrix Tectonites	23
Sandstone Petrology	25
Fissile Sheared Mudstone	31
Broken Formation	33
Olistostromal Conglomerates	35
Clasts	35
Matrix	38
Field Relations	38
Lithologies Occurring in Block in Matrix Tectonites	38
Black Limestone	39
Chert	40
Petrology	41
XRF	41
Hornblende Andesite	43

Cobble Conglomerate	44
Heath Creek Conglomerates	44
Staff Hut Conglomerates	46
Lake Head Conglomerate	47
North Shore Conglomerate	48
Structure	49
 CHAPTER FIVE: MATAKI FAULT BOUNDED SLICE	
INTRODUCTION	54
MATAKI BASALTS	54
M CREEK FORMATION	55
Conglomerates	55
Laminated Siltstones and Sandstones	56
SALISBURY CONGLOMERATE	58
STRUCTURE	59
 CHAPTER SIX: JUNCTION FAULT BOUNDED SLICE	
JUNCTION FORMATION	62
Petrology	65
STRUCTURE	66
 CHAPTER SEVEN: PETROLOGY AND GEOCHEMISTRY OF IGNEOUS ROCKS	
BALLOON FORMATION ANDESITES	69
Major Element Geochemistry	70
Trace Element Geochemistry	70
MATAKI FORMATION BASALTS	72
INTRUSIVE ROCKS	80
Basic Intrusives	80
Geochemistry	81
Other Intrusives Rocks	82
ANALYTICAL METHODS	82
 CHAPTER EIGHT: STRUCTURES COMMON TO ALL TECTONIC SLICES	
INTRODUCTION	84
BOUNDING FAULTS	84
Balloon Fault	84
Mataki Fault	86
Junction Fault	86
Cobb Thrust	88
OVERPRINTING DEFORMATION	88
FAULTING	94
East West Cross Faults	94
Kink Bands/Crenulation	95
 CHAPTER NINE: CONCLUSIONS	97

ACKNOWLEDGEMENTS	101
REFERENCES	102
APPENDICES	
1 Sample Identification	106
2 Fossil Age Control	107

List of Figures

	Page
1.1 General Geology of NW Nelson (after Cooper 1979).	1
1.2 Map of study area showing geology of Grindley (1980).	3
2.1 Central Belt stratigraphy of Grindley 1961 and 1980.	10
4.1 Logged section, south shore of Cobb Reservoir.	Map pocket
4.2 Measured stratigraphic section, Balloon Formation, Cobb Reservoir.	24
4.3 Boudinaged sandstone beds exposed in glaciated pavement, Reservoir shore.	26
4.4 Disrupted margin of thick sandstone bed. Reservoir shore.	26
4.5 Sandstone rich block in matrix tectonite Reservoir shore.	27
4.6 More typical outcrop, showing lemon-pip shape of clasts wrapped by foliation. Reservoir shore.	27
4.7 Disrupted sandstone and mudstone. Reservoir shore.	28
4.8 Block in matrix tectonite exposed in glaciated pavement on Reservoir shore.	28
4.9 Slabbed surface of blocky tectonite cut perpendicular to lineation. Sylvester Rd.	30
4.10 QFR ternary diagram of Balloon Formation sandstones.	30
4.11 Slabbed sample of intensely disrupted and fractured mudstone and siltstone. Reservoir shore.	32
4.12 Highly sheared fissile mudstone with relict cherty siltstone beds. Reservoir shore.	32
4.13 Broken Formation. Reservoir shore.	34
4.14 Olistostromal conglomerate. Reservoir shore.	37
4.15 Olistostromal conglomerate. Reservoir shore.	37
4.16 Contact between hornblende andesite and olistostromal conglomerate.	45
4.17 Stereographic plots of poles to beddings, plotted by domains.	51
4.18 Strongly boudinaged sandstone, in blocky tectonite. Reservoir shore.	52
4.19 Elongated sandstone inclusion. Reservoir shore.	52
5.1 Disrupted pillow basalts, Deep Creek.	57
5.2 Matrix supported angular debris flow conglomerate, Mataki Creek.	57
5.3 Salisbury Conglomerate, Balloon Creek.	60
5.4 Stereographic plot of bedding and foliation in Salisbury Conglomerate.	60
6.1 Thinly bedded sandstones of Junction Formation, Deep Creek.	63
6.2 Soft sediment deformation, Junction Formation, Deep Creek.	63
6.3 Flames and load casts, Junction Formation, Cobb River.	64
6.4 Shear plane offsetting thin bedded sandstones of the Junction Formation, Galena Creek.	64

6.5	Stereographic plot of poles to bedding, Junction Formation. Balloon, Deep and Mataka Creeks, Flora and Takaka Rivers.	67
6.6	Stereographic plot of poles to bedding, Junction Formation, Diamond Lake Stream and Cobb River.	67
7.1	Alkalis Silica diagram.	71
7.2	AFM diagram.	73
7.3	K ₂ O-Silica diagram.	71
7.4	Cr-Y discrimination diagram.	73
7.5	Ti-Sr-Y discrimination diagram.	74
7.6	Ti-Zr discrimination diagram.	75
7.6a	Ti-Zr plot of comparative data of andesites from active calc-alkaline arcs.	75
8.1	Exposure of Balloon Fault, Lake Lillie Stream.	87
8.2	Exposure of Junction Fault, Deep Creek.	87
8.3	Exposure of Cobb Thrust, Cobb River below dam.	89
8.4	Stereographic plots of foliation and lineation, plotted by domain.	91
8.5	Stretched Battey Conglomerate.	93

List of Tables

1	Major and Trace element XRF analyses for Balloon Formation cherts and cherty mudstones.	42
2	Major and Trace element XRF analyses of igneous rocks.	77

List of Maps

1	Data Map of Cobb Reservoir Area - Field Observations
2	Interpretative Geological Map of Cobb Reservoir Area

CHAPTER ONE

INTRODUCTION

REGIONAL GEOLOGY

The Lower Paleozoic rocks of N.W. Nelson, N.Z., divide naturally into three sedimentary belts, termed Western, Eastern and Central Belts (Cooper, 1979). (figure 1.1) The Central Belt, bounded east and west by major N-S trending faults, comprises a diverse range of lithologies including volcanics and volcanogenic sediments containing fossils of

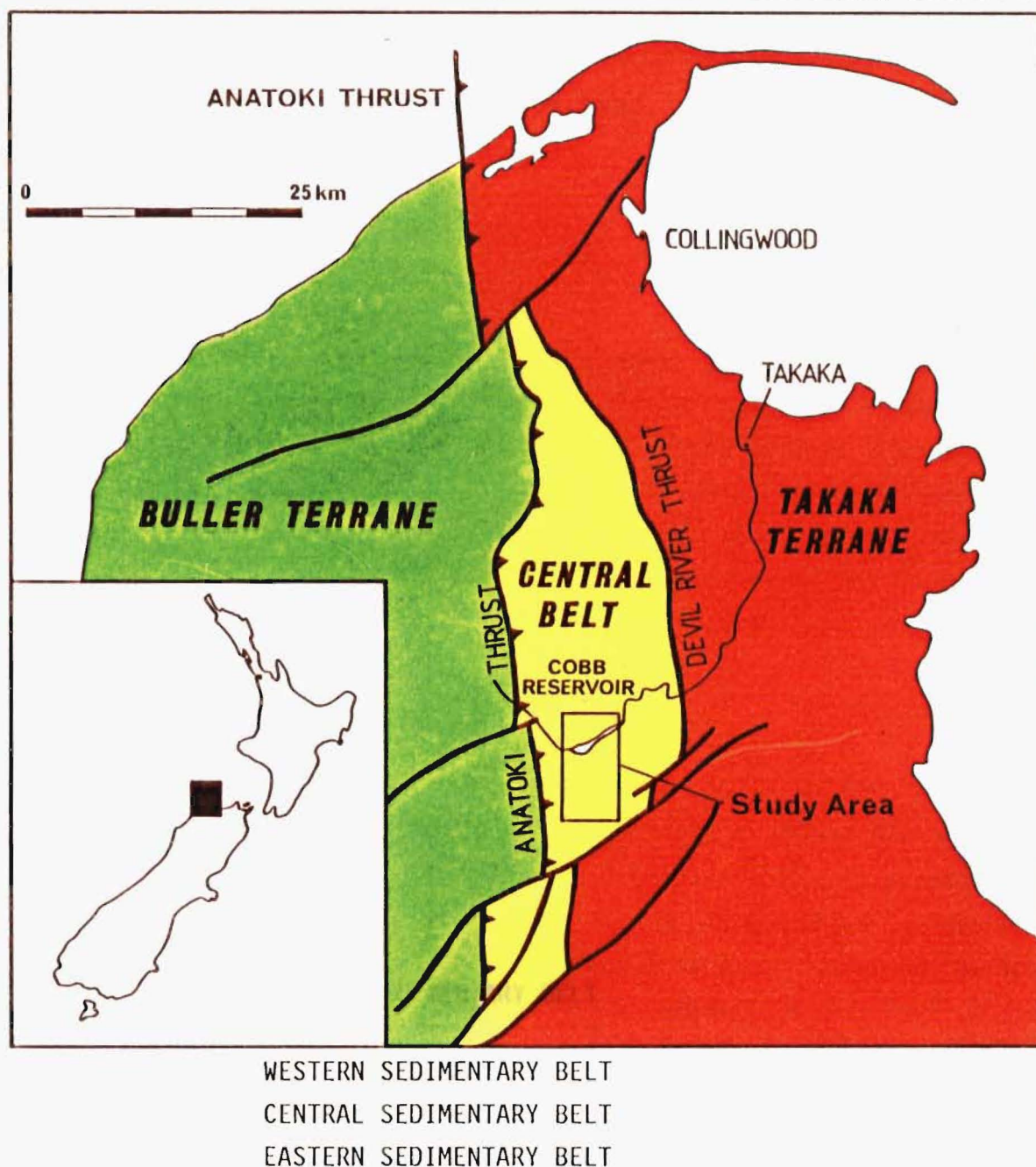


Figure 1.1. General geology of N.W. Nelson (after Cooper 1979).

Cambrian to Lower Ordovician age. It is structurally complex, poorly exposed and one of the least well understood sections of New Zealand geology. The most detailed and complete interpretation of the Central Belt is presented in two 1:63,360 geological maps, S8 Takaka and S13 Cobb (Grindley 1971,1980). He has proposed a stratigraphy for the Central Belt involving seven concordant formations, separated into two Groups; the Cambrian Haupiri Group and the Lower Ordovician Mount Patriarch Group. The Haupiri Group comprises five concordant formations of Middle to Upper Cambrian age. From oldest to youngest these are: Balloon Formation; Devil River Volcanics; Tasman Formation; Lockett Conglomerate and Anatoki Formation. However this interpretation has been criticised, and alternative and radically different regional interpretations have been proposed by Cooper (1979,1984,1986). Chapter 2 is a review of previous work.

AIM

The objective of this thesis was to examine a portion of the Balloon Formation of Grindley(1981) including the type section in Balloon Creek, to ascertain the stratigraphic relationship of the Balloon Formation to other Central Belt units. In light of the results of extensive field mapping, it is now necessary to describe the geology around the Cobb Reservoir and discuss the implications of these findings for Central Belt structure and stratigraphy.

STUDY AREA

The study area, approximately 80 km² of the N.W. Nelson State Forest Park, is centered on the Cobb Reservoir (figure 1.2). It extends from the Lockett Range in the north to Salisbury Hut in the south. Vehicular access is provided by the Cobb Hydro Road from Upper Takaka to the head of the Reservoir. The rest of the area is accessible by foot track, untracked forest, rivers and ridge crest. Three N.Z.F.S huts, Salisbury Lodge, Balloon Hut and Bushline Hut, were used as field bases.

An uplifted Early Tertiary peneplain surface is the most outstanding physiographic feature of the area, being clearly visible from S.H. 60 on

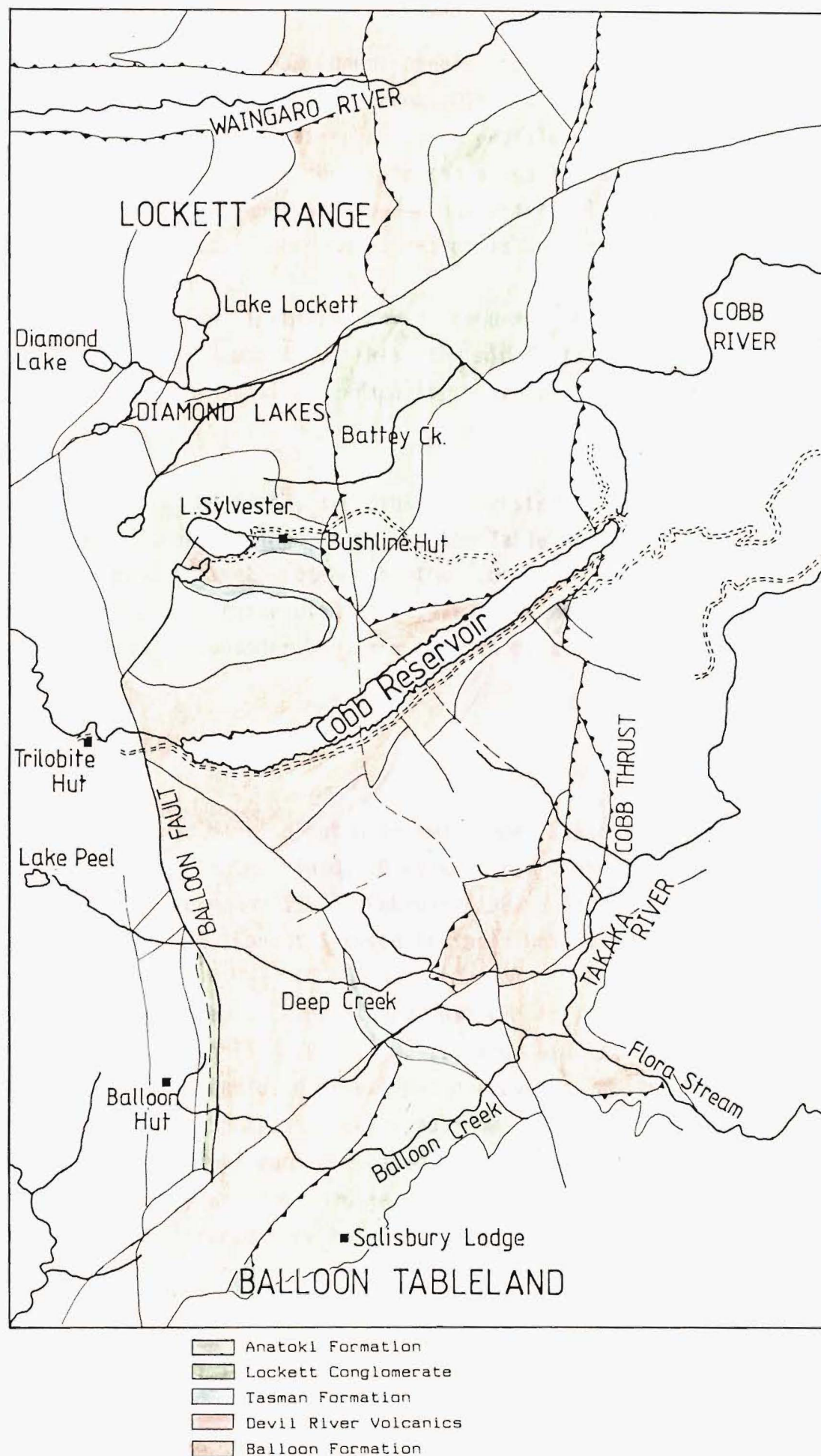


Figure 1.2 Map of study area showing geology of Grindley (1980).

the Takaka Hill. This has been deeply incised by Late Pleistocene glaciation, producing the Deep Creek, Diamond Lake Stream and Cobb River valleys, good examples of steep sided, U profile valleys. The peneplain is well preserved in the south, in the so-called Tablelands area (1100m asl) but is preserved only as broad ridge crests in the Lockett Range (1500m asl). Resultant topographic relief is in excess of 700m.

A transgressive Tertiary cover sequence originally blanketed the peneplain surface. Remnants of this, the mid Tertiary Takaka Limestone, remain on the peneplain surface south of the Reservoir, forming steep bluffs.

Valley walls and floors are densely forested with mature *Nothofagus*-*Podocarpus* forest. Ridge tops and the Tableland are generally covered with sub-alpine tussock, although the Lockett Range crest is bare. Outcrop is largely restricted to stream beds, ridge tops, odd bluffs and lakeshores and is considerably less than 1% of area.

FIELD WORK AND MAPS

Field work was carried out over two summer seasons. A total of 22 weeks was spent in the field, 10 weeks during February - April 1986 and 12 weeks during November 1986 - February 1987. Accommodation was kindly provided by the N.Z. Forest Service in their Hostel at Cobb Reservoir.

Aerial photographs were found useful for locating in fairly open terrain. Runs SN c5676 L9-11, M9-11 and N10-11 were particularly useful. In more enclosed creeks paced traverses and altimeter readings were used. Field sheets were enlarged from NZMS 1 S13 Cobb and NZMS 270 M26D and M27B. Final maps are based on M26D and M27B and are at 1:10000 and 1:25000. They are included in the map pocket at the rear of the thesis. Grid references are taken from the metric grid.

SPECIMENS

Thin sections, rock samples and powders are stored in University of Canterbury collections, catalogued with official University of Canterbury

numbers. Field numbers used on the map are indexed to U.C numbers in Appendix 1. Fossil collections are held by the N.Z. Geological Survey, Lower Hutt.

CHAPTER TWO

REVIEW

INTRODUCTION

The N.W. Nelson area has had a long history of geological investigation. This chapter reviews published work and attempts to summarise the regional interpretations of Central Belt structure that have been proposed. The implications of these interpretations and the significance of the Balloon Formation will be discussed.

BACKGROUND

The first geological mapping in N.W. Nelson was by McKay(1879) who divided the rocks of the Mt. Arthur-Wangapeka area into three Lower Paleozoic units

- : Mt. Arthur series (Lower Silurian)
- : Baton River Series (Upper Silurian)
- and : an unnamed "Upper Devonian" series of aphanitic breccias and green sandstones which were found on the Mt. Arthur Range and the Mt. Peel-Tableland area.

These "Upper Devonian" rocks were later included by Park(1890:p237) in a belt of upper Devonian "*.. red and green slates, indurated blue and green sandstones, coarse conglomerates, and fine breccias often green in colour. They stretch continuously from Snows River to Mount Peel, and from there to the head of the Karamea and Wangapeka, occupying a belt of country several miles wide.*" He correlated this belt with the Te Anau Series of southern New Zealand and the name was adopted. Park also suggested the name Aorere series for what are now Western Sedimentary Belt rocks and ascribed a "Lower Silurian"¹ age to these from the presence of graptolites. His map quite clearly shows Te Anau series rocks folded in a synclinorium within the Aorere Series.

¹ Note that Park and McKay were using Lower Silurian in the Murchison or Continental way. Equivalent to what we call the Ordovician - the last system to be named.

In 1907 Bell and others proposed that the Te Anau Series be renamed the Haupiri Series, "*.. a new name of no definite age signification.*" Based on presence of pebbles of Aorere Series in basal conglomerates of the Haupiri Series (on Brown Cow Ridge near Anatoki Thrust) they attested that the Haupiri was younger than the Aorere. In common with Park they felt that (Bell et al, 1907:p22).. "*In general the structure of these sedimentary rocks is that of a great synclinorium. The Haupiri rocks occur near the centre of the synclinorium.*"

Henderson in 1923 (and later in 1959), following from previous workers, identified four stratigraphic units. In decreasing relative age he called these

- 1: Mt. Arthur Series (now Mt. Arthur Group)
- 2: Aorere Series (now Aorere Group)
- 3: Baton River Series (now Baton River and Ellis Groups)
- 4: Haupiri Series (now Haupiri Group)

Age diagnostic fossils were sparse and existed only for the Mt. Arthur (Lower Silurian¹), Aorere (Silurian¹) and Baton River (Devonian) Series.

More detailed age control was provided in an important paper by Keble and Benson (1929) who reported Middle to early Late Ordovician graptolites from the Aorere Series in the Cobb Valley. The presence of Late Ordovician graptolites from lithologically similar shales of the Mt. Arthur Series at Mount Lodestone led them to conclude that (Keble and Benson 1929:849): "*.. the rocks occurring east and west of the broad belt of Haupiri Series belong to the same group of strata. The sequence of faunas shows that the beds were deposited, if not continuously, at least without any considerable break. Clearly the Haupiri rocks which are of vast thickness, cannot be regarded as part of the sequence from which the graptolites considered in this paper were obtained. Probably they owe to folding or faulting their position between belts of Ordovician strata differing little in age.*" This paleontologic similarity established a linkage in space and time between rocks east and west of the Haupiri Series which is fundamental to Grindley's later interpretations.

The discovery in 1956 by Benson of Cambrian trilobites at Trilobite Rock overturned ideas on the position of the Haupiri Series within the existing stratigraphy. It meant that the Haupiri Series, whilst

apparently occupying a generally synformal position, was flanked by younger strata. Obviously any new regional geological interpretation necessarily required a complex structural model to explain this.

THE NEW MODEL

A new model was provided in 1961 with the publication of the 1:250000 geological map Sheet 13 (Golden Bay) by Grindley, who proposed that the Haupiri Group (renamed from the Haupiri Series) was emplaced as a series of three discrete nappes thrust from the south over an autochthonous basement of Eastern and Western Belts and subsequently folded and tilted into a broad synformal shape. This model fits the constraints of synformal geometry and "inverted" ages well.

Supporting evidence is poorly documented in the accompanying discussion but rests mostly on 1:(indirectly) map interpretation and

naming of nappe structures. If nappes are present then large tectonic transport is implied

2:the presence of long isoclinal folds adjacent to the fault-bounded margins of the nappes which have hinges trending at a high angle to the margins and plunging down the regional east dip of the beds

and 3: the presence of steeply plunging folds in Mt. Arthur Group sediments which are overturned northwards, thought to imply a northward transport of nappes over an autochthonous floor of Mt. Arthur Group sediments

It is interesting to note that no indication of fold closures can be found on the map or accompanying sections.

Grindley(1961) subdivided the Haupiri Group into three concordant formations :

Anatoki Formation	
Tasman Formation (upper Mid Cambrian)	
Devil River Volcanics	

All the rocks of the Cobb area were included within the Anatoki Formation. Mapping of Mount Arthur Group sediments in both the Western and Eastern Belts clearly indicates their assumed genetic relationship beneath the Central Belt

Over the following twenty years intensive mapping as part of the N.Z.G.S. 1:63,360 mapping program saw production of the four 1:63360 sheets covering the Central Belt:-

S3 Farewell-Kahurangi	Bishop(1971)
S8 Takaka	Grindley(1971)
S13 Cobb	Grindley(1980)
S19 Wangapeka	Coleman(1981)

All the authors have adopted a stratigraphic-structural model expanding and supporting Grindley's 1961 model. The Takaka and Cobb sheets were mapped in conjunction despite being published nine years apart, and are the most important, covering the major part of the Central Belt.

The Haupiri Group (and all the Cambro-Ordovician) stratigraphy underwent major revisions in both 1971 and 1980 (see figure 2.1; for details see Grindley 1980:p39). In 1971 as well as the three existing formations Grindley recognized two new formations. The Lockett Conglomerate, previously included in the Anatoki Formation as the Haupiri Conglomerate, was introduced *"resting disconformably on the Tasman Formation, the Balloon Formation and the Devil River Volcanics"* and *"overlain by and probably passing laterally into the Anatoki Formation"*. The Balloon Formation, another subdivision of the Anatoki Formation described as *"dark sheared micaceous argillite, phyllite and pelitic schist, and dark massive siliceous sandstone and chert frequently boudinaged and auto-brecciated"*, was also introduced. It was thought to *"underlie the Tasman and Anatoki Formations"* and be *"contemporaneous with the Devil River Volcanics and locally with the Tasman Formation."* In studying the map and legend and accompanying booklet it is interesting to note that the legend does not depict all stated stratigraphic relationships. For instance Balloon Formation is not shown in contact with Anatoki Formation on the legend, but is shown so on the map (Anatoki Nappe - Snowden Range).

Grindley (1980), based on mapping in S13 (Cobb) of the Balloon -Devil River Volcanic contact (including a contact within the study

AGE	FORMATION (GRINDLEY 1961)	FORMATION (GRINDLEY 1980)	GROUP
LOWER ORDOVICIAN		SUMMIT LIMESTONE	MOUNT PATRIARCH
UPPER CAMBRIAN	ANATOKI	PATRIARCH	
MIDDLE CAMBRIAN		ANATOKI	HAUPIRI
		LOCKETT CONGLOMERATE	
	TASMAN	TASMAN	
LOWER CAMBRIAN	DEVIL RIVER VOLCANICS	DEVIL RIVER VOLCANICS	
		BALLOON	
		COBB IGNEOUS COMPLEX	

Figure 2.1 Central Belt stratigraphy of Grindley 1961 and 1980.

area), revised the position of the Balloon Formation. It was now thought to be the oldest formation in the Haupiri Group conformably underlying the Devil River Volcanics. This change was in part prompted by new age considerations. Acritarchs of supposedly Vendian to Lower Cambrian age had been identified from the supposed base of the sequence and trilobite fragments of Mid Cambrian age from the top. However the acritarchs are now known to range up into the Upper Mid Cambrian and the trilobite fragments have never been refound and are considered to be contamination (R.A. Cooper, pers. comm.).

Grindley (1980) recognised a stack of three major (and two minor) nappes, Each of the major nappes is considered to contain an overlapping portion of the stratigraphy. The northern most (first emplaced) nappe contains the youngest rocks, and the later emplaced nappes contain older portions of the stratigraphy. These nappes Grindley considered to have been later folded into a broad synformal shape, dismembered and eastward tilted by N.S oriented F2 folding, thereby exposing the basal thrust and repeating the lowest nappe on the outside of the Central Belt. The three main nappes (lowest to highest) are

- :Anatoki Nappe - exposed along the Western side of the Central Belt adjacent to the Anatoki Thrust. Exposed again along the East margin within the Waingaro Schist Zone. Composed largely of Anatoki Formation (unconformably overlying Balloon Formation in places).
- :Waingaro nappe - A large nappe with complex internal thrusting. Contains all Haupiri Group formations.
- :Haupiri Nappe - sandwiched between Anatoki and Waingaro nappes. Composed largely of Devil River Volcanics.

The inferred source for the nappes is given first (Grindley, 1961) as the Baton River, Mt. Patriarch area, then the Anatoki "Eugeosyncline" (Grindley 1978p118) in the Rotoroa Complex area. Timing of over-thrusting is inferred to be Silurian based on identification of Haupiri Group pebbles in the basal conglomerate of the Lower Devonian Baton River Formation.

Eastern and Western Belt stratigraphies were also substantially revised in 1971 and 1980 following paleontological work by Cooper (1965,-68,-71), Cooper and Druce (1975) and Cooper and Wright (1972) and others. No rock units common to both of the Belts were now recognized.

In 1980 Grindley summarised the evidence supporting his model. The strongest lines of evidence advanced were

- 1: Mapping of the basal thrust plane (Anatoki and Devil River Thrusts) as closing to the north around the end of the Central Belt.
- 2: The recognition of a set of discrete nappes containing overlapping stratigraphy with younger rocks at the bottom and older rocks at the top, which Grindley(1981:p26) states "must be considered prima-facie evidence for major overthrusting."
- 3: The presence of mesoscopic and macroscopic "reclined recumbent" folds with axes trending east, and an axial planar cleavage (S1) and elongation b-lineation (L1)
- 4: The presence of reclined northward overturned recumbent folds in both Eastern and Western belts near the boundary thrusts

Grindley(1980) also recognised a major tectonic event occurring prior to emplacement of the nappes, the "Haupiri disturbance", in which *"the lower part of the Central Belt sequence was uplifted by block faulting and minor thrust faulting"* and accompanied *"by the emplacement and rapid unroofing of the Cobb Igneous Complex"*. The Lockett Conglomerate, the most characteristic consequence of the event, is inferred to have been derived from a block faulted source to the east (predominantly the underlying Cambrian rocks). Evidence for the Haupiri Disturbance, Grindley claims, can be seen within the geology of the Waingaro Nappe which contains two distinctive sequences separated by the Mid Cambrian Balloon fault. West of the Balloon fault an undisturbed conformable Haupiri sequence from Devil River Volcanics through Tasman Formation to Lockett Conglomerate is exposed. East of the fault, the deformed lower part of the Haupiri Group (the Balloon Formation) is overlain by the Devil River Volcanics south of the Reservoir and the

Lockett Conglomerate (with minor Tasman Formation) to the north. The Balloon Fault, separating the Balloon and Tasman Formations in the Cobb Valley, and necessarily having a large displacement there, is mapped as dying out upwards over a remarkably short distance into the Lockett Conglomerate. It was supposedly active during the Haupiri Disturbance and Lockett Conglomerate sedimentation.

WEAKNESSES IN THE ALLOCHTHONOUS CENTRAL BELT MODEL

The Allochthonous Central Belt model requires large scale tectonic movements of older over younger rocks. There are considerable constraints on such a model with respect to gross geometry of the nappes, structure within the nappes, structure within the sub-nappe basement, and geology within that basement.

STRUCTURE

Problems of gross nappe geometry have been discussed in considerable detail by Bradshaw (1982). In particular he points out problems with naming and correlation of thrust planes, age relations within thrust sheets and unfolded (pre F2) geometry of nappes, as well as the relationship of F2 folds to F1 structures. It is crucial to Grindley's model that F1 folds and thrusts are contemporaneous and dynamically related. In a number of examples on S13 thrusts clearly truncate axial planes of F1 folds and must therefore postdate development of the F1 structures. Grindley (1982) interprets this discordance to be due to later tilting and rejuvenation of thrusts during the F2 compressional phase.

Well documented examples of large scale nappe structures from overseas (e.g. Swiss Alps) are accompanied by a distinctive and restricted range of structures including isoclinal folds with fold hinges at high angles to the direction of transport (frequently with lower limbs excised) and high strain within the lower limbs. Strain on these examples generally produces elongation lineation parallel to the direction of nappe transport (Ramsay and Huber 1984). Grindley (1980) maintains that pebble elongations occur perpendicular to the inferred transport direction and parallel to F1 fold axes and cites presence of these lineations as evidence of F1 folding. Since Grindley's mapping

documentation of sheath folds (Ramsay and Huber 1987) shows that simple correlation between hinge orientation and tectonic transport is unwarranted.

The geometry of F1 folds is rather peculiar involving large sheets of rock folded back on themselves over considerable distances. The Christmas Anticline in the Haupiri Nappe on S8 Takaka has an axial plane trace 20 km long with limbs parallel and of equal thickness along this whole length, implying that a 40 km sheet of rock has been folded back on itself without excision of either limb or evidence of extreme strain - a geometrical nightmare. No such folds are described anywhere in the literature. For more detailed comments on structural inconsistencies the reader is referred to Bradshaw (1982).

To a large extent in any geological mapping of moderately to poorly exposed terrain, identification of fold (and thrust) structures relies on correct interpretation of stratigraphy. If stratigraphy is incorrect then structural interpretations have no basis.

STRATIGRAPHY

From examination of the maps S8 and S13 and the accompanying booklets it is apparent that Central Belt formations are identified principally by gross lithologic type. While formations must be based on lithology, for them to be meaningful and applicable mapping units they must be accompanied by descriptions of components and variability. Formal descriptions accompanying the Central Belt Formations are brief and include no logged sections or stratigraphic detail, and in most cases have no designated Type Section. Furthermore the descriptions contain considerable overlap. Hence recognition of a particular gross lithology (e.g. conglomerate) cannot be used to assign the rocks to a particular formation on a rigorous basis.

Probably the most perplexing problem of the Allochthonous Central Belt model concerns the affinity of the Western and Eastern Belts. Grindley (1982, p376) states that "*No significant tectonic or sedimentary facies changes can be recognised between the two belts, and both may be contiguous parts of a single sedimentary basin.*" However Cooper in 1979 first recognised that the affinity between the Central and Eastern Belts

is much stronger than that between the Eastern and Western Belts both containing virtually identical Lower Ordovician stratigraphies. He proposed that the Central Belt represents the uplifted substratum to the Eastern Belt and is of unknown relationship to the Western Belt, a model known as the "Autochthonous Central Belt" model.

More recent work has confirmed these affinities and led Cooper (1984,1986) to propose that the N.Z. Paleozoic comprises two tectono-stratigraphic terranes, the Buller (W. Belt) and Takaka (C. and E. Belts) Terranes separated by the Anatoki Thrust (see figure 1.1). Ward(1984,1986) has recognised this same terrane boundary in Fiordland.

The Autochthonous Central Belt model assumes the basic within-belt stratigraphy of Grindley (1971,1980). It offers no interpretation Central Belt structure other than to suggest that uplift was likely to have occurred along internal thrust planes. However at a Workshop organised in the Geology Department, University of Canterbury in August 1986 Cooper(1986b) advanced a new interpretation of Central Belt structure. Following mapping of the West side of the Belt he has suggested that it is comprised of a *"collage of at least 8 tectonic (probably thrust) slices, each bounded by major faults"*. Stewart(1986) also presented preliminary results that supported this interpretation and these are expanded in this thesis.

CHAPTER THREE

GENERAL FIELD RELATIONSHIPS

Early in the course of mapping it became apparent that application of the simple regional stratigraphy of Grindley (1971,1980) to my field area did not work. I found it meaningless to assign lithologies to one of the five Central Belt formations, since the formal descriptions of the Formations given by Grindley are inadequate and the formations have many features in common. Furthermore the boundaries of formations as mapped by Grindley could not be located or followed and no evidence of a layer cake stratigraphy was observed.

Identification of a number of distinctive lithologies and structural styles plus mapping of faults has led to recognition of three (possibly more) major fault bounded structural entities, each of contrasting depositional and deformational history (see Map 2, back pocket). Interpretation is based on very detailed field mapping and collection of a large amount of field data. This data constitutes the basis of the thesis and the text should be read in conjunction with the map.

The subsequent layout for this thesis reflects the findings outlined above. Description of the geology (lithology, distribution and structure) of the three fault bounded slices is outlined in Chapters 4,5 and 6. Chapter 7 describes and compares the petrology and geochemistry of igneous rocks associated with the slices, while Chapter 8 describes structures common to all.

This interpretation closely parallels that of Cooper (1986) who identified "9 separate fault bounded slices, each with its own distinct stratigraphy" comprising the western part of the Central Belt.

Over recent years a working hypothesis of mapping coherent rock bodies bounded by faults as primary structural units has proved useful in analysis of areas of active and ancient convergent and translational margins. This approach is known as "terrane analysis" and the individual crustal blocks as "terrane" (Howell 1985).

The accepted definition of terranes, that they are *"fault bounded geological entities of regional extent that are characterised by a geological history different from that of neighbouring terranes"*, is relatively straight forward {Coney (1980) in Cooper (1987)}. However the use and application of the terrane concept is still under active discussion. The important point is that fault bounded blocks are treated as distinct separate entities until it can be established that they have a common and closely related stratigraphic history.

It is a matter of debate whether the fault bounded blocks identified during the course of this mapping and those identified by Cooper (1986) should be regarded as terranes. Cooper (1986) suggests that they should not, stating that the distinctness between blocks "is not so great as to suggest that the slices have had distinctly different geological histories and should be regarded as separate terranes. Rather they suggest a tectonically dismembered and truncated, originally diverse, terrane (representing an island arc environment)."

In this thesis I shall leave this question open until the concluding chapter where the question will be addressed in the light of the data presented.

CHAPTER FOUR

BALLOON FAULT BOUNDED SLICE

INTRODUCTION

The Balloon Fault Bounded Slice (or just Balloon slice) is a complex fault bounded lithologic assemblage, composed predominantly of a disrupted sandstone/mudstone sequence. The name Balloon slice applies to the structural entity bounded by the Balloon, Mataki and Junction Faults (see Map 2, back pocket). Rocks occurring within the Balloon slice have been assigned to one of two informally named formations, the Balloon Formation or the Battey Conglomerate. It is important to distinguish between the Balloon slice (an interpretative structural feature) and the Balloon Formation (a lithologic mapping unit).

The Balloon fault bounded slice has been mapped from the Balloon Tablelands in the south to the Lockett Range in the north. The internal structure of the slice is poorly understood. While the gross geology south of Lake Sylvester is understood with a reasonable degree of certainty, interpretation north of this area is still at a preliminary stage and further field work is necessary before conclusions can be drawn.

Of the two formations (mappable lithologic units) recognised within the Balloon slice, the Balloon Formation and the Battey Conglomerate, the Balloon Formation is volumetrically the larger component, and is described in detail in this thesis. The Battey Conglomerate is being studied by Kate Pound (University of Otago) and will not be examined in detail here.

BATTEY CONGLOMERATE

The Battey Conglomerate is an informal name proposed by R.A. Cooper (pers. comm.) for distinctive green to maroon coarse cobble conglomerates outcropping south of Lake Sylvester and in a belt through Battey Creek and Diamond Lake Stream. This name is informally adopted here. The conglomerate was previously mapped by Grindley (1980) as two bodies of

Lockett Conglomerate, a western tongue stratigraphically overlying Balloon Formation (sensu Grindley, 1980) and in continuity with the type Lockett, and an eastern area structurally overlying the Balloon via the Sylvester Thrust (see figure 1.2).

The Battey Conglomerate is a clast supported coarse granule to coarse cobble conglomerate. Clasts are subrounded to subangular and poorly to moderately sorted. Bedding where present is defined by thin lensoidal medium to coarse sandstone beds. Clasts include chert, quartz, silicic tuff (?), grey to green sandstones, highly deformed chloritic volcanics and medium grained igneous (? gabbroic) pebbles. In Battey Creek distinctive maroon siltstone clasts also occur.

On the ridge south of Lake Sylvester, Battey Conglomerate is surrounded to the north, west and south by the Balloon Formation. It is uncertain whether the conglomerate rests in stratigraphic or low angle fault contact on the Balloon Formation (i.e. whether it is an outlier or a klippe). The conglomerate does not reach, or cross the Balloon Fault, and is nowhere in contact with Lockett Conglomerate. In one outcrop (M26 797105), strongly deformed conglomerate is in conformable contact with foliated laminated siltstone and sandstone, which is in turn in concordant contact with foliated blocky tectonite some 10's of metres away. No firm conclusion could be reached as to the nature of this latter contact.

On the north side of the conglomerate bedding dips at 20°- 30° S or SE and the contact vees into Sylvester Creek, while to the south bedding dips steeply (80°) to the NW. The most obvious interpretation is that the conglomerate is folded into an asymmetric syncline (see Map 2).

In lower Battey Creek and Diamond Lake Stream, the conglomerate forms a slab about 600m thick striking NE and dipping consistently 60° SE. On the SE side the conglomerate is in conformable contact with strongly rodded green carbonate siltstones, which are in fault contact with sandstones of the Junction Slice. To the NW it is in concordant (? conformable) contact with blocky tectonite of the Balloon Formation.

It is not known how (or if) these two conglomerate bodies are related. It does not appear possible that they form part of a single

structure and no sensible structural interpretations can be constructed from the available map data. Given the paucity of outcrop it is doubtful that further mapping will cast much light on the problem. One possibility is that the two conglomerates are unrelated, as suggested by Stewart (1987), and that the conglomerate and silstones of Battey creek and Diamond Lake Stream may comprise separate fault bounded slices. It is hoped that the petrological work of Kate Pound may help elucidate the affinities of these conglomerates.

BALLOON FORMATION

INTRODUCTION

Use of the name Balloon Formation as defined by Grindley (1971) has been retained in this thesis. However I amend its usage, so that it is no longer considered to be an in-situ and integral part of a systematic stratigraphic succession in the Central Belt, but to be a formation occurring within a fault bounded unit.

Reference Section

The type section of the Balloon Formation has only been indirectly not formally stated. Grindley clearly intended it to be in Balloon Creek stating (1971, p3) "*.. The type section is in Balloon Creek in Sheet S13, where a minimum thickness of 1000m is exposed.*" However in the S13 booklet covering Balloon Creek Grindley (1980, p5) merely states "*The most complete sequences are on the south side of Cobb Reservoir, and in Deep and Balloon Creeks.*"

Apart from brief descriptions of lithology in map booklets, no description of the presumed type section or the nature of contacts is given.

I nominate as the reference section (or reference locality) the South Shore of the Cobb Reservoir from M27 787082 to 817095. This section, best exposed at low lake levels, was exceptionally well exposed

during the summer of 1986-87 and enabled a detailed pace and compass and visually estimated section of 1700m true thickness to be logged (see figure 4.1 back pocket). This lakeshore section provides a far more complete and representative section than Balloon Creek which is atypical of the unit as a whole. It is very useful, as numerous clean glaciated pavements enable textural relationships to be seen. Elsewhere outcrop morphology is strongly controlled by foliation and lineation fabric and little internal structure is discernable.

Age of the Balloon Formation

The age of the Balloon Formation is equivocal and poorly constrained. A locality of limestone rip-up conglomerate (M27 f192/195) on the north shore of Cobb Reservoir (M27 789085) has yielded an assemblage almost identical to that from Trilobite Rock and indicates an Early Boomerangian age. This limestone occurs as an unfaulted sliver within cobble conglomerates and is of unknown affinity to the surrounding sediments.

A new fossil locality in Heath Creek (M27 f181, M27 806067) discovered by R.A. Cooper and the author, has yielded trilobites of Floran age, the oldest fossil age from the Central Belt. A Middle Cambrian age (Floran to Boomerangian) is also indicated for sparsely fossiliferous carbonate nodules (M27 f198) outcropping in a tributary of Deep Creek (M27 807048), roughly along strike from the previously mentioned locality.

The age contrast between these two localities is problematic. Cooper (1986) suggests that the sequence of conglomerates, andesites and siltstones containing Floran trilobites is in fault contact with the blocky tectonites of the Balloon Formation and names this sequence the Heath Slice. In view of the fact that no fault contact was observed and that the sequence appears to be conformable, these rocks are, for now, included within the Balloon Formation. This problem will be discussed later in this chapter.

General Character Of The Balloon Formation

Pervasive disruption of the rocks and destruction of primary sedimentary features is considered to be a characteristic of the unit. Nowhere within the field area can disrupted rocks be traced into an undeformed sequence.

The formation consists of sparse lenses of resistant lithologies (limestone, chert, volcanics and cobble conglomerate) within a "foliated block in matrix" tectonite (diamictite of earlier descriptions).

While in previous studies of deformed rocks of this nature [e.g. Bradshaw (1972), Botsford (1983), Cowan (1982) etc.] it is common to describe initial (i.e. pre-deformational) lithologies or lithologic associations, in this case the deformation is so pervasive as to constitute the most distinctive feature of the rocks. No undisrupted sequences have been observed. This chapter describes distinctive lithologic types and styles of deformation recognised, and discusses the possible origins of the deformation.

Lithologies of the Balloon Formation can be grouped under two headings :1, "Block in Matrix" type lithologies and :2, distinctive lithologies occurring within these block in matrix tectonites.

BLOCK IN MATRIX TECTONITES

Introduction

The problem of classifying and interpreting disrupted rocks is well illustrated by the number of classification schemes found in the literature. A recent review by Raymond (1984) provides a classification scheme which is becoming relatively accepted by many workers. However it is not readily applicable to rocks of the Balloon Formation. They cannot be classified as Mélange or Dismembered Formation (Raymond 1984) as commonly a gross sense of stratigraphy is preserved. However generally rocks are significantly more disrupted than the definition for Broken formation allows, although broken formation is recognised.

Diamictite has been used previously by Cooper (1979) and Grindley (1971, 1980) to describe the rocks of the Balloon Formation. "Diamictite" is a non-genetic term proposed by Flint et al (1955, 1959) to describe a *"non-sorted or poorly sorted, non-calcareous, terrigenous sedimentary rock that contains a wide range of primary particle sizes in a finer grained matrix."* As such it can only be used to describe rocks in which block in matrix texture is of sedimentary origin. While some of the Balloon Formation is interpreted to be of olistostromal origin (i.e. true diamictite), the origin of most of it is interpreted to be a tectonic process. In this thesis the rocks are given the name "Block in Matrix" tectonite or "blocky tectonite, unless a more specific name can be applied.

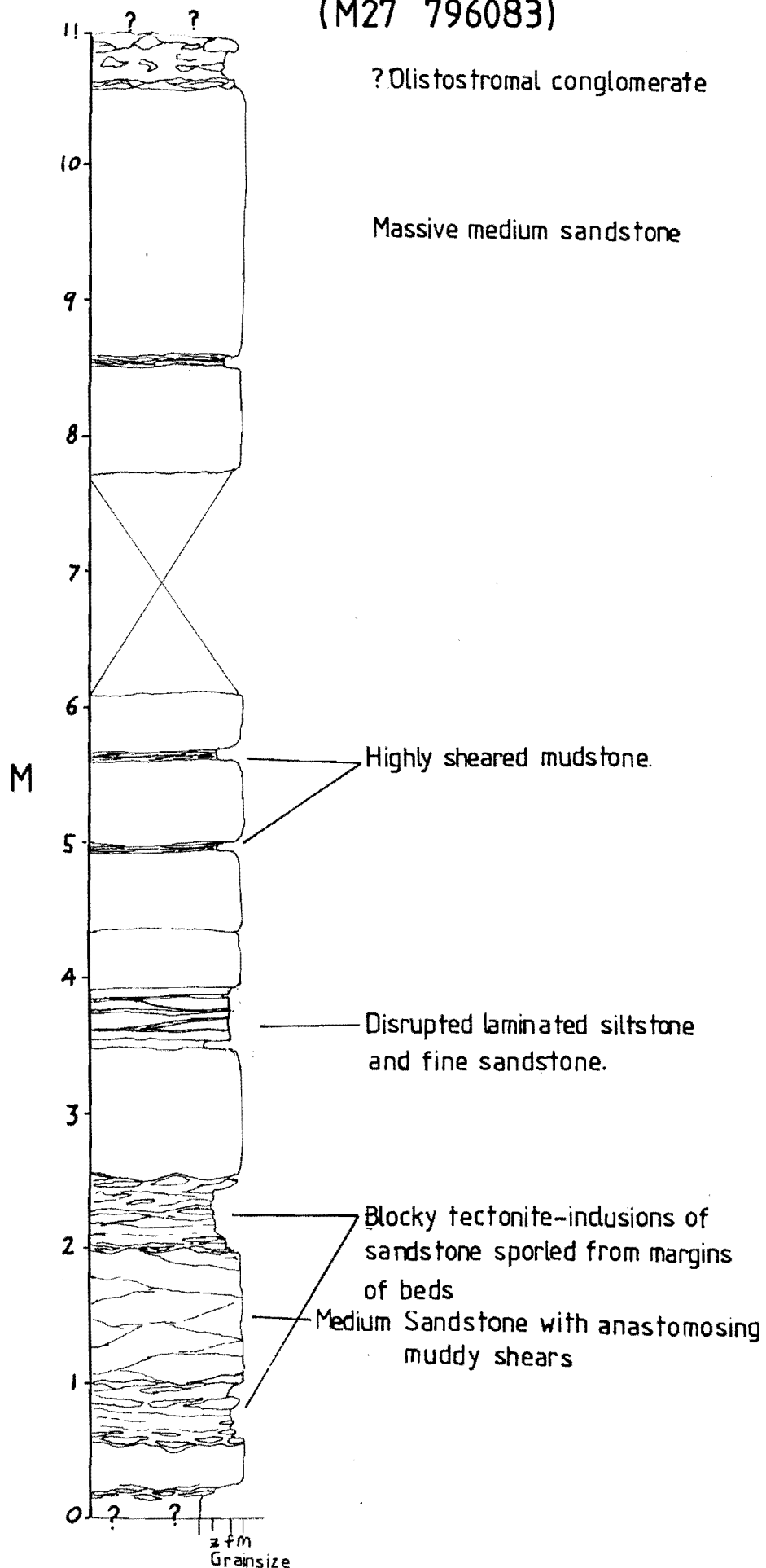
Block in Matrix Tectonites

Block in matrix tectonite is volumetrically the most important unit of the Balloon Formation. It can roughly be subdivided into two major overlapping categories - sandstone rich (50-90% sst) and sandstone poor (20-50% sst). Often the two are intimately admixed and grade from one to the other. This obviously reflects the original sand/mud ratio of the sediments irrespective of the process of mixing, so mapping of sandstone percentage in blocky tectonite should delineate primary sediment distribution. Unfortunately insufficient 2D (or 3D) outcrop exists to enable any patterns sediment distribution to be mapped. A very broad range of tectonite types are observed on the shore of Cobb Reservoir where good exposures of sandstone/mudstone textures are found in glaciated pavements. The textures are best described by photograph. Elsewhere textures are not generally observable. It did not prove possible to subdivide the range of textures observed into usable mapping units.

The degree of disruption is variable, from sequences where original bedding is still recognisable to outcrops containing discrete sandstone inclusions scattered in a foliated mudstone matrix, and every gradation between. A gross sense of original bedding is found over most of the area, defined by sandstone rich/sandstone poor layering (figure 4.1). A small section where disruption is at a minimum was logged on the lakeshore at M27 796083 (figure 4.2). No sedimentary features could be

Figure 4.2 Measured stratigraphic section, Balloon Formation, Cobb Reservoir (M27 796083).

Measured Section - Intact Bedding (M27 796083)



observed. Sandstone beds 40 cm to 1 m thick are separated by either sheared siltstone and mudstone or disrupted mudstone with blocks of sandstone. Bedding roughly equates to the Medium Bedded sandstone association of Botsford (1982). Bedding contacts are strongly modified and blocks of sandstone are detached from the sandstone beds and tectonically included in the mudstone. Beds are frequently lense shaped and thin or boudinage along strike (figure 4.3).

Sandstone rich tectonite comprises sandstone with a coarsely anastomosing veinwork of mudstone. This can be observed in figure 4.4 and in the lower part of figure 4.5. Contacts between sandstone rich and sandstone poor tectonites are gradational and are marked by a decrease in size and abundance of inclusions.

Sandstone poor blocky tectonite is generally comprised of discrete sandstone inclusions floating in a mudstone matrix. Inclusions range in size from sandgrain size up to many metres. They are often 'lemon pip' shaped (figure 4.6) and have a preferred orientation with long axes of clasts aligned. Other inclusions have irregular shapes (e.g. figures 4.7, 4.8, 4.5) but still generally have a preferred orientation. Shape is in part determined by sandstone-mudstone ratio. In sandstone poor outcrops inclusions are predominantly lemon-pip shaped, while in sandstone rich outcrops inclusions are irregular in outline.

Margins vary from sharp well defined boundaries, particularly parallel to foliation, to being indistinct and apparently gradational with matrix (figure 4.9).

Generally inclusions are monolithic, comprising predominantly fine to medium feldsarenite sandstones although sparse siltstones and coarser sandstones are found (e.g. figure 4.8).

Sandstone Petrology

A total of 20 sandstones were examined in thin section. All are substantially altered and original mineralogy is difficult to estimate. Development of solution cleavage planes marked by concentrations of opaques indicates an unknown volume loss by solution. The rocks now have 20 - 50 % matrix of chlorite, sericite, quartz, opaques, abundant



Figure 4.3 Boudinaged sandstone beds exposed in glaciated pavement (M27 796087). Hammer handle 60cm long. Reservoir shore.

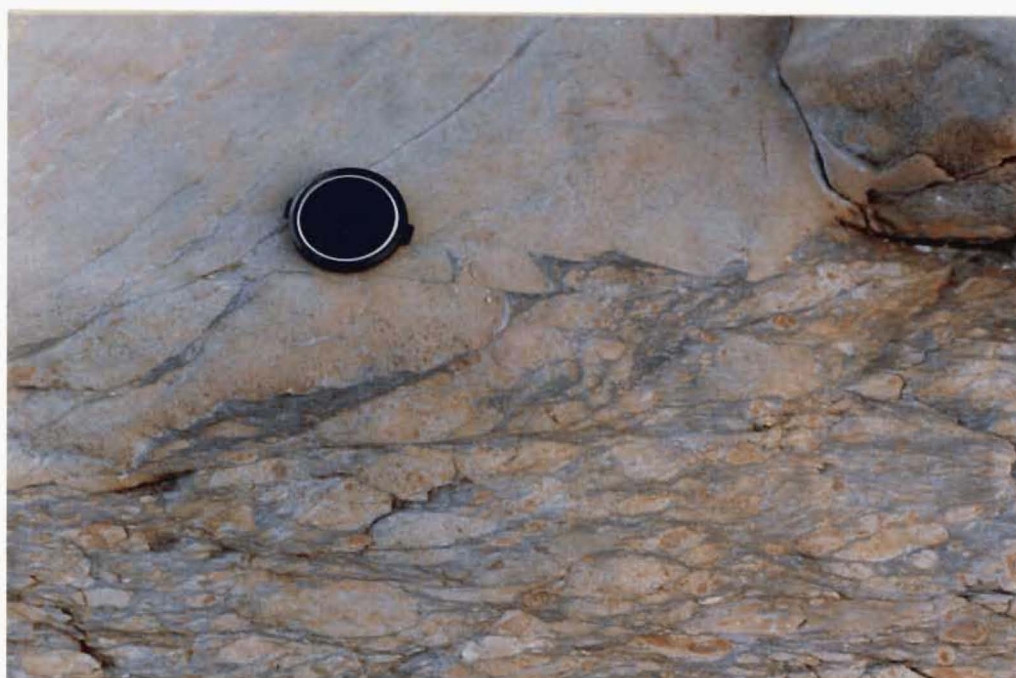


Figure 4.4 Disrupted margin of thick sandstone bed. Note intact blocks of sandstone separated from main body of bed. (M27 812091). Reservoir shore.

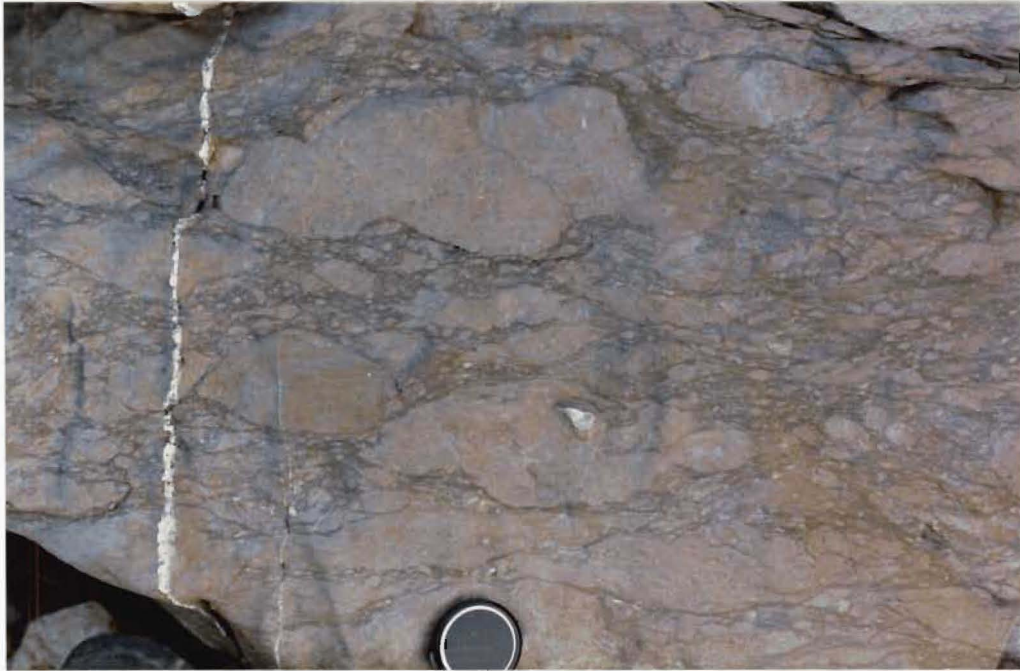


Figure 4.5 Sandstone rich block in matrix tectonite (M27 812091). Reservoir shore.



Figure 4.6 More typical outcrop, showing lemon-pip shape of clasts wrapped by foliation (M27 794082). Width of field of view approximately 6m. Reservoir shore.



Figure 4.7 Disrupted sandstone and mudstone (M27 788082). Note the irregular inclusion shapes and often poorly defined margins. Foliation is defined by long axes of inclusions and fissility in matrix. Orange colour due to weathering of secondary ankerite in sandstone. Reservoir shore.



Figure 4.8 Block in matrix tectonite exposed in glaciated pavement on Reservoir shore (M27 788082). Coarse granule sandstone inclusions may be derived from an originally continuous bed. Note that inclusion above and right of pencil, appears to have deformed by ductile processes.

carbonate and minor epidote, either recrystallised from the original matrix or alteration products after feldspar.

Composition

Visual estimation of modal % was undertaken in five relatively unaltered samples of medium to fine grain size. Point counting was not employed, as mineral identification is commonly difficult, and solution, replacement and alteration have modified original mineralogy. Sandstones plot in a broad scatter straddling the feldsarenite-lithic feldsarenite classification (figure 4.10). The sandstone analyses do not cover the full range of sediments present and further work is warranted.

Quartz: Quartz grains vary from relatively fresh to embayed, corroded grains showing chloritic replacement or patchy carbonate replacement. They frequently have sharp margins parallel to cleavage and sericite beards occupying pressure shadows at the ends of grains. The quartz population is dominated by the unstrained, monocrystalline variety, although strained and polycrystalline quartz is present in minor quantities. Polycrystalline quartz is generally replaced along subgrain boundaries. Grains are frequently subangular to angular, angularity being increased by solution and alteration, from (?) originally subangular to subrounded.

Feldspar: The feldspar population (20-30 modal %) is dominated by sodic plagioclase, which is largely sericitised and/or replaced by carbonate. Microcline is an important minor component in most sandstones and is generally fresher and less altered than plagioclase. It is present in the proportion trace to 2%, with one sample (U.C 12633) containing 20%. Microcline is suggestive of a plutonic igneous source (Shelley 1975). Scattered grains of myrmekite appear in one sample (U.C 12634).

Rock Fragments:

Sedimentary rock fragments occur in variable proportions. Minor siltstone grains with preexisting phyllosilicate fabrics constitute from trace to 3%. Fine grained, equigranular chert clasts are locally abundant. They are subangular, constitute the coarser mode in most samples, and are often partly replaced by small rhombs of carbonate.



Figure 4.9 Slabbed surface of blocky tectonite cut perpendicular to lineation. Note the near circular cross sections of some sandstone inclusions and poor definition between matrix and clasts. Sylvester Rd.

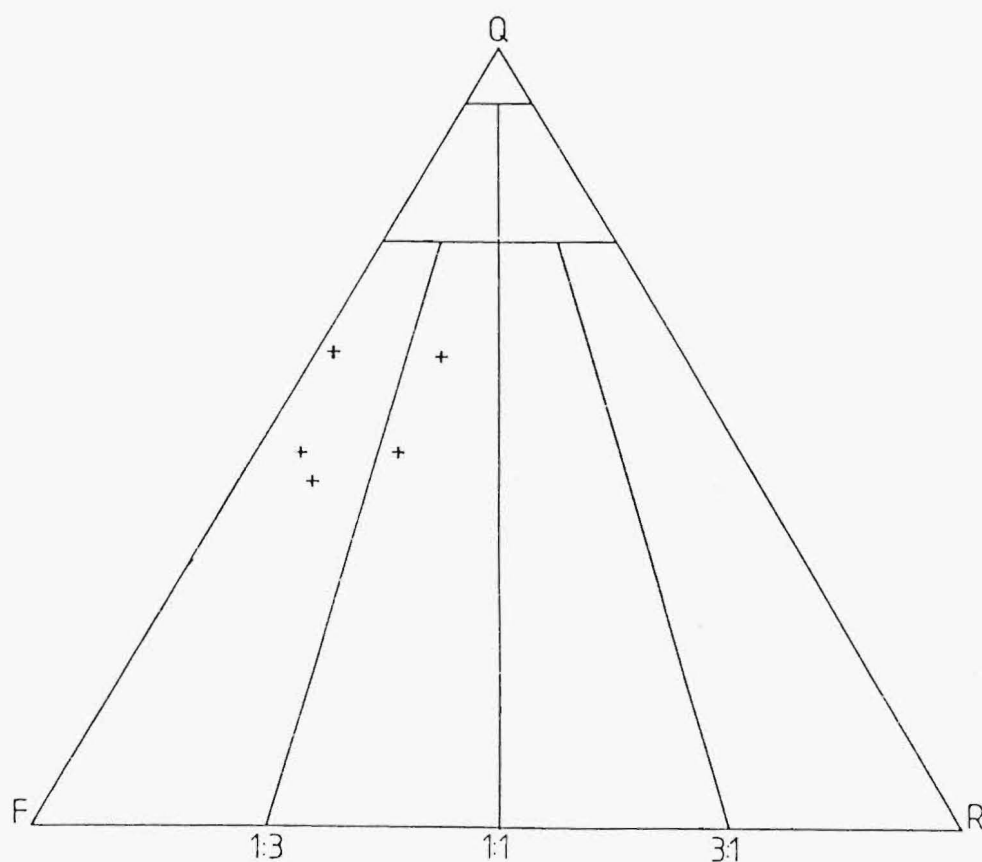


Figure 4.10 QFR ternary diagram of Balloon Formation sandstones. Arenite classification after Folk et al (1970).

Minor volcanic rock fragments of unknown affinity are inferred from altered patches of a fine grained chlorite, carbonate and quartz assemblage. Minor quantities of intergrown alkali feldspar and quartz are interpreted as plutonic rock fragments.

Others: Detrital mica is locally abundant, constituting up to 3 modal % and is present in all sample. It is commonly bent and kinked around grain boundaries and by solution planes. It is a distinctive component in hand specimen.

Fissile Sheared Mudstone

At a number of localities in the Lakeshore section fissile, fine-grained sediments commonly with strongly streaked out relict bedding are found. At M27 787082 (see figure 4.1 +42m) a 4m thick outcrop of light to dark grey, vaguely laminated, fissile mudstone and very fine siltstone, with lozenges of chert and cherty mudstone, outcrops. In cut slab this lithology is seen to be very intensely disrupted, with no sense of original bedding preserved (fig 4.11). Mudstone has been semi-ductilely deformed and brecciated producing irregular and folded lozenges. Small isoclinal fold hinges are preserved floating in the foliated mudstone. The presence of fold hinges suggests soft sediment processes may be in part responsible for the disruption.

At M27 794082 (see figure 4.1 +600m) another outcrop of fissile dark to light grey mudstone with 2 cm thick relict cherty mudstone beds is found (see figure 4.12). It contains up to 50 cm long elongate lozenges of disrupted sandstone, some 5-10 cm long elongate chert blocks, minor black pyritic mudstone and a few isolated isoclinal fold hinges. In cut surfaces, bedding can still be recognized (parallel to foliation). The presence of isoclinal fold hinges suggests that deformation was in part a soft sediment process.

In a 6m thick disrupted but moderately well bedded sequence exposed at M27 796083 (figure 4.2), fissile dark grey mudstone and laminated siltstone is found interbedded with massive sandstone beds. Contacts have been modified by tectonic movement and large strains accommodated within the mudstone layers.



Figure 4.11 Slabbed sample of intensely disrupted and fractured mudstone and siltstone, Reservoir shore.



Figure 4.12 Highly sheared fissile mudstone with relict cherty siltstone beds (M27 812091). Width of outcrop approximately 0.5m. Reservoir shore.

Broken Formation

At one 40m outcrop (M27 805086) on the lakeshore (figure 4.1 1120-60m) Broken Formation (Raymond, 1984) is found. It comprises angular and lozenge shaped blocks of sandstone and siltstone in a disrupted finer grained matrix in which bedding and laminations are commonly still visible. Inclusions are commonly bounded by pairs of bedding planes and shear fractures at moderate (30-60°) angles to bedding, and are irregularly oriented although tend to parallelism to foliation. The rock as a whole has a strong lineation and foliation and the range of lithologies present is similar to that in the sequence as a whole

Deformation appears to be primarily extensional (note the repeated normal fault offsetting of siltstone layers in figure 4.13), and has apparently occurred predominantly by brittle fracturing processes. In slabbed section it can be seen that the sandstone inclusions are penetratively laced with darker grey surfaces. These surfaces are difficult to recognize in outcrop. Where visible they form a dense intermeshing network and commonly end in embayments or fractures at inclusion margins. Shear movement is sometimes apparent from offset of margins. These surfaces are similar to Web Structure described by Byrne (1984).

Within the same area of outcrop, the degree of stratal disruption varies in scale from microscale up to (?)10 m patches within which original stratigraphy is largely intact. A number of large (8m x 3m) sandstone lozenges are present. Deformation is apparently brittle on all scales.

It is interesting to note that this zone of brittle deformation roughly coincides with the top of the belt of chert bodies.

Brittle fracture is NOT indicative of tectonic deformation or even lithification of sediments. Crittenden et al (1980) have reported cataclasis and grain breakage in gravitationally driven slide blocks, and Lundberg and Moore (1981) have noted the same features in unlithified DSDP cores. Thus this deformation may be produced by the same event as produces ductile failure in surrounding rocks and it may reflect an



Figure 4.13 Broken Formation (M27 805085). Note repeated normal offset of siltstone beds (arrowed) and angular lozenges bounded by shear fractures and beddings. Reservoir shore.

initial variation in lithification state. Little constraint on the timing of this event can be made; it may be due to slope processes or tectonic processes or some mixture of the two.

Olistostromal Conglomerate

Matrix supported conglomerates or "diamictites" with coarse sand to boulder sized clasts in a dark grey mudstone matrix are an important component of the Balloon Formation. They are abundantly developed and well exposed on the Reservoir shore comprising up to 10% of the exposed sequence (see figure 4.1 and Map 1), and also outcrop around the shores of Lake Sylvester and Little Lake Sylvester, and in Deep Creek.

It is this conglomerate that Grindley (1980) calls "diamictite", an accurate name as it is quite clearly of sedimentary origin.

The conglomerate or "diamictite" is distinguished from blocky tectonite in general by the following criteria.

- A greater angularity and random orientation of clasts.
- A greater range of clast lithologies including sandstone/ laminated siltstone/ black pyritic mudstone/ mudstone/ chert/ limey siltstone and sparse volcanics.
- Better sorting. Clast sizes predominantly range from granule to pebble size.
- Interstratification with bedded sediments.

Clasts

Clasts range from rounded to angular (predominantly sub-angular) and grade from coarse sand size up to pebble and even sparse cobble/boulder size. Predominant grainsize is granule to fine pebble.

Clasts include

- Sandstone The dominant clast type. In outcrop pale grey-green to grey fine to medium sandstones, generally massive but sometimes displaying bedding (and rarely cross-bedding) in larger clasts. Sands are very similar compositionally to the sands of the surrounding tectonites

comprising altered and carbonate replaced plagioclase with minor microcline and detrital biotite and muscovite. Clast boundaries are well defined.

- Siltstone/laminated siltstone Quartz and feldspar rich siltstone with a strong matrix sericite fabric. Clast fabric oriented at all angles to surrounding matrix. Some clasts contain mm laminations.
- Quartz grains Up to 1mm. Generally monocrystalline and unstrained or slightly strained. Largely unaltered although sometimes have a rim of chloritic/sericitic alteration.
- Plagioclase <.8mm. Ranges from moderately fresh to intensively sericite and carbonate altered. Generally twinned and of albitic composition.
- Microcline Moderately fresh often with a rim of carbonate alteration.
- Black pyritic mudstone Generally small clasts (< 1 cm) which weather to a rust orange (figure 4.14).
- Mudstone Various dark grey to black mudstones found as small angular flakes.
- Chert Generally as small pebble size clasts (see fig 4.15); also as sparse clasts up to 1.5m long.
- Carbonate siltstone/limestone Generally small clasts (see 4.14, 4.15) but one rafted inclusion 8m x 3m found on the Reservoir shore (M27 797082). This proved unfossiliferous (Appendix 1).
- Volcanics Sparse volcanics have been reported by Cooper (1979). None were observed in this study.

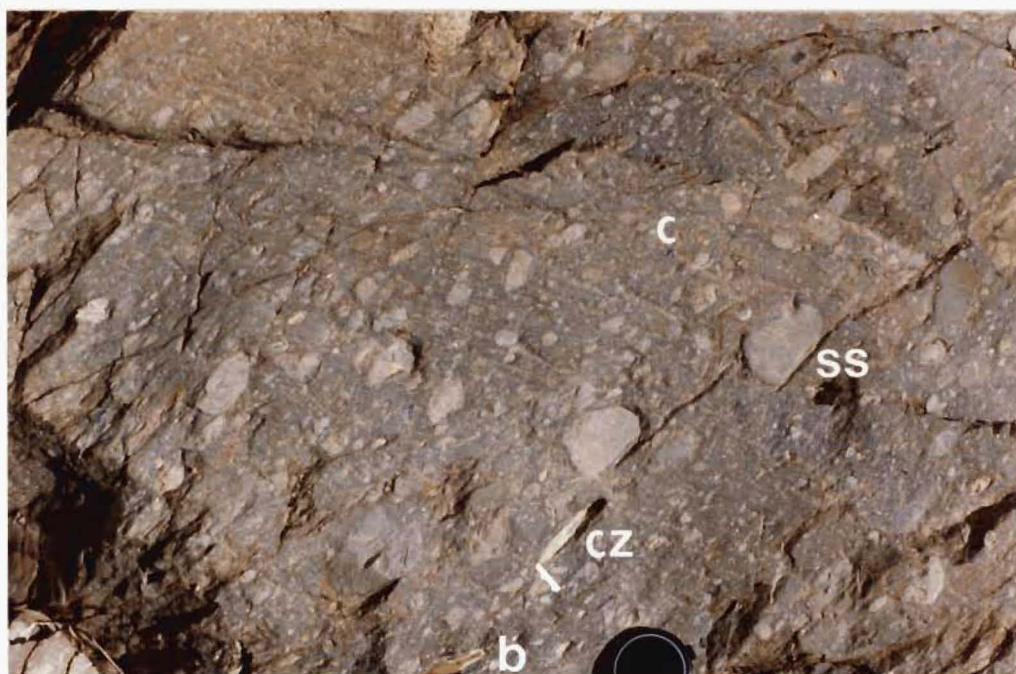


Figure 4.14 Olistostromal conglomerate (M27 797083). Note restricted range of clast sizes and also orange weathering after pyritic mudstone. ss = sandstone, cz = cherty siltstone, c = chert, b = black pyritic mudstone. Reservoir shore.



Figure 4.15 Olistostromal conglomerate (M27 797083). Note abundant chert (c) and cherty siltstone (cz) clasts. Tape case is 6cm. Reservoir shore.

Sharp clast boundaries, pre-existing clast fabrics and generally angular clast shapes indicate that clasts were at least partially lithified prior to inclusion in the debris flow.

Matrix

Subdivision into clasts and matrix is rather arbitrary as a more or less continuous gradation in grain size from mud to cobbles exists, but matrix is defined as anything less than very fine sand size (.1mm). The matrix consists of quartz, albite and sericite with minor carbonate replacement. Sericite has a weak to strong preferred orientation defining a planar fabric which wraps around clasts.

Field Relations

In Deep Creek (M27 794057) good granule to pebble olistostromal conglomerate is found interlayered with sandstone rich block in matrix tectonite. Although gross bedding sense can be determined, bedding contacts have undergone disruption and are not clear. The sedimentary diamictite grades into rock in which the block in matrix texture is interpreted to be a tectonic feature. To what extent this gradation is primary (a depositional feature), due to soft sediment slumping or mixing, or to subsequent deformation is not clear.

On the Reservoir shore similar bedding relations are seen. Bedding attitude can sometimes be determined from thin deformed mudstone interbeds, or from subtle lithologic variation. Too much deformation has occurred (and too little 3D exposure exists) to be able to see channeling or lensoidal geometry characteristic of olistostromes.

LITHOLOGIES OCCURRING IN BLOCK IN MATRIX TECTONITES

The following distinctive lithologies are found outcropping within the disrupted sediments of the Balloon Formation.

Black Limestone

Limestone occurs as small (<10m) pods within the disrupted sediments. It is commonly associated with chert and sometimes black pelagic mudstone, especially south of the Reservoir. The limestone is a black, fine-grained, very indurated massive limestone with a distinctive outcrop appearance. One sample contains probable algal oncoliths. Ten samples were disaggregated in glacial acetic acid and picked for trilobites and brachiopods. No fossils were found.

Petrographically the limestone is composed almost entirely of micrite (<4um), microsparite (4-15um) and spar (up to 40um) (classification of Folk (1959)). A gradational range of grainsizes from micrite to spar indicates spar is probably the product of recrystallisation from micrite.

A characteristic orange rust weathering colour indicates an iron/magnesium rich carbonate species. This was confirmed by optical identification of dolomite, which contains / in the obtuse angle between intersecting glide twin planes (Shelley, 1975). Lack of glide twinning also suggests dolomite.

Identification by XRD confirms presence of Fe/Mg rich carbonate, the 100% peak being shifted 1 - 1.5° 2 theta from calcite. Most traces match well with the dolomite end member composition given on JCPDS XRD cards. However, slight variation in peak intensity and position indicates non-stoichiometric forms, possibly of the Ankerite-Dolomite solid solution series.

Two deformation features are apparent in thin section. Firstly, an episode of extensional veining represented by thin (.05mm) veins of sparite and wider (2mm) composite veins of quartz and calcite. Secondly, a spaced solution stylolite cleavage which is marked by concentrations of opaques and which cuts veins at a high angle. The composite veins in general have an outer fringe of sparite (dolomite) with antitaxial quartz fibres in the centre and a well developed median line of microspar. Thin veins most likely represent incipient or failed fractures, both cutting and being cut by the thicker veins. Morphologically similar veins in surrounding sandstone are post metamorphism.

One sample (U.C 12635) contains probable algal structures. Delicately preserved, concentrically layered bands marked by fine laminae of opaques, are interpreted to be oncoliths. Aside from three trilobite and brachiopod localities these are the only organic structures identified in the field area. The oncoliths are surrounded by a mosaic of quartz, which appears to be recrystallised from a mature quartz sandstone. No other sediments of such high maturity are found in the Balloon Formation and it is not known how this outcrop is related to the surrounding rocks

Chert

Chert is found as prominent lens shaped outcrops up to 200m long and 50 m thick. The outcrops are largely confined to a broad-belt running roughly from Balloon Creek to the Cobb Reservoir (M27 790030 to M27 802085) although chert does occur outside of this belt. The chert is dark grey to black, bedded and massive, and has a conchoidal fracture. Bedding, typically 2-5 cm ribbon bedding, is difficult to identify in weathered outcrop, and appears to be complexly and irregularly folded. Muddy cherts or cherty mudstone are commonly associated with cherts, either interbedded or in gradational contact. They are well bedded (1-5 cm) with thin muddy partings.

Chert bodies are most numerous and best exposed in Balloon Creek where they stand out as spectacular ridges. Structure in this area is complex and poorly understood. Chert bodies are not continuous along strike and no folding is apparent. It is likely that significant fault displacement and repetition, of unknown geometry, has occurred.

Margins to chert bodies in Balloon Creek are often rather poorly defined, chert grading into muddy chert. Elsewhere (especially on the Reservoir shore) margins are sharp and are probably tectonically modified. Chert bodies are frequently quartz and/or carbonate veined and in places brecciated and recemented in a quartz matrix.

Petrology

The cherts where unaltered are uniform, very fine grained, interlocking aggregates of microcrystalline quartz, with sparse sericite and opaques (Trace - 1%). No evidence of any microfossils were observed in thin section. The cherts have a faint crystallographic preferred orientation, but exhibit little evidence of recrystallization. Ankerite /dolomite occurs as small euhedral rhombs (.005-.2 mm) in most samples (<1%). Morphologically the groundmass rhombs are very similar to euhedra occurring in carbonate veins invading groundmass, suggesting that they formed post chertification. Both groundmass euhedra and carbonate veins are cut by later quartz veining.

Muddy cherts have a predominantly sedimentary mudstone texture of fine grained elongate sericite, quartz and minor feldspar, and a strong dimensional and crystallographic preferred orientation, defining a planar fabric. The fabric is considered to be a metamorphic fabric (c.f. diagenetic or compactional) as it is parallel to the regional foliation and is observed to cut bedding obliquely in some outcrops.

Muddy cherts also contain small anhedral siderite (U.C 12625) or dolomite (U.C 12626) crystals. In U.C 12625 these are zoned and contain, in their centres, inclusions of matrix displaying fabric parallel to the enclosing rock. This indicates porphyroblasts formed post- fabric development.

XRF

X Ray fluorescence of nine samples was carried out by Mark Lawrence of the University of Canterbury. The analytical method is the same as that outlined in Chapter 7. Samples were analysed as HCl insoluble residues and two were also analysed untreated. Analyses are presented in Table 1. Cherts contain high SiO₂ (92 - 99%) and low levels of other majors and trace elements, commonly at or near the level of detection. Minor Al₂O₃ and K₂O is contributed from sparse sericite and Fe from iron oxides (e.g. U.C 12624). Comparison of analyses of HCl insoluble residues and untreated samples shows that all major elements except silica decrease after treatment by acid (Fe, Al, Mn, Mg and K particularly). Mn, Mg and

SAMPLE NO.	137A IR	137B IR	152A IR	152B IR	152B	155 IR	159 IR	178	178 IR	189 IR	193 IR
GEOCHEM NO	13441	13442	13443	13445	13444	13446	13447	13448	13449	13450	13451
U of C No.	12624	12625	12626	12627	12627	12628	12629	12630	12630	1263	12632
LOCATION	M27	M27	M27	M27	M27	M27	M27	M27	M27	M27	M27
	786058	786058	791037	791037	791037	794037	795038	797034	797034	781082	794074
SiO2	92.48	71.62	67.16	98.37	94.7	94.17	98.98	82.45	98.47	98.69	96.99
TiO2	.16	.57	.67	.08	.08	.12	.04	.17	.17	.04	.04
Al2O3	2.56	11.2	13.67	.98	1.54	1.88	.54	1.94	1.04	<.2	<.2
Fe2O3	1.65	5.38	6.07	.03	.78	1.23	.08	2.34	.06	.42	.07
MnO	.08	.37	.17	<.01	.11	.04	<.01	.18	<.01	.07	<.01
MgO	.51	1.92	2.4	<.01	.38	.39	<.01	2.05	<.1	<.1	<.1
CaO	.37	.23	.19	<.01	.46	.03	<.01	3.91	<.01	<.01	.01
Na2O	.2	1.08	1.66	<.01	<.1	<.01	<.01	<.1	<.1	<.1	<.1
K2O	.62	2.65	3.05	.3	.5	.49	.15	.37	.2	.11	.11
P2O5	.09	.07	.09	<.05	.12	<.05	<.05	<.05	<.05	<.05	<.05
TOTAL	99.73	100.08	100.34	100.45	99.86	99.48	99.91	100.29	100.25	100.25	98.08
BA	4	16	20	<2	<2	4	<2	3	2	<2	<2
PB	13	31	4	8	8	8	6	6	3	2	9
RB	24	106	131	21	21	20	5	14	13	4	6
SR	36	55	40	35	35	6	5	109	23	4	6
TH	3	16	22	<1	<1	3	<1	5	4	<1	<1
Y	5	26	30	5	5	5	7	13	11	3	4
BA	154	399	391	46	78	115	49	70	51	23	46
CE	15	82	91	<10	18	14	<10	50	48	15	20
CR	12	74	64	<5	6	11	<5	13	9	<5	<5
LA	5	38	54	4	5	<5	4	10	10	<2	<2
NB	<5	12	16	<5	<5	15	<5	<5	<5	<5	<5
ND	11	32	37	<10	10	13	16	23	29	<.10	<10
NI	14	44	67	6	6	9	<5	14	<5	<5	<5
V	11	70	85	<5	7	9	9	21	9	<5	<5
ZN	21	84	85	4	12	23	3	25	4	3	5
ZR	29	106	128	16	15	19	10	44	45	7	5

! = INSOLUBLE RESIDUE

TABLE 1: Major and Trace element XRF analyses for Balloon Formation cherts and cherty mudstones.

Fe are likely to be removed with carbonate (ankerite) and K, Al and Fe by acid leaching of mica and clay minerals.

Cherts are formed by the chertification (silica replacement) of sediments. Silica can be supplied (with increasing burial) from remobilization of silica from silicic organisms (radiolaria), from clay mineral transformations or from metamorphic reactions. The composition of the chert will be a product of both original rock characteristics and chemistry of replacing fluids. Chertification of fine grained sediments generally leaves a signature of higher Al, Fe, Mg, Na and K due to feldspar, mica and clay minerals. On the other hand chertification of carbonates generally results in complete replacement of CaCO_3 by silica and low residue levels of major and trace elements (M. Lawrence pers. comm.).

Textures, high silica content and low abundances of majors and traces indicate that these cherts are likely to be the products of chertification of an original carbonate. This is supported by the observation that some limestones have been partly or wholly (e.g. U.C 12635) replaced by silica. No inferences of the source of the silica or timing of chertification can be made.

The two cherty mudstones analysed have compositions similar to typical siltstones or mudstones (Pettijohn, 1971) and are the products of partial chertification of clastic sediments.

Hornblende Andesite

Andesites occur as elongate lensoidal bodies intercalated within blocky tectonite and bedded sediments of the Balloon Formation. They are generally pale green coloured with distinctive pale, remnant feldspar phenocrysts, and in fresh outcrop, abundant hornblende. The rock is very resistant and breaks into regular, joint bounded blocks. Petrographically and geochemically the rocks are calc-alkaline hornblende andesites. Petrology and geochemistry will be discussed in Chapter 7.

The andesites outcrop on the crest of the Lockett Range, in Iron Lake Stream, on the shores of Cobb Reservoir and in Heath Creek and creeks to

the south. They are most voluminous in Heath Creek where they are intercalated with cobble conglomerate, laminated siltstone and green nodular carbonate siltstones, and comprise approximately 40% of the total succession. The outcrops range in size up to 300m along strike and 60 m thick. They are everywhere parallel to foliation and gross stratigraphy.

Contact relationships of the andesites are ambiguous. One outcrop on the Lakeshore (M27 816094) suggests the andesite may be extrusive, as overlying mass flow conglomerates containing blocks of andesite, appear to be in primary sedimentary contact with them (see figure 4.16). Whether these are actual clasts or have been tectonically included is uncertain. Margins of other andesite bodies have been clearly disrupted with lozenges of andesite obviously becoming detached. No evidence of intrusive contact, such as baking or discordant margins, is observed. The andesites occur over a wide stratigraphic range and a wide area, which suggests that they are more likely to be intrusive. Given the structural complexity and the possibility that fault repetition may have occurred, it is possible that they are both intrusive and extrusive.

Cobble Conglomerate

Heath Creek Conglomerates

Near the eastern margin of the Balloon Formation south of Cobb Reservoir, abundant conglomerates are found intercalated with fossiliferous carbonate siltstones and laminated grey siltstones. Contacts are concordant and where observed are conformable. This sequence is found on the Bullock Flat, in the streams draining north from Peat Flat and to maximum development in Heath Creek. Trilobites indicate a Floran age for the sequence, two stages older than fossils in limestone on the north shore of the Reservoir. The sequence also contains abundant hornblende andesite sheets, interpreted as of intrusive origin.

Cooper (1986) maps these rocks as the Heath Slice, a separate fault bounded unit to the Balloon Slice containing the above lithologies and the Mataki Basalt and M Creek Formation (see Chapter 5). However it is felt that the conglomerates, siltstones and andesites are in sequence with the Balloon Formation as no fault or evidence of a fault is found



Figure 4.16 Contact between hornblende andesite and olistostromal conglomerate. Blocks of andesite (A) occur within the sediment and appear to be clasts, but may be tectonically included. Note that the andesite is banded and appears to include grains of sediment (M27 815094). Slabbed sample from Reservoir shore.

between this sequence and the block in matrix tectonites. Also the igneous rocks of this area, which were all included in the Heath slice, are now recognised to belong to two totally unrelated sets (see (Chapter 7)).

The conglomerate consists of a green sub-angular to sub-rounded, poorly sorted, clast supported granule to pebble conglomerate. Visual handspecimen and outcrop estimates of composition indicate a significant proportion of volcanic clasts (up to 50%) plus medium to fine sandstone, siltstone, mudstone and chert. This is confirmed petrologically. Visual estimation of a thin section (U.C 12636) indicates approximately

60-70% volcanic clasts:

- a) inter locking qtz + feldspar laths with interstitial chlorite after mafics = a qtz andesite - similar to hornblende andesites),
- b) Other indeterminate volcanics with fine grained qtz/fspar groundmass with plag phenocrysts and chlorite/epidote replacing mafic minerals,
- c) Other indeterminate dark fine grained rock with a chloritic matrix and chlorite amygdales/pseudomorphs,

25% sandstone clasts

Generally altered and recrystallised quartz rich mature fine sandstones. Some largely unaltered quartzite,
<5% Phyllite and chert.

Clasts in general are flattened and elongate parallel to the fabric in tectonite. The rock shows abundant evidence of solution, with concentrations of opaques bounding long edges of grains. The conglomerates are not found on the Reservoir shore.

Staff Hut Conglomerates

Rounded cobble (to boulder) conglomerates occur as two large outcrops (>20m) on the slope south of Cobb Reservoir (M27 795078). These outcrops appear to be lensoidal shaped and fall within approximately the same foliation plane horizon. It is possible that they are boudinaged and extended from within the same stratigraphic horizon. However conglomerates are generally lensoidal and laterally discontinuous. Bedding is observed in only one of these outcrops where it is parallel to surrounding foliation (030/40° SE).

The conglomerate is a pale green rounded to subangular, clast supported, moderately sorted granule to cobble conglomerate. No

systematic clast counting or petrology has been done. However from field and hand specimen descriptions clasts comprise, in decreasing relative abundance, grey-green micaceous medium to fine sandstone, green volcanics (? intermediate) and assorted finer grained lithic clasts including dark grey mudstone and chert. Bedding is poorly defined by a single coarse sandstone bed in otherwise massive conglomerate.

Pebbles are flattened parallel to bedding and stretched parallel to the regional lineation. In an adjacent creek bed outcrop the conglomerate is seen to be interbedded with disrupted very fine sandstone and mudstone.

A thin (2m) cobble conglomerate of igneous and lithic clasts outcrops on the lakeshore (M27 789082) admixed in a disrupted bedded sequence. It lies in a similar foliation plane to the conglomerates just described, and may be from the same stratigraphic horizon.

Lake Head Conglomerate

At the west end of Cobb Reservoir a coarse green cobble conglomerate outcrops as a prominent glacially smoothed ridge across the valley. It has previously been described as an "agglomerate" (Grindley, 1980) and as an "igneous conglomerate interbedded with turbidites - possibly the product of a submarine lahar" (Grindley, 1978). It also outcrops on the hill slope to the south and in two unconnected outcrops on Peel Ridge.

The conglomerate comprises a 35m thick-bedded sequence of distinctive green, well rounded pebble to boulder conglomerate with sparse lensoidal laminated siltstone, sandstone and (?) tuff interbeds. The sequence dips at 25° to the east (parallel to regional dip) and is thought to be the right way up, but this is not certain. Two samples slabbed to find a face direction produced only inconclusive and equivocal results. Signs of minor disruption and modification were apparent.

At the structural base the sequence grades rapidly up from a sparse dark grey angular pebbly mudstone, very similar to olistostromal conglomerate lithologies, into a light grey to green angular coarse sandstone to chip conglomerate, containing well rounded volcanic

(andesitic) pebbles and cobbles. To the west the pebbly mudstone is in fault contact with structurally sliced but bedded siltstones. This fault is of unknown magnitude but is suspected to be significant. The top (east) contact is not exposed and is thought to be faulted. Detailed observations on sedimentology were not carried out owing to the poor definition of internal structures in outcrop.

In thin section volcanics are seen to comprise predominantly andesitic volcanics containing phenocrysts of hornblende and/or clinopyroxene and altered plagioclase in a microcrystalline quartz/feldspar/chlorite matrix. Petrologically these rocks are andesitic to quartz andesites. Clasts are well rounded with sharply defined margins, indicating that they have undergone considerable transport and abrasion. Filling interstices are medium sand to granule sized quartz, microcline, plagioclase, chert and minor siltstone. Subhedral, fresh hornblende and pyroxene crystals are probably of detrital origin, as they are seen in places to have matrix attached (very difficult to identify as matrix of volcanic rock is very similar to conglomerate matrix). Surrounding these clasts is a very fine grained matrix of recrystallised quartz.

The clast supported nature of the conglomerate plus the presence of laminated and low angle cross bedded sandstones and the well rounded nature of indurated volcanic clasts suggests tractive current deposition and considerable transport of larger clasts.

North Shore Conglomerate

On the north shore of Cobb Reservoir a large outcrop of pebble to boulder conglomerate forms a promontory into the lake. It is lithologically very similar to the outcrops found on the hill south of the Reservoir. On the south west side it is in conformable contact with bedded sandstones and siltstones which have unknown relationship to the disrupted sediments. To the north east no contact is exposed.

This conglomerate contains two outcrops (? fault repeated ?) of redeposited limestone rip-up conglomerate (similar in texture to Trilobite Rock (MacKinnon, 1985)). The limestones contain a faunal

assemblage (U.C 12580, M27 f192/195) almost identical to that found at Trilobite Rock and indicate an early Boomerangian age (Late Middle Cambrian). This limestone is in fault contact with the conglomerate and is therefore of unknown affinity to both the conglomerate and the enclosing sediments.

STRUCTURE

As described in the previous section, the Balloon Formation is characterised by a "block in matrix" texture. Disruption is pervasive on all scales, such that mapping of any discrete or continuous bodies is not possible. Some outcrops do contain a more or less intact bedding and a number of distinctive lithologies are found but these are surrounded by more disrupted sediments.

Whatever mechanism is invoked to account for the disruption is constrained by what appears to be a discrete segregation into belts with inclusions of a particular lithology, suggestive of an original stratigraphy. Chert inclusions are largely confined to a belt running from the Reservoir shore to Balloon Creek (see Map1), while andesites occur in a belt to the east of this.

Unequivocal olistostromal conglomerates occur throughout the area and are clearly distinct from the blocky tectonites.

Overall the texture is dominated by strong evidence of extension and elongation. Inclusions generally have elongate, lemon pip shapes with axial ratios of the order of 3:2:1. Their long axes are strongly aligned parallel and define a regional lineation described in Chapter 8, and intermediate and long axes define a plane of foliation. Quartz extensional fibres filling discrete fractures and joints, and necking and boudinage of relatively intact sandstone beds record extension parallel to this lineation. Extensional boudinage and fracturing are also indicated perpendicular to the lineation direction.

In many outcrops a 'sense' of bedding is retained, at best by pinch and swell of relatively intact beds (e.g. figure 4.3, at worst by a vague alignment of similar size or composition inclusions. More generally

bedding is indicated by boudinaged sandstone beds (e.g. figure 4.18), trains of inclusion or a gross compositional layering in matrix. Where observed bedding is always parallel to foliation. It shows a similar variation in orientation to foliation also (e.g. figure 4.17, c.f. figure 8.4).

Deformation appears to have occurred by both brittle and ductile processes. In general inclusions display no evidence of brittle fracturing and have symmetrical cross sections parallel to lineation (e.g. figure 4.6). In some inclusions deformation has been predominantly brittle. A 2 m thick outcrop of cobble conglomerate exposed on the Reservoir shore at M27 789082 has been necked to 20 cm by repeated normal fault offstepping. In slabbed section some sandstone inclusions are seen to be laced with dark grey shear surfaces along which modification of clast shapes has occurred (e.g. figure 4.19). Fractured inclusions generally show a marked asymmetry, however no consistent sense of shear is recognised. Broken Formation (e.g. figure 4.13) is characterised by brittle fracturing and angular shear bounded inclusions, and has a strong linear fabric parallel to that in blocky tectonites. This range in deformation styles presumably reflects a variation in competence contrasts at the time of deformation.

Folding is notably absent in the Balloon Formation. Apart from minor rootless isoclinal fold hinges in fissile mudstone, no evidence meso or macroscopic folding was observed. No evidence of turbulent mixing can be seen either.

The textures observed in the Balloon Formation are very similar to those described from mélanges. The origin of mélanges have been ascribed to three main processes

- 1) Tectonic disruption (Needham and MacKenzie 1987, Bell 1987, Byrne 1985, Botsford 1982).
- 2) Olistostromal or gravity induced process (Cowan 1982, Gucwa 1975, Boles and Landis 1982, Page and Suppe 1981).
- 3) Mud diapirism (Williams et al 1984)

Figure 4.17 Stereographic plots of poles to beddings, plotted by domains (all lower hemisphere equal area projection).

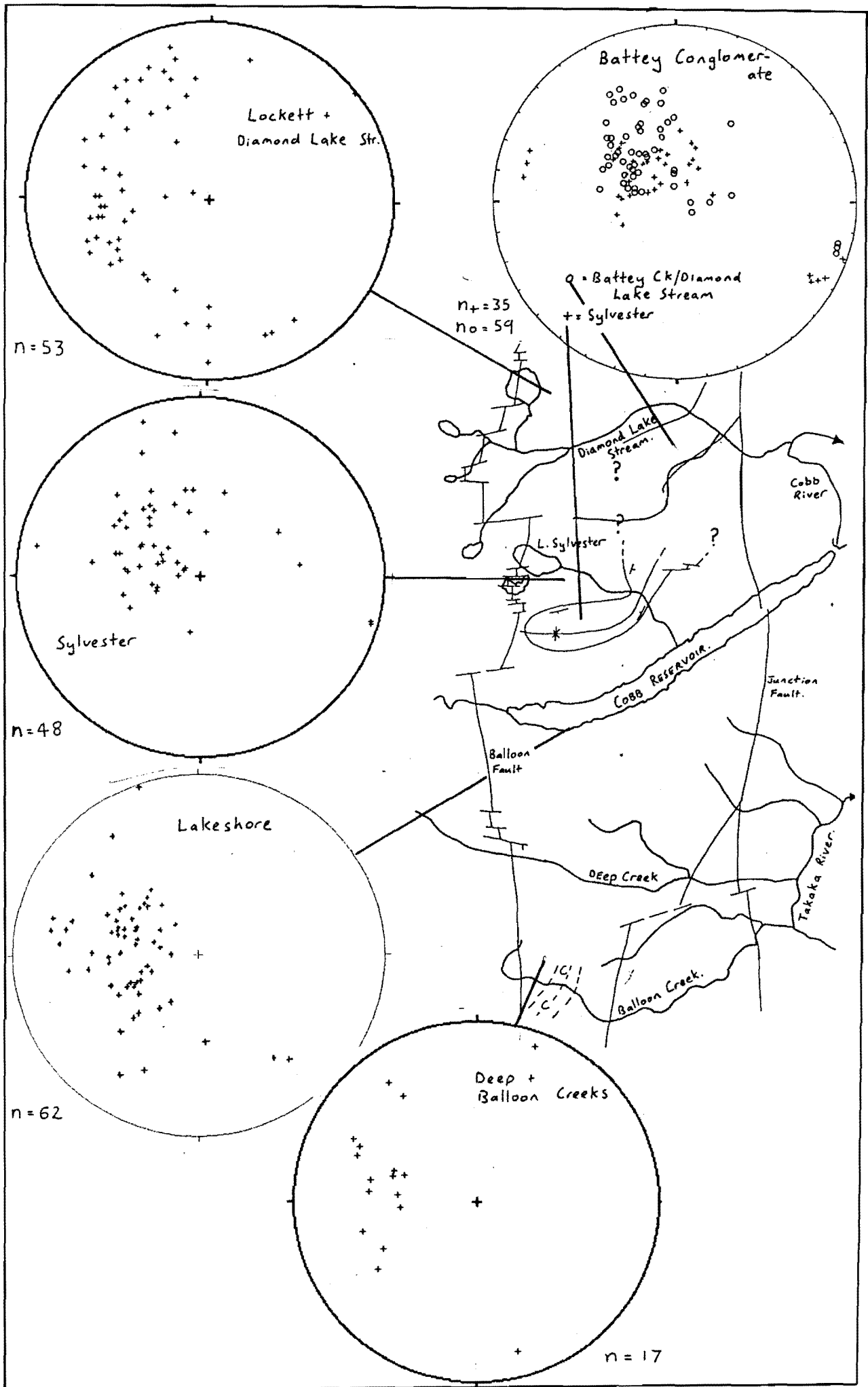




Figure 4.18 Strongly boudinaged sandstone, in blocky tectonite. Reservoir shore (M27 812091).



Figure 4.19 Elongated sandstone inclusion. Note dark grey shear surfaces lacing inclusion, along which shape modification has occurred. Sample from Reservoir shore (M27 812091).

It is felt that an olistostromal origin can be discounted in this case as deformation occurred under metamorphic conditions. Microscopic evidence for synkinematic metamorphism includes

- 1) A strong matrix phyllosilicate fabric which anastomoses around inclusions and is most marked in bands of shear between more intact sandstone.

- 2) Growth of quartz and sericite beards in pressure shadows at the ends of inclusions.

- 3) Extensional quartz and chlorite fibres in the necks of boudinaged sandstone inclusions and infilling brittle fractures in quartz and chert grains. These record extension parallel to the lineation.

Similarly a diapiric origin for the Balloon Formation can be discounted as a general sense of stratigraphy is preserved.

Two alternative models for the origin of the disruption can be put forward. Firstly a two stage model in which disruption is the product of an earlier event overprinted by the regional extensional deformation. Strong alignment of the inclusions parallel to the regional lineation may be due to either fortuitous coaxiality of the deformations or to rigid body rotation during the second deformation. No evidence of any overprint relationships was observed. Rigid body rotation is not felt to be likely, as the high strains required to produce such a strong lineation are not indicated by other strain markers e.g. deformed conglomerates.

Alternatively, a single stage model in which disruption is a product of the extension and elongation process can be invoked. Linear tectonite fabrics parallel to transport direction are commonly described from regimes of simple shear (Ramsay and Huber 1984), but these are generally not accompanied by disruption of bedded sequences. Recently Needham and MacKenzie (1987) have interpreted a linear fabric in *mélange* as transport parallel fabric resulting from disruption during elongation. It is felt that this may be an applicable model to the rocks of the Balloon Formation.

Further work on mesoscopic fabrics is necessary to enable interpretation of these rocks.

CHAPTER FIVE

MATAKI FAULT BOUNDED SLICE

INTRODUCTION

A fault bounded area of rock previously identified as Devil River Volcanics and Lockett Conglomerate (Grindley 1980), but in fact of uncertain affinity, is informally assigned a new name, the Matakai Fault Bounded Slice (or Matakai slice). It outcrops in Balloon Creek, Matakai Creek and Deep Creek, and is bounded on the west by the Matakai Fault and on the east by the Junction Fault.

The rocks of the Matakai slice fall into three lithologic groups: 1/ basaltic volcanics and associated sediments: 2/ volcanic rich, matrix supported debris flow conglomerates and: 3/ red and green chert and volcanic rich conglomerates and sandstones. The three lithologic groups have been assigned the informal names Matakai Basalt, M Creek Formation and Salisbury Conglomerate respectively. Relationship between these units are equivocal and poorly understood. No age control exists for the Matakai slice.

Rocks are dominated by lower greenschist facies metamorphic assemblages which destroy initial mineralogies and texture, making even distinction of sedimentary rocks from igneous difficult.

MATAKI BASALTS

Basaltic volcanics and associated sediments outcrop in Balloon, Deep and Matakai Creeks. The reference locality for the Matakai Basalts is designated to be Deep Creek (M27 820055 to 822057). In general, outcrop is highly altered and appearance is dominated by metamorphic minerals, making identification of basalts from sediments difficult. The petrology and geochemistry of the basalts will be discussed in Chapter 7.

The basalts are medium to dark green, finely crystalline and generally massive, and commonly have a felted texture in fresh surface. They are distinguished from sedimentary rock by green colour, texture,

lack of visible grains and presence of small carbonate filled pocks interpreted as amygdales. Green colour is due to abundant iron rich metamorphic phases (e.g. chlorite/ epidote/ tremolite). Weathered rocks show a pale dove grey colour, and have a homogeneous fine-grained texture on broken surfaces.

Due to poor exposure, few margins were identified and in most cases field evidence does not permit distinction between extrusive (pillow lavas or flows) and intrusive (dykes or sills) bodies. In one outcrop dark grey interstitial sediments define rounded pillow shapes (Figure 5.1); pillows were tentatively identified in several other outcrops. Variable (weak to intense) shearing is also apparent in most outcrops. Note in figure 5.1 that pillow margins have been offset by shear surfaces.

Geochemically the basalts are tholeiitic and are distinct from and unrelated to the calc-alkaline hornblende andesites of the Balloon Formation (see Chapter 7).

Sediments associated with the basalts are volumetrically insignificant, and include pale silicic siltstones with faint laminations, and dark grey siltstone. Contacts where exposed are concordant.

In Balloon and Matakiki Creeks volcanics and interbedded siltstones strike N-S and dip at a moderate angle to the east, parallel to a weak foliation in both sediments and volcanics.

M CREEK FORMATION

In Matakiki Creek a sequence of laminated siltstones and matrix supported conglomerates, here called the M Creek Formation is found.

Conglomerates

Conglomerates are green, poorly sorted, matrix supported and basalt rich. Basaltic clasts, petrographically similar to the basalts described

above, predominate and range in size from granule to coarse cobbles. Clasts are commonly angular with cusped embayments (e.g. figure 5.2) and appear to have deformed semiplastically during inclusion in the rock.

Other clasts include fine sandstones, carbonates and mudstone; the latter clasts are generally of coarse sand to granule size, angular and appear to be rip up clasts. Most clasts are randomly oriented and have sharp margins. Reddish sub-angular to sub-rounded chert clasts are volumetrically insignificant, but are obvious in outcrop due to their induration and lack of alteration.

Matrix is a grey to green slightly foliated fine sandy mudstone. In thin section (U.C. 12637, 12638) it comprises quartz, plagioclase and lithic grains dispersed through a dark groundmass. Lithic clasts are difficult to distinguish from matrix but become apparent under low magnification and illumination.

In the field the conglomerate was tentatively identified as a pyroclastic deposit. Thin section examination of matrix indicates a sedimentary origin as no features of pyroclastic deposits (e.g. cusped shards, vitric material) were identified. Bedding is sometimes defined by a crude layering of clasts.

The matrix supported nature of the conglomerate, general random size and orientation of clasts and lack of internal structure suggests deposition by mass flow processes.

Laminated Siltstones and Sandstones

Sediments associated with the conglomerate include intercalated dm bedded sandstone, cm laminated siltstones and silty mudstones. No facing directions were identified. A thin section (U.C. 12639) shows the sandstone to be a lithic feldspathic sandstone with approximately 20-25 modal % quartz, 20-25% plagioclase, 3% rock fragments, 1% biotite and 50% secondary matrix minerals. Feldspars have undergone saussurization and been extensively replaced by carbonate, sericite and minor quartz, making estimation of original feldspar percentage difficult. It is likely that the original feldspar proportion may have been as high as 35 - 40%.



Figure 5.1 Disrupted pillow basalts, Deep Creek (M27 821057). (Hammer 30cm long).



Figure 5.2 Matrix supported angular debris flow conglomerate, Matakiki Creek (M27 811048). Note clasts of (?) basalt (arrowed).

Lithic fragments include minor chert, siltstone and volcanic rock fragments. No grading was apparent in the field.

Debris flow conglomerates and siltstones mostly outcrop in Matakī Creek which flows approximately along strike at 040-060°. They dip at about 45° to the east. Bedding attitude is similar in adjacent creeks.

SALISBURY CONGLOMERATE

A distinctive red and green conglomerate, previously mapped as Lockett Conglomerate, outcrops in Matakī Creek, and is here called the Salisbury Conglomerate. This conglomerate is being studied in detail by Kate Pound of the University of Otago. This thesis will consequently comment mainly on field relationships, field descriptions and structure.

The Salisbury conglomerate consists of an interbedded sequence of medium to coarse sands and poorly sorted granule to cobble conglomerates. Conglomerates are usually clast supported, although very poor sorting results in large clasts surrounded by finer material. Clasts are well rounded to rounded and are commonly discoid or blade shaped (an original feature as well as a product of later deformation). They include mauve siltstone, red chert, green mudstone, green siltstone and green chloritic volcanics.

The matrix is a medium to coarse sand sized lithic feldsarenite containing approximately 10 modal % quartz, 30% plagioclase, 2% alkali feldspar, 6% chert, 10% basaltic and andesitic rock fragments, 2% siltstone and 40% fine grained secondary minerals.

Conglomerates are poorly bedded to massive. Bedding is poorly defined and consists of thin, irregular sandy interbeds (see fig 5.3). Bedding contacts are not sharp and commonly coarse clasts project into or across finer grained beds. No imbrication, grading or facing direction was observed.

In Balloon Creek the sequence becomes finer grained to the east; conglomerate beds become sparse and dm bedded medium to coarse sandstone predominates. In Matakī Creek the sequence comprises mainly dm bedded

pebbly coarse sandstones with laminated fine sand/silt interbeds and sparse pebble to cobble conglomerate beds.

Bedding attitudes in the conglomerates and sandstones are variable and indicate folding of some nature. However no clear pattern emerges from either form line mapping or stereographic projection (e.g. figure 5.4). Bedding divides roughly into two domains - an eastern domain in which bedding dips consistently 40 - 60° south east and a western area in which the bedding has steep dip and variable strike.

The sequence is overprinted by a foliation (flattening and stretching, see Chapter 8) which falls into two similar domains. In the western portion foliation dips at a steep angle to the south while in the east it dips at a moderate angle to the south east (parallel to bedding). Foliations (and associated bedding) were stereographically restored to a common plane to see if this variation was an effect of later folding. The resultant bedding plot still displayed no clear pattern. While the progressive swing in strike of bedding in the western area appears to be a product of folding, variation between the east and west domains is not simply explained by folding. An alternative hypothesis is that a fault of unknown orientation, magnitude or importance separates the two domains.

Insufficient data exists to be able to solve this problem at present.

STRUCTURE

The structure of the three assemblages is poorly understood. While they are here grouped together as a single fault bounded entity, in fact the relationship between units is poorly controlled.

The Mataka Basalts and Salisbury Conglomerate are in contact in Mataka and Deep Creeks. In Mataka Creek the contact is clearly a discordant fault contact. In Balloon Creek the contact appears concordant. However both conglomerate and basalt become sheared near the contact and a fault is suspected.



Figure 5.3 Salisbury Conglomerate, Balloon Creek. Well rounded, pebble to cobble, clast supported conglomerate with coarse sand beds (M27 810033).

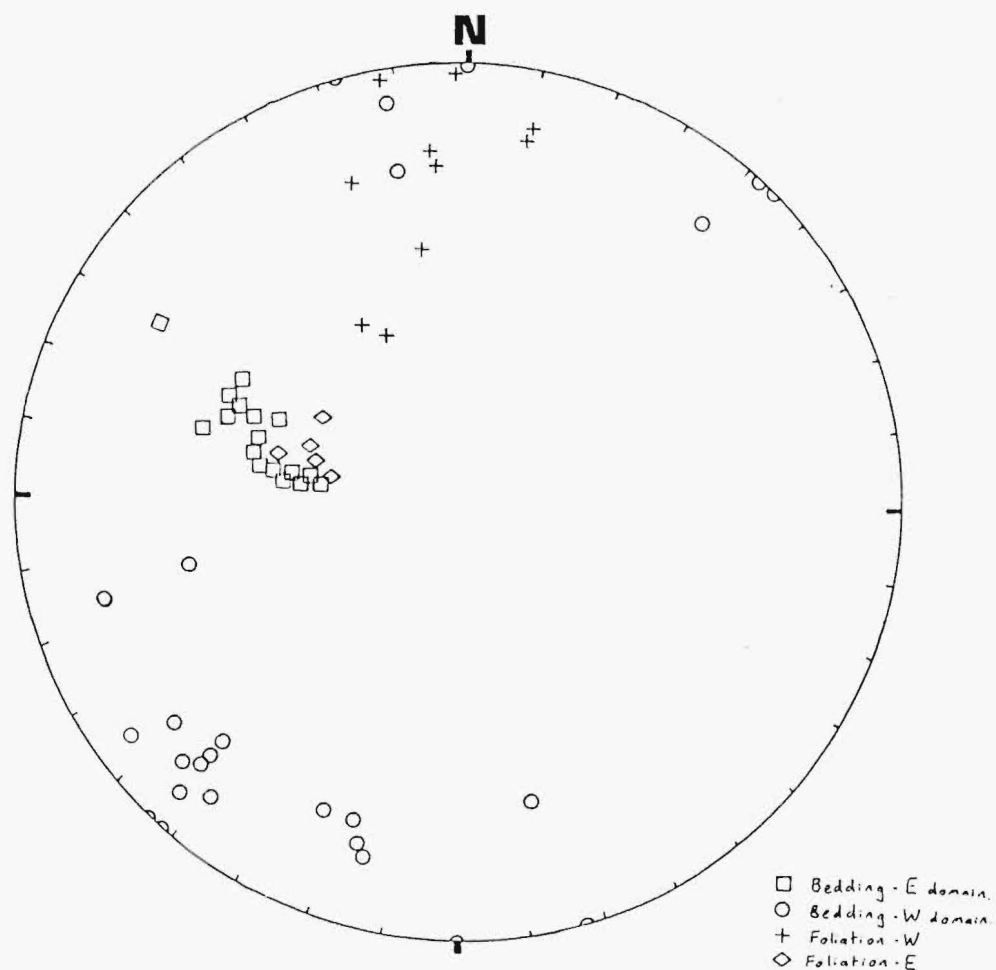


Figure 5.4 Stereographic plot of bedding and foliation in Salisbury Conglomerate (lower hemisphere equal area projection). No simple pattern of folding matching outcrop data can be recognized

The Salisbury Conglomerate and conglomerates of the M Creek Formation are in apparent concordant contact in Mataki Creek (M27 818051). The actual contact is not exposed and its position is only constrained to within 40m. The conglomerates show apparent parallelism over a strike distance of approximately 1.5 km. Neither unit displays more shearing than usual near the contact.

Mataki Basalt and M Creek Formation both outcrop in Deep Creek but their relationship is not clear as the units are difficult to differentiate in the field. M Creek Formation apparently outcrops west of M27 820055 while basalt outcrops to the east. One basalt sample (U.C. 12594) collected from within M Creek conglomerate was analysed. It is chemically similar to the other basalts and appears to be from the same suite, implying connection between these lithologic groups (see Chapter 7).

Interrelationships between the lithologic units are equivocal. If the M Creek Formation is linked to the basalts and also in conformable contact with the Salisbury conglomerate some peculiar geometry must be invoked to bring basalts and Salisbury conglomerate into fault (or even more unlikely, conformable) contact.

The Salisbury conglomerate contains evidence for folding which is not reflected in the contacts with the other units. It is therefore possible that the Salisbury conglomerate is not related to either of the other units and may be a separate fault bounded block. Further detailed mapping may help to resolve the problem, however virtually all outcrop in the area has been visited.

CHAPTER SIX

JUNCTION FAULT BOUNDED SLICE

A sequence of folded interbedded sandstones and siltstones outcrops in a narrow elongate belt from Flora Creek and Takaka River in the south to Cobb River and Diamond Lake Stream in the north. The sequence is fault bounded on the west by the Junction Fault and to the east by the Cobb Thrust. The body of rock bounded by these faults is here assigned a new informal name, the Junction Fault Bounded Slice (or Junction Slice).

The rocks of the Junction Fault Bounded Slice have been previously mapped as both Balloon and Anatoki Formations by Grindley (1980). However they bear little or no resemblance to the type areas of either of these formations, and instead are included in a new formation, informally called the Junction Formation.

JUNCTION FORMATION

The reference section for the Junction Formation is designated as the Flora River from M27 832048 (Upper Junction) to M27 835046. No stratigraphic succession can be identified due to structural complexity and no base or top of the unit are recognised.

The age of the Junction Formation is restricted to the Middle Cambrian (R.A. Cooper, writ. comm.) on the basis of a single fossil locality on the Sylvester Road (M27 833112, M27/f194, see Appendix 1).

The Junction Formation is composed of a well indurated sequence of interbedded sandstones and siltstones. Sandstones are predominantly grey to green cm to 0.5m bedded fine to medium sands with sparse coarse sand to granule conglomerate beds. Most beds appear massive in outcrop although some beds have normal grading. Coarser beds infrequently have channelized bases but typically bedding is regular and repetitive (e.g. figure 6.1, 6.2). Facing directions are from grading and flame structures (e.g. figure 6.3) but are not common.



Figure 6.1 Thinly bedded sandstones of Junction Formation, Deep Creek (M27 831057).



Figure 6.2 Soft sediment deformation, Junction Formation, Deep Creek (M27 827057). Undisturbed parallel laminated siltstones to either side of contorted horizon. Sequence faces to the right.



Figure 6.3 Flames and load casts, Junction Formation, Cobb River (M26 829133).



Figure 6.4 Shear plane offsetting thin bedded sandstones of the Junction Formation, Galena Creek (M26 825107).

Sandstones commonly weather to a distinctive orange/brown colour (e.g. figure 6.4) which produces a distinctive banded outcrop appearance. The colour is due to weathering of Fe/Mg rich carbonate species (ankerite-dolomite) and reflects a higher percentage of secondary carbonate in coarser grainsizes.

Siltstones are light to dark grey and are commonly parallel laminated. In slabbed section, wispy indistinct dark grey to black laminations appear to be a cross bedding feature. However in thin section these are observed to be concentrations of opaque minerals on cleavage or minor shear planes. Minor thin pale grey to cream coloured carbonate beds also occur within the sequence.

Soft sediment deformation is generally confined to thin (<30 cm) layers bounded above and below by parallel bedded sediments (e.g. fig 6.3). More pervasive disruption of bedding is attributed to brittle tectonic processes (see Chapter 8).

Petrology

Sandstones have been moderately or strongly altered by metamorphism. However original mineralogy and textures can still be recognized in a number of samples. One sample (U.C 12640) is subangular to subrounded, moderately sorted fine sand and contains approximately 40% matrix and 60% clasts. The clasts comprise approximately 75-80% quartz, 16-20% plagioclase, 4% alkali (anorthoclase), 1% siltstone and traces of chert, muscovite and sphene. The matrix is composed of secondary carbonate, sericite, chlorite, epidote and quartz. Feldspar is commonly highly altered and sausseritized and probably contributes to matrix, hence the original feldspar proportion may have been considerably higher than at present. The rock is estimated to have originally been a felds- or subfeldsarenite. Other sandstones are more altered but appear to have similar mineralogy to this sample.

Coarser grained samples (e.g. U.C 12641,12642) contain abundant chert and cherty siltstone clasts. Original modal percentage in some samples is estimated to be as high as 20% chert.

STRUCTURE

This section presents preliminary structural observations from the Junction fault bounded slice. A number of structural elements can be recognised prior to the regional elongation deformation.

- 1/ Soft sediment deformation: Mobilised argillite horizons are the most common soft sediment deformation structures. They are generally small scale features.

- 2/ Low angle faulting: Ubiquitous in thinly bedded sandstones and argillite is the development of small discrete shear planes (see Figure 6.4). Shear planes are at a moderate to low angle to bedding and have displacements ranging from cm to m + scale. Displacement varies along the length of the faults and frequently dies out into argillite layers, presumably being accomodated by bedding parallel shear. The sense of offset is invariably normal.
 More pervasive disruption of original bedding is observed in Cobb River. Sandstone beds have been totally dismembered by faulting and blocks of sandstone are now surrounded by mudstone.
 The faulting appears to have accompanied a generally extensional deformation, however the significance of the deformation is unknown. Deformation appears to have been by essentially brittle processes.

- 3/ Folding The most obvious structural feature of the Junction Unit is a set of rather irregular but consistently east plunging mesoscopic folds.

In the Flora Creek and Takaka River area the folds are predominantly upright, open to tight, gently plunging asymmetric chevron folds with axial planes dipping steeply to the south. A weakly developed axial planar cleavage is found only in the hinges of some folds. Variation in fold orientation is indicated by a wide scatter of bedding poles around and away from the best fit pi girdle (Figure 6.5). The average fold orientation is similar to orientations of fold axes measured in the field. Too few face directions were identified to be able to determine gross facing direction or macroscopic structure of the whole unit. The folds have a Z asymmetry when viewed down plunge.

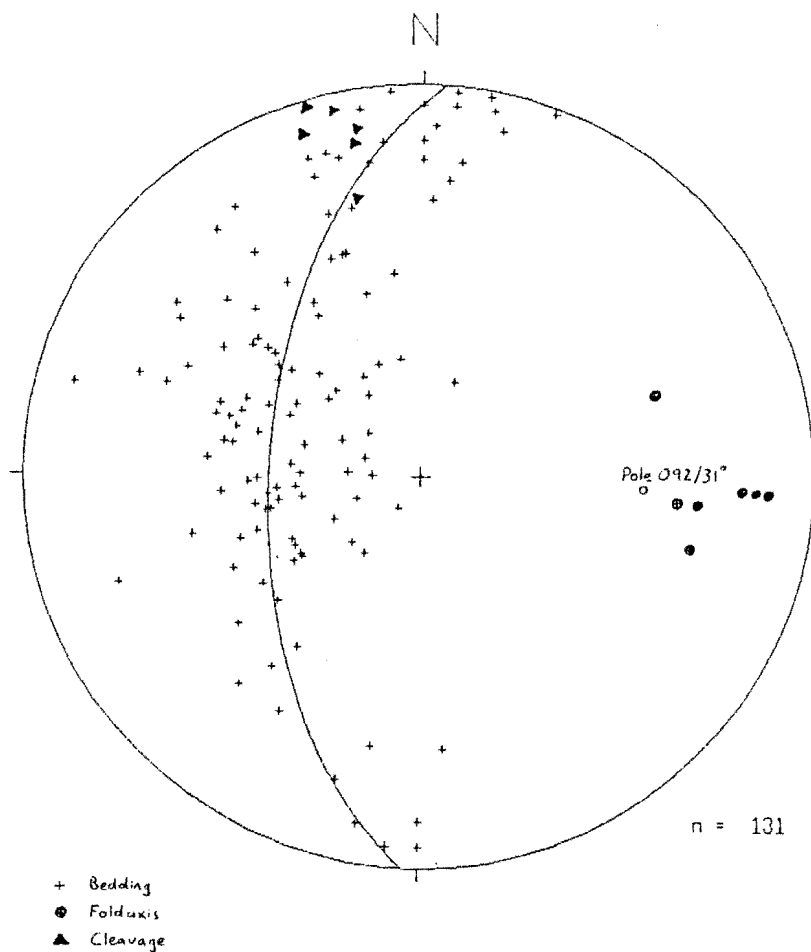


Figure 6.5 Stereographic plot of poles to bedding, Junction Formation. Balloon, Deep and Mataki Creeks, Flora and Takaka Rivers (lower hemisphere equal area projection).

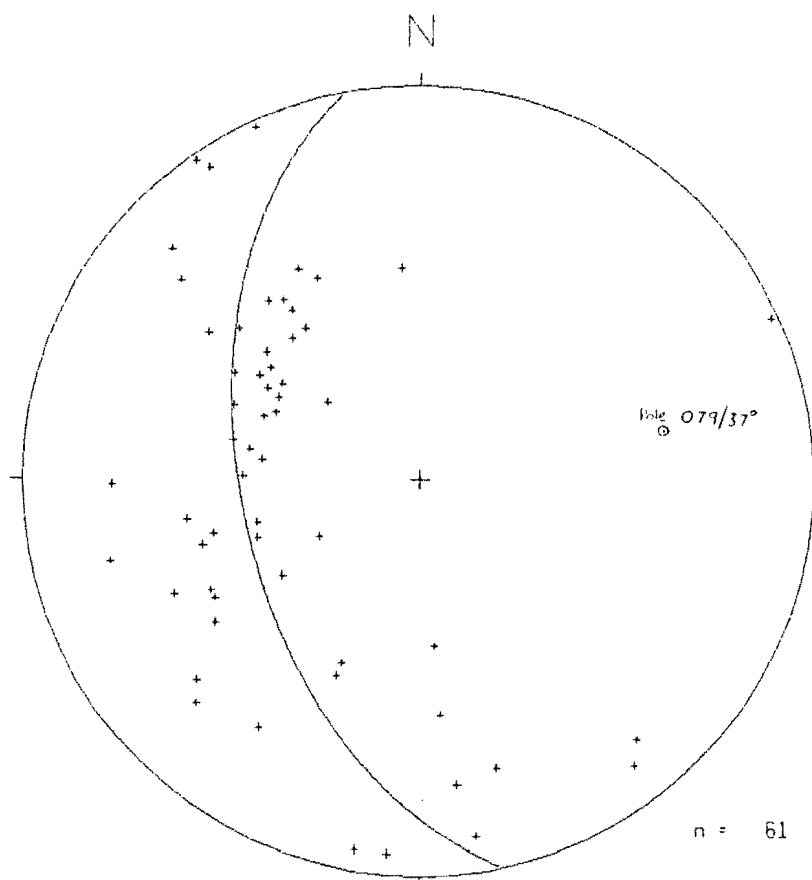


Figure 6.6 Stereographic plot of poles to bedding, Junction Formation, Diamond Lake Stream and Cobb River (lower hemisphere equal area projection).

In Cobb River and Diamond Lake Stream, the sequence is again folded around gently east plunging fold axes. A fold exposed at the junction of these two streams is gently to moderately plunging and moderately inclined. In contrast to the folds of Flora River it has an axial plane dipping 40° to the east. Poles to bedding again define a pi girdle with a pole parallel to fold axes observed in the field (figure 6.6).

In Diamond Lake Stream and Cobb River minor isoclinal fold hinges were observed in float and outcrop. The size or importance of these folds could not be determined in the field. However on a macroscopic scale disparate face directions imply that an early phase of tight to isoclinal folding may be present. In Diamond Lake the sequence appears to be dominantly upright, while in Cobb River the sequence dips S.E and is dominantly overturned. Further work is necessary to help elucidate structure within the Junction Formation.

The Junction Fault Bounded slice is overprinted by a strong linear (and planar) fabric which will be described in Chapter 8.

CHAPTER SEVEN

PETROLOGY AND GEOCHEMISTRY OF IGNEOUS ROCKS

Two geographically distinct groups of extrusive rocks were identified during field mapping; andesites occurring in the Balloon Slice, and basalts within the Mataki Slice (see Map 1, back pocket). A suite of medium grained basic intrusives occurs in all of the tectonic slices. Assorted other heavily altered igneous rocks are of unknown affinity.

BALLOON FORMATION ANDESITES

Andesites are found intercalated within diamictite and olistostromal conglomerate of the Balloon Unit, from the Lockett Range in the north, to Balloon Creek in the south. They occur as elongate tabular pods up to 300m long and up to 60(?)m thick and are concordant with the gross stratigraphy. They are identified as andesites by both petrographic classification (Streckeisen) and silica content.

The andesites are interpreted as intrusive sheets as they occur over a broad stratigraphic range. They are generally pale green coloured with distinctive pale remnant feldspar phenocrysts and, in fresh unaltered outcrops, abundant hornblende. Field relationships are described in Chapter 4.

Texturally, the rocks are hypocrySTALLINE with 0.5 - 5 mm phenocrysts of hornblende and plagioclase set in a fine grained, semi-opaque matrix. Phenocrysts comprise up to 40% of the rock mass and are randomly orientated. Plagioclase is albitised (An 6%) and partially or wholly sausseritised to a quartz, sericite, chlorite assemblage. Hornblende has distinctive green to yellow-brown pleochroic colour and occurs as euhedral crystals. It is commonly totally altered to an assemblage of leucoxene, chlorite, sericite, albite, quartz, carbonate and epidote. Quartz is also found as sparse phenocrysts. Groundmass material comprises quartz + albite + carbonate + sericite + chlorite + opaques ± zeolites and exhibits an apparent devitrification texture.

A xenolith from sample 20316 has a packed porphyritic texture with euhedral phenocrysts of hornblende, plagioclase in a fine grained matrix. Irregularly cracked patches of serpentine with rims of Fe oxide are interpreted to be pseudomorphs after olivine. Petrologically the xenolith is an olivine hornblende andesite and is probably a cognate hypabyssal equivalent of the andesite lavas.

Major Element Geochemistry

Analytical data for andesite samples are presented in Table 2 (1 - 17). The samples vary in degree of alteration. Bulk chemistry does not appear to be significantly affected by degree of alteration as fresh and altered samples (e.g. 20315 cf 20306) have similar analyses.

The andesites have low concentrations of Cr and Ni and high concentrations of the mobile elements Rb, Ba and Sr. Significant carbonate metasomatism is indicated by a high proportion of secondary Fe/Mg carbonate (up to 10%) and is probably responsible for enrichment of Rb, Ba and Sr. Major and other trace element proportions and concentrations do not appear to have been significantly affected.

The andesites plot firmly in the calc alkaline fields on the Alkalis-Silica diagram (figure 7.1) and the AFM plot (figure 7.2). According to Ewart's subdivision of the K₂O Silica diagram (figure 7.3) most samples are classified as high silica andesites, with one sample (20059) a dacite and one (20320) a rhyolite. These last two samples have high LOI and are heavily altered to carbonate.

Trace Element Geochemistry

The trace element characteristics of modern day volcanics reflect the geotectonic environment in which they form. Certain trace elements remain immobile under alteration and metamorphism up to greenschist (and even amphibolite) facies and thus provide a potentially useful tool for determining tectonic environment of ancient volcanics.

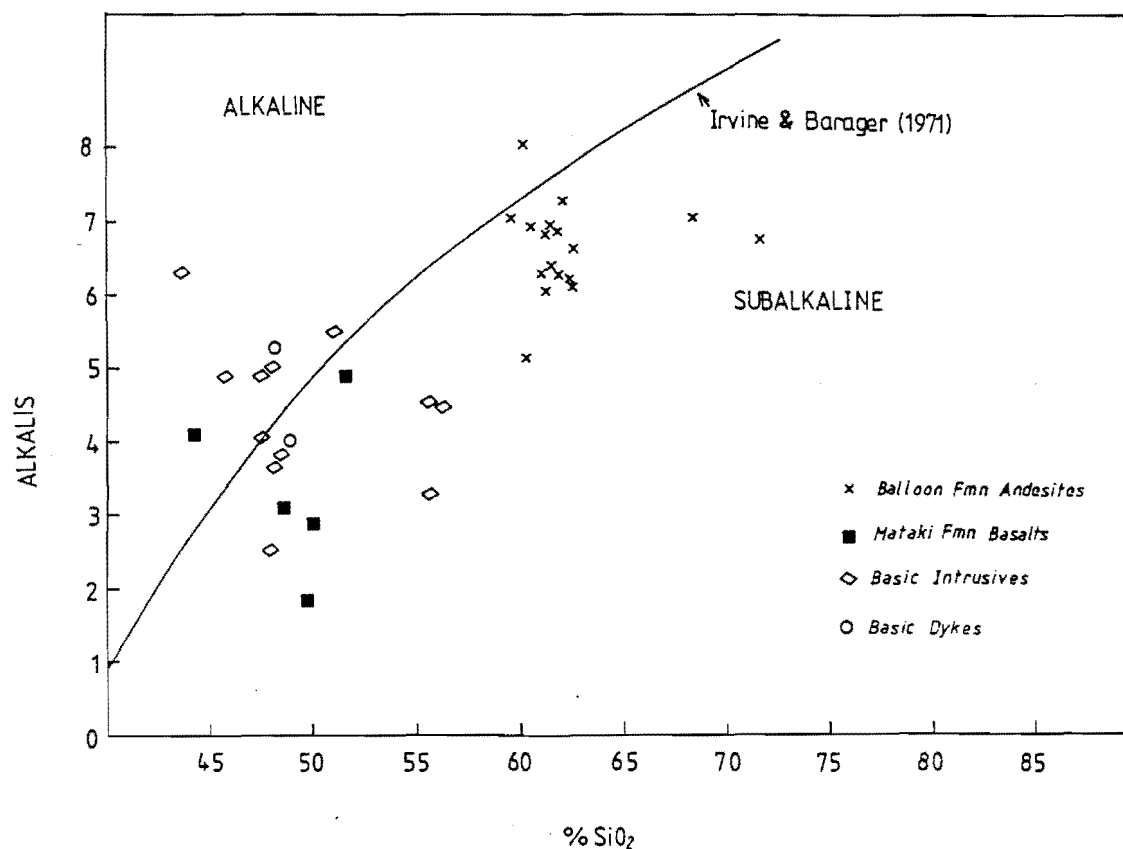


Figure 7.1 Alkalis Silica diagram.

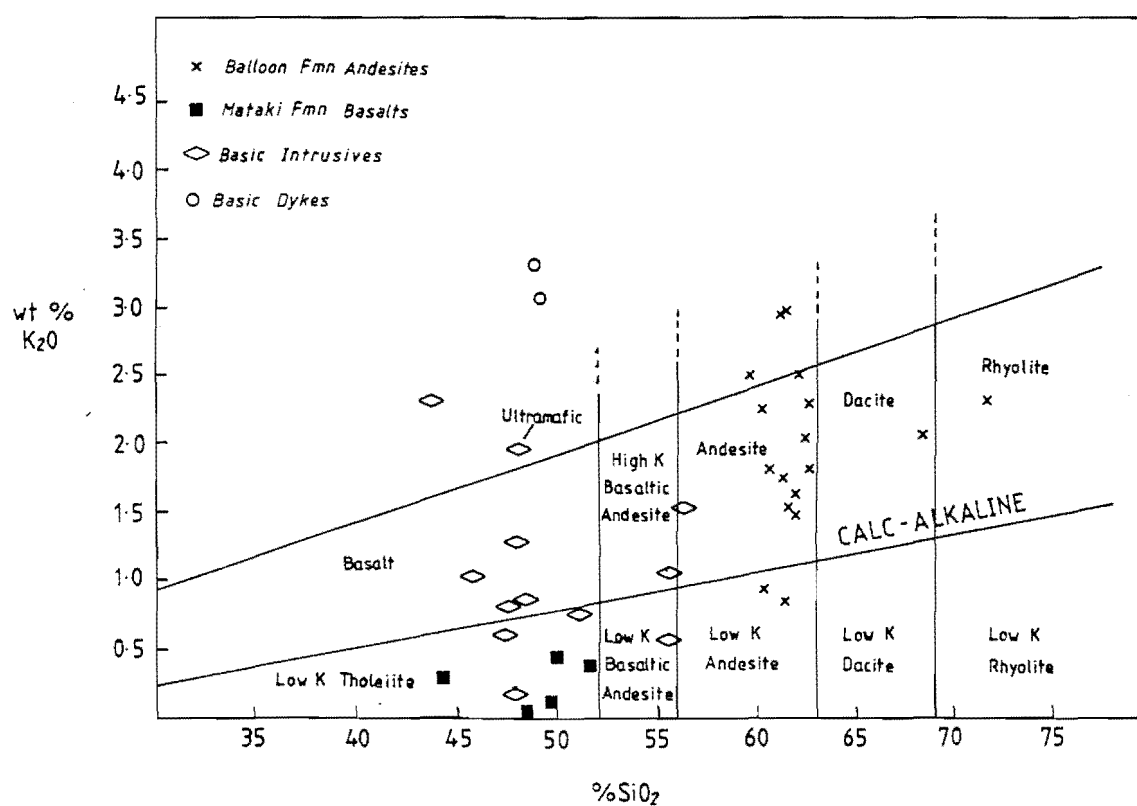


Figure 7.3 K₂O-Silica diagram. Fields of Ewart (1982).

The Cr-Y diagram has proved to be a useful discriminator (Pearce 1982) for distinguishing volcanic arc rocks from within plate basalts and Mid Oceanic Ridge Basalts (MORB's). On a Cr-Y plot (figure 7.4) the andesites all fall well within the volcanic arc compositional field.

On the Ti-Zr-Y ternary plot (figure 7.5) the andesites plot on the high Zr edge of the field of calc alkaline lavas (Pearce and Cann 1973). This diagram is strictly for basaltic rocks only and the high Zr and low Ti of the Balloon andesites reflects their more evolved compositions. On the Ti-Zr diagram (figure 7.6) all samples plot within the volcanic arc field of Pearce (1982).

These andesites have similar compositions to many modern calc alkaline arc lavas. Comparative data from the Tongariro Volcanic Centre, New Zealand (Cole 1978, 1979, 1982, Graham and Hackett 1987), Mexico (Robin 1982) and the Andes (Ewart 1982) are plotted on Figure 7.6a.

Thus both major and trace element characteristics point towards a clear calc-alkaline signature and a convergent margin origin for the andesites. Major element abundances do not appear to have been significantly affected by metamorphism or alteration.

MATAKI FORMATION BASALTS

Basalts occur in a thin belt on the eastern side of the Mataki Block. In one outcrop, unequivocal pillow structures were observed (figure 5.1) and were tentatively identified in other outcrops. The field relationships of this unit are not clear. Sediments associated with the basalts are clastic and include laminated siltstones and mass flow conglomerates/breccias containing basalt clasts petrographically similar to the flow rocks.

Basaltic composition is indicated by high concentrations of Fe, TiO₂, Zr and V and low concentrations of Mg, K and Cr. The rocks have evidently suffered Na metasomatism as plagioclase now has compositions of albite to oligoclase (An 0 - 25%). Petrologically the basalts comprise an assemblage of plagioclase, chlorite and opaques with an equigranular,

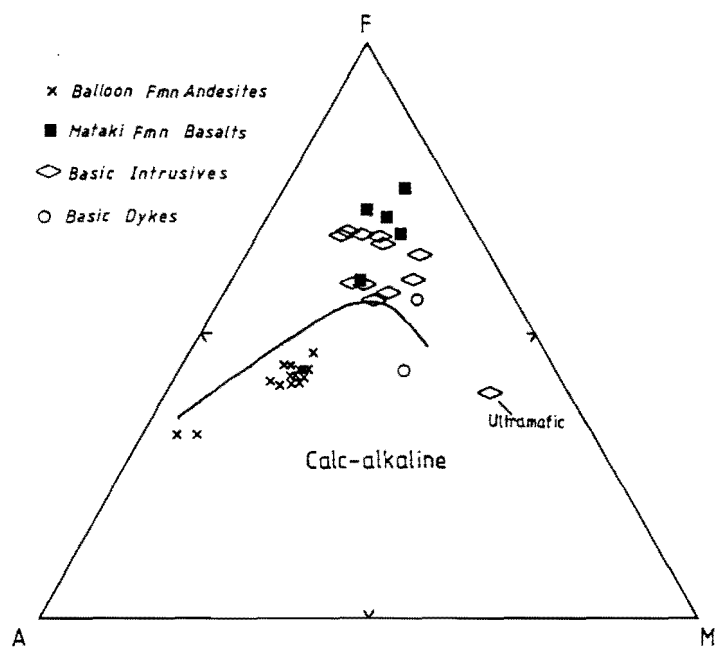


Figure 7.2 AFM diagram. Calc-alkaline/Tholeiitic dividing line of Irvine and Barager (1971).

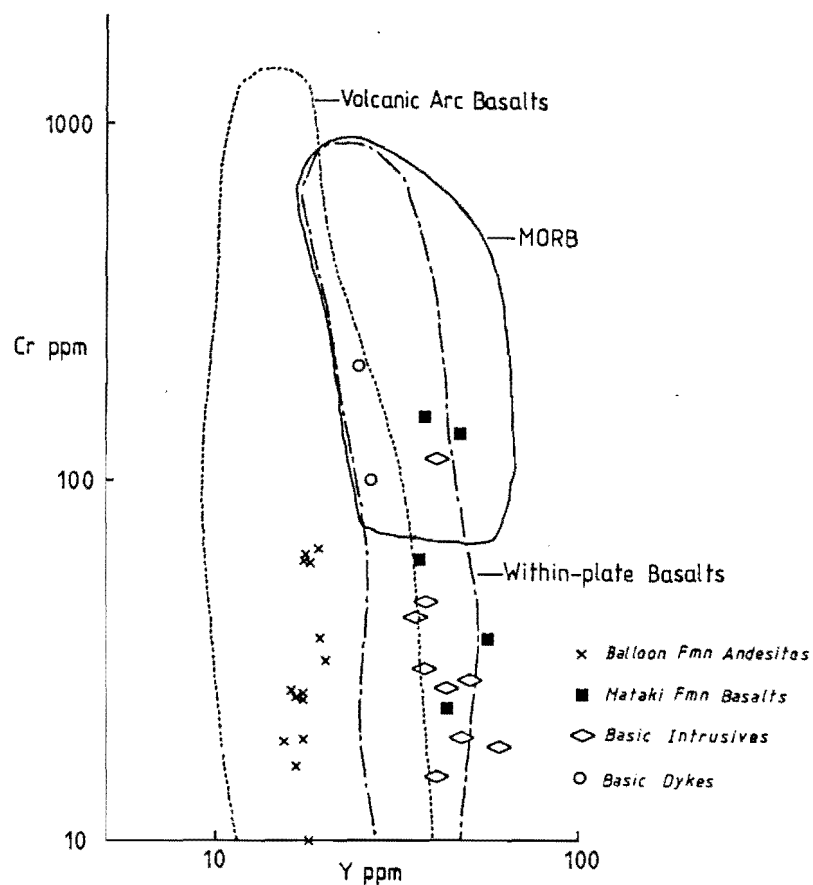


Figure 7.4 Cr-Y discrimination diagram. Compositional fields of Pearce (1982).

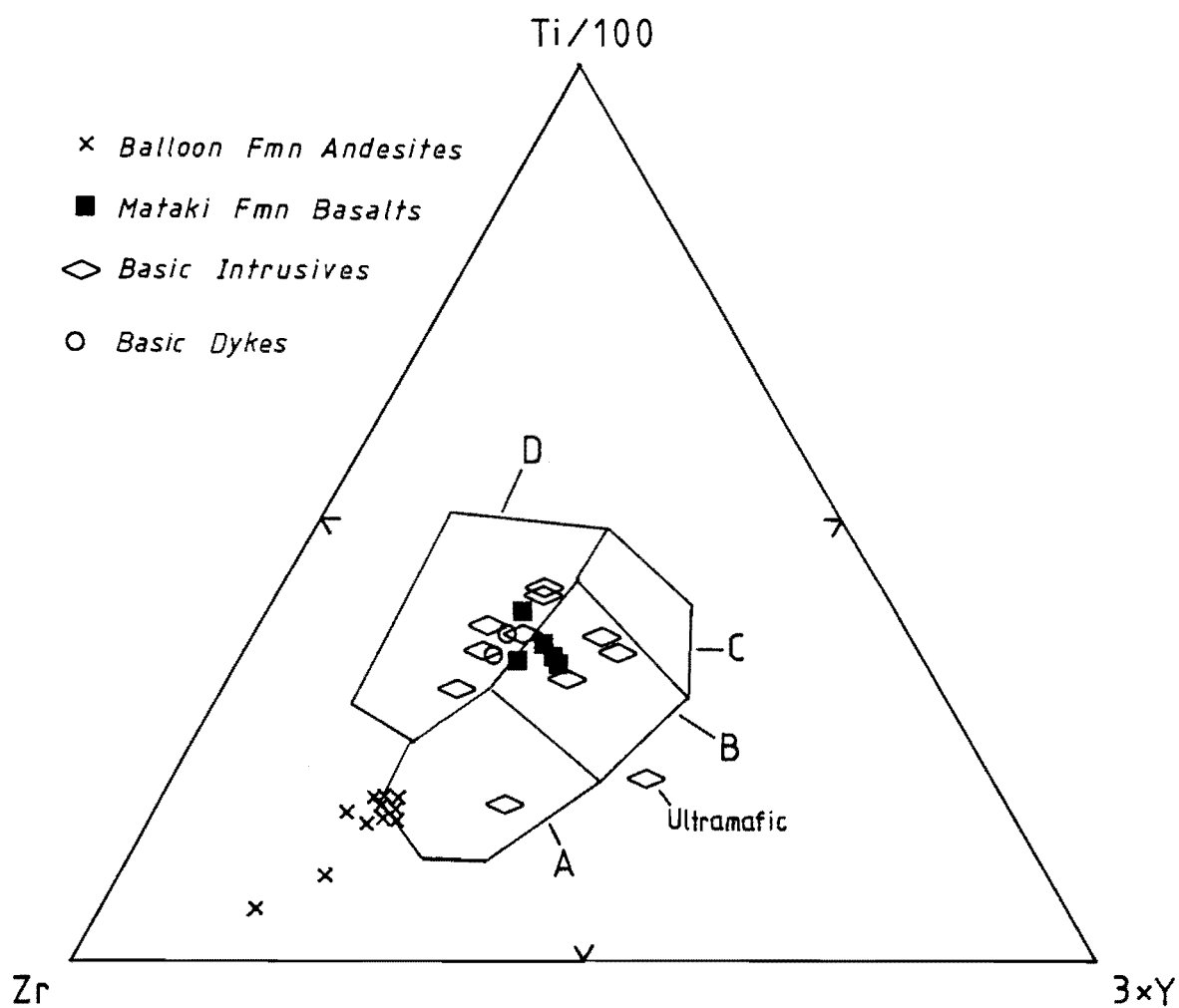


Figure 7.5 Ti-Sr-Y discrimination diagram. Compositional fields of Pearce and Cann (1973).

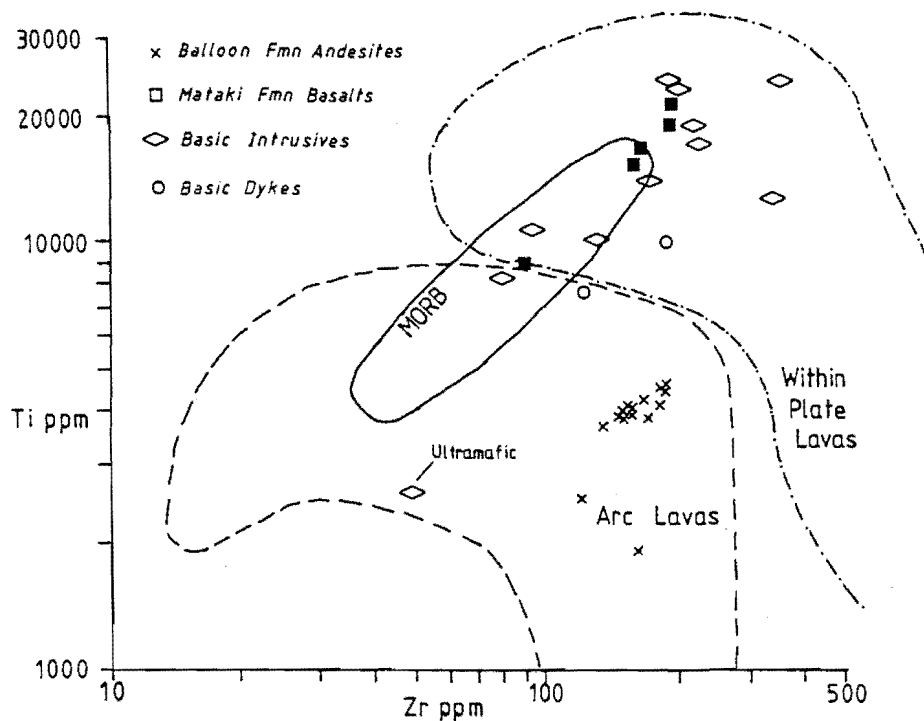


Figure 7.6 Ti-Zr discrimination diagram. Compositional fields of Pearce (1982).

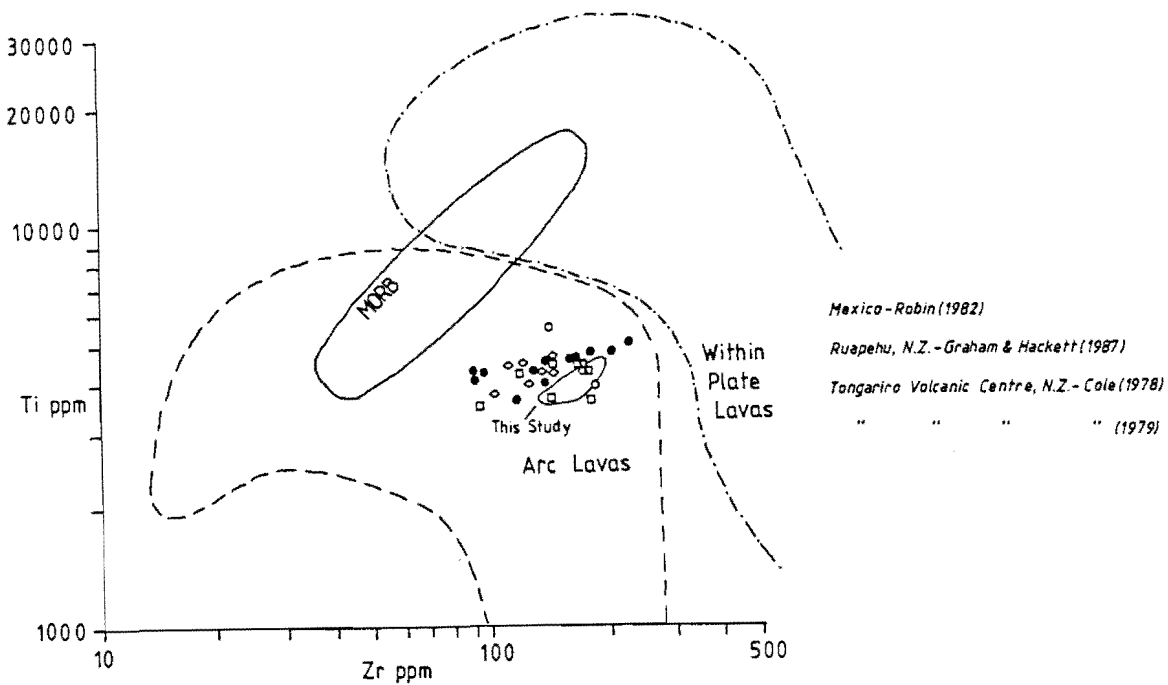


Figure 7.6a Ti-Zr plot of comparative data of andesites from active calc-alkaline arcs.

microcrystalline quench texture. Both oligoclase laths and groundmass are largely replaced by carbonate. Round patches infilled with carbonate are interpreted as amygdales. Little else could be determined in thin section owing to the fine grained and altered nature of these rocks.

Analytical data for basalts are presented in Table 2 (17-21). The samples have high LOI (5-10%) which reflects a high degree of carbonate alteration. Basalts plot in the field of iron enrichment on the AFM ternary (figure 7.2) and are classified as low K tholeiites on the K_2O - silica diagram (figure 7.3). Two of the samples contain normative olivine, and one (20066) contains normative nepheline.

A specific tectonic environment for the basalts is not unequivocally indicated by the trace element data. Analyses show a fairly wide range in composition which may be genuine heterogeneity or alteration due to carbonate metasomatism or shearing.

On all the discrimination diagrams mentioned in the previous section basalts fall in the field of within plate basalts but also scatter into the fields of MORB or ocean floor basalts. Ti values for these basalts are high, up to 3.5% TiO_2 , which are typical values for ocean floor or within plate basalts and much higher than for volcanic arc rocks (figure 7.6). On the Cr-Y plot also (figure 7.4) the basalts fall in the within plate field, with two samples falling in the MORB field. The basalts are clearly not of volcanic arc origin.

The Ti-Zr-Y ternary is a good discriminator of modern within plate basalts from MORB or ocean floor basalts. These samples plot roughly on the dividing line between the two fields (figure 7.5).

Hence trace element discrimination diagrams do not conclusively distinguish a unique geotectonic environment for these basalts. However when integrated with the field relations of the basalts, it is inferred that they are probably of seamount or oceanic island origin. Most importantly sediments associated with the volcanics are clastic and not of deep sea origin (i.e. pelagic ooze, chert, metal rich suspensions).

	1	2	3	4	5	6	7	8	9	10	11	12	13	14
FIELD NO	239	252	253	228	313	314	317	319	320	340	363	501	510	512
GEOCHEM NO	20059	20060	20061	20069	20301	20302	20303	20304	20305	20306	20309	20315	20316	20317
U of C NO	12583	12584	12585	12593	12599	12600	12601	12602	12603	12604	12607	12614	12615	12616
SiO2	65.69	61.59	60.11	61.14	58.77	59.84	61.13	60.73	61.15	57.82	59.06	57.50	59.20	59.68
TiO2	.31	.63	.65	.62	.74	.58	.61	.58	.59	.74	.60	.64	.69	.67
AL2O3	15.90	16.71	16.45	16.46	16.61	16.67	16.68	17.13	16.64	16.19	16.49	15.21	15.34	15.62
FeO	3.27	6.06	6.14	5.93	6.74	6.11	5.85	5.97	5.73	6.70	6.07	6.43	6.37	6.28
MNO	.11	.13	.12	.12	.12	.14	.12	.11	.11	.11	.17	.12	.12	.14
MGO	.95	3.05	2.94	2.99	3.06	2.73	2.68	2.41	2.66	3.04	2.40	3.27	3.20	3.31
CaO	2.61	3.94	5.23	3.52	3.09	4.90	4.25	3.34	4.33	3.58	4.61	3.66	5.41	4.20
Na2O	4.97	5.58	4.37	4.43	5.90	4.25	4.26	4.86	4.38	5.06	4.86	5.79	3.42	4.05
K2O	1.93	1.41	1.67	2.16	2.13	.92	1.94	2.40	1.71	1.70	1.42	.78	2.77	2.80
P2O5	.15	.25	.26	.24	.39	2.96	.22	.26	.22	.39	.26	.23	.24	.22
LOI	3.68	1.00	1.94	2.71	3.30	.24	2.24	1.55	1.53	4.06	4.38	5.91	2.66	2.47
TOTAL	99.57	100.35	99.88	100.32	100.85	99.34	99.98	99.34	99.05	99.39	100.26	99.54	99.42	99.44
Ap	.34	.55	.58	.54	.87	6.56	.49	.58	.49	.89	.59	.54	.54	.50
Il	.61	1.20	1.26	1.20	1.44	1.11	1.18	1.12	1.15	1.47	1.19	1.29	1.35	1.31
Mt	1.05	1.88	1.93	1.87	2.13	1.90	1.84	1.88	1.81	2.16	1.95	2.11	2.03	1.99
Or	11.85	8.34	10.02	13.01	12.83	5.47	11.67	14.42	10.31	10.47	8.70	4.89	16.82	16.97
Ab	43.72	47.28	37.56	38.21	50.89	36.21	36.69	41.84	37.82	44.66	42.66	52.03	29.74	35.15
An	12.44	16.41	20.66	16.20	12.79	5.00	20.00	15.13	20.45	15.87	19.70	14.03	18.84	16.59
Di	0.00	1.27	3.29	0.00	.20	0.00	0.00	0.00	0.00	0.00	1.89	3.03	5.91	2.74
Hy	7.00	14.85	13.85	15.41	16.47	14.93	14.50	14.02	14.33	16.82	13.44	16.01	13.67	15.43
Ol	0.00	0.00	0.00	0.00	0.00	0.00	0.00	0.00	0.00	0.00	0.00	0.00	0.00	0.00
Ne	0.00	0.00	0.00	0.00	0.00	0.00	0.00	0.00	0.00	0.00	0.00	0.00	0.00	0.00
C	1.30	0.00	0.00	1.03	0.00	6.92	.38	1.11	.24	.47	0.00	0.00	0.00	0.00
Q	21.67	8.22	10.86	12.54	2.38	21.90	13.24	9.89	13.41	7.18	9.88	6.06	11.10	9.33
Total	100.00	100.00	100.00	100.00	100.00	100.00	100.00	100.00	100.00	100.00	100.00	100.00	100.00	100.00
A	60.08	41.67	38.22	40.75	43.22	35.19	40.31	44.53	40.28	39.20	40.71	38.68	37.59	39.97
M	8.27	18.18	18.60	18.49	16.47	18.58	17.42	14.78	17.60	17.63	15.56	19.25	19.43	19.31
F	31.64	40.15	43.18	40.75	40.31	46.22	42.27	40.69	42.12	43.17	43.73	42.07	42.98	40.72
Q	55.19	51.51	52.25	52.78	49.69	56.29	52.94	52.04	52.99	51.11	51.97	50.81	52.30	51.79
M	4.89	11.06	11.66	10.68	11.95	11.03	10.13	9.94	9.96	12.04	10.70	12.91	13.09	12.31
L	39.92	37.42	36.09	36.54	38.36	32.68	36.93	38.02	37.05	36.85	37.34	36.28	34.61	35.90
GA	16	17	17	17	16	17	17	15	15	18	17	16	17	16
PB	6	7	7	7	14	8	6	6	5	7	9	8	8	17
RB	58	25	41	62	45	34	64	69	60	59	45	30	108	94
SR	682	991	1048	862	556	559	881	1012	695	572	342	489	965	726
TH	10	8	5	7	13	7	8	9	7	11	8	8	6	7
Y	14	16	17	17	22	15	16	17	15	20	17	17	17	16
BA	1274	855	744	960	845	375	777	1130	653	655	506	363	802	1285
CE	78	60	65	62	100	61	58	66	57	94	71	45	65	67
CR	6	23	23	23	31	8	18	10	25	36	14	60	59	55
LA	43	31	32	29	50	30	22	33	26	49	40	31	26	29
NB	20	14	13	12	19	17	17	20	16	17	18	16	16	15
ND	31	27	27	25	43	31	28	31	30	44	28	30	28	28
NI	5	12	12	12	18	11	11	6	14	16	9	16	17	17
V	29	124	124	128	132	113	115	98	113	135	108	133	148	131
ZN	49	61	49	61	73	62	65	57	191	57	73	68	65	107
ZR	144	126	129	136	170	117	135	150	128	168	131	133	147	161

TABLE 2: Major and Trace element XRF analyses of igneous rocks.

	15	16	17	18	19	20	21	22	23	24	25	26	27	28
FIELD NO	523	363	426	260	230	381	382	402	256	258	169	225	391	387
GEOCHEM NO	20320	20470	20474	20066	20070	20311	20312	20472	20062	20064	20067	20068	20313	20471
U of C NO	12618	12619	12623	12590	12594	12609	12610	12621	12586	12588	12591	12592	12611	12620
S102	69.11	59.27	58.34	39.72	44.10	48.15	44.27	47.48	46.90	53.23	43.95	46.86	44.32	51.91
T102	.15	.61	.72	3.04	2.73	2.09	1.27	2.30	3.70	1.91	3.76	3.83	1.71	2.05
AL2O3	14.62	16.45	16.35	12.91	12.91	16.20	11.74	14.96	15.27	13.78	14.70	13.49	14.87	13.45
tFE2O3	2.97	6.06	6.66	16.43	14.81	11.47	16.18	14.55	16.29	13.19	16.76	16.16	12.73	12.58
MNO	.13	.11	.14	.21	.18		.19	.20	.22	.24	.37	.23	.22	.15
M60	.57	2.46	3.39	3.64	4.18	4.11	4.33	5.22	3.53	2.73	4.43	5.32	5.78	4.02
CAO	2.19	4.31	4.85	9.69	8.59	6.10	9.25	7.18	6.37	5.40	6.06	8.23	10.34	5.39
NA2O	4.44	4.58	4.69	3.53	2.83	4.31	1.60	2.39	3.80	3.46	3.83	3.31	2.20	2.62
K2O	2.19	1.52	2.38	.25	.03	.35	.07	.40	1.22	1.00	.97	.77	.15	.50
P2O5	.08	.26	.36	.30	.41	.30	.13	.29	.38	.70	1.03	.30	.18	.71
LOI	4.03	4.23	1.65	9.29	8.83	5.91	10.37	4.46	1.67	4.24	3.49	1.90	6.93	6.76
TOTAL	100.48	99.86	99.53	99.01	99.60	99.16	99.40	99.43	99.35	99.88	99.35	100.40	99.43	100.14
Ap	.18	.59	.80	.72	.98	.70	.32	.66	.84	1.59	2.33	.66	.42	1.65
Il	.30	1.21	1.39	6.35	5.65	4.22	2.67	4.55	7.11	3.76	7.36	7.30	3.48	4.13
Mt	.95	1.95	2.09	5.58	4.98	3.77	5.54	4.68	5.09	4.22	5.34	5.01	4.21	4.12
Dr	13.37	9.34	14.29	1.62	.19	2.19	.46	2.46	7.27	6.11	5.89	4.55	.95	3.13
Ab	38.84	40.31	40.32	19.05	26.02	38.70	14.97	21.02	32.45	30.26	33.33	28.04	19.89	23.48
An	10.69	20.47	16.80	20.46	24.38	25.28	27.25	30.05	21.20	19.76	20.63	19.70	32.33	23.41
Di	0.00	0.00	4.35	25.55	15.99	3.97	19.08	4.18	6.93	2.73	2.84	16.03	17.61	0.00
Hy	5.85	14.54	15.14	0.00	21.73	16.04	25.90	29.47	7.18	22.34	2.96	7.96	14.44	26.36
Ol	0.00	0.00	0.00	13.24	0.00	5.12	0.00	0.00	11.92	0.00	19.32	10.75	6.67	0.00
Ne	0.00	0.00	0.00	7.43	0.00	0.00	0.00	0.00	0.00	0.00	0.00	0.00	0.00	0.00
C	1.20	.06	0.00	0.00	0.00	0.00	0.00	0.00	0.00	0.00	0.00	0.00	0.00	.53
Q	28.62	11.52	4.81	0.00	.09	0.00	3.82	2.94	0.00	9.23	0.00	0.00	0.00	13.19
Total	100.00	100.00	100.00	100.00	100.00	100.00	100.00	100.00	100.00	100.00	100.00	100.00	100.00	100.00
A	63.14	39.88	39.58	14.72	12.17	21.66	6.96	11.54	18.83	20.41	17.23	14.91	10.55	14.77
M	5.43	16.08	18.98	14.18	17.79	19.10	18.06	21.59	13.24	12.50	15.90	19.45	25.95	19.03
F	31.43	44.03	41.44	71.10	70.04	59.24	74.98	66.87	67.92	67.09	66.86	65.64	63.50	66.19
Q	56.79	52.42	50.43	45.57	46.66	47.87	48.64	48.04	46.98	50.49	47.43	46.87	48.04	51.66
M	3.85	10.30	13.25	31.33	29.26	21.12	30.50	25.99	25.97	20.70	26.64	29.83	27.29	21.83
L	39.36	37.28	36.32	23.11	24.08	31.01	20.86	25.97	27.04	28.81	25.93	23.30	24.68	26.51
GA	17	16	19	23	22	18	16	21	26	24	22	23	19	16
PB	10	8	16	6	6	4	4	8	6	6	9	10	4	10
RB	79	47	62	7	1	7	2	8	31	23	21	18	4	21
SR	164	331	724	213	202	211	142	251	555	462	546	373	388	363
TH	11	9	12	2	3	4	1	3	1	3	1	1	3	3
Y	8	18	21	43	54	37	23	46	48	77	60	47	35	39
BA	349	526	782	90	<20	116	<20	111	360	546	1879	246	<20	1026
CE	59	53	86	43	34	28	8	32	37	76	76	41	10	53
CR	1	13	62	13	26	130	48	121	8	5	17	18	30	76
LA	38	34	48	11	19	14	<3	11	14	27	33	12	<3	20
NB	20	19	17	23	20	20	14	17	20	34	21	19	9	14
ND	30	29	37	16	12	19	7	20	16	36	37	22	12	21
NT	2	8	25	32	21	56	36	38	13	5	35	36	32	23
V	9	105	124	441	411	321	287	327	447	47	257	593	388	191
ZN	40	72	83	156	130	112	108	127	143	150	178	116	97	84
ZR	122	134	169	189	189	161	87	159	185	335	368	181	93	na

TABLE 2: Continued.

	29	30	31	32	33	34	35	36	37	38
FIELD NO	234	235	261	458	516	522	359	409	257	343
GEOCHEM NO	20071	20072	20073	20314	20318	20319	20308	20473	20063	20307
U of C NO	12595	12596	12597	12612	12616	12617	12606	12622	12587	12605
SIO2	52.52	38.96	46.70	45.64	45.33	47.18	42.40	43.41	75.84	42.61
TIO2	1.70	2.90	2.29	2.82	.45	1.56	1.31	1.65	.10	1.02
AL2O3	14.91	16.88	14.65	15.95	14.36	13.44	15.73	15.64	12.65	13.27
Fe2O3	10.11	12.79	12.56	13.48	10.70	14.99	8.97	11.02	1.20	11.51
MNO	.09	.12	.18	.20	.21	.23	.13	.15	.08	.23
MgO	4.68	4.54	4.73	6.41	14.39	7.61	6.64	6.64	.75	7.62
CaO	4.73	6.66	4.91	6.11	5.17	8.35	7.72	6.33	1.15	3.01
Na2O	2.89	3.74	4.46	4.26	1.71	3.01	1.78	1.04	1.17	3.14
K2O	1.38	2.01	.67	.55	1.82	.79	2.81	2.54	3.19	.46
P2O5	.20	.42	.36	.62	.13	.13	.23	.35	.04	.08
LOI	6.81	11.05	8.70	3.08	4.87	2.44	12.46	10.69	3.40	16.68
TOTAL	100.02	100.07	100.21	99.12	99.14	99.73	100.18	99.46	99.57	99.63
Ap	.47	1.03	.86	1.40	.30	.29	.57	.86	.09	.21
Il	3.44	6.13	4.71	5.53	.90	3.01	2.82	3.50	.20	2.31
Mt	3.33	4.39	4.20	4.30	3.48	4.71	3.14	3.80	.39	4.25
Or	8.67	13.18	4.28	3.34	11.31	4.73	18.77	16.73	19.56	3.24
Ab	25.99	12.53	40.77	36.21	15.22	25.84	14.72	9.81	10.28	31.66
An	23.56	25.90	19.42	23.45	26.08	21.13	30.11	32.47	5.65	17.17
Di	0.00	6.43	3.63	2.96	0.00	16.57	9.37	0.00	0.00	0.00
Hy	24.93	0.00	9.53	0.00	13.50	4.59	0.00	29.51	3.70	32.13
Ol	0.00	18.16	12.61	22.32	28.70	19.12	19.24	2.74	0.00	6.26
Ne	0.00	12.24	0.00	.49	0.00	0.00	1.25	0.00	0.00	0.00
C	.58	0.00	0.00	0.00	.51	0.00	0.00	.57	5.48	2.77
Q	9.04	0.00	0.00	0.00	0.00	0.00	0.00	0.00	54.65	0.00
Total	100.00	100.00	100.00	100.00	100.00	100.00	100.00	100.00	100.00	100.00
A	21.15	23.47	21.54	18.36	11.84	13.54	21.65	15.93	67.66	14.99
M	23.19	18.53	19.86	24.47	48.27	27.11	31.32	29.56	11.64	31.74
F	55.66	58.01	58.60	57.18	39.89	59.35	47.02	54.51	20.70	53.27
Q	50.76	45.36	48.09	48.40	50.51	48.88	49.19	47.95	62.31	48.51
M	19.35	24.42	22.93	24.28	27.16	28.61	22.02	23.75	2.12	26.46
L	29.89	30.22	28.98	27.32	22.33	22.51	28.79	28.31	35.57	25.03
GA	19	25	23	22	12	18	15	18	12	12
PB	6	4	5	5	4	5	3	3	8	4
RB	38	53	21	14	68	13	115	108	111	14
SR	117	343	358	563	128	195	332	363	122	341
TH	1	2	1	1	3	1	1	1	4	1
Y	26	38	48	40	22	33	24	26	16	23
BA	736	184	138	384	295	173	694	325	2216	642
CE	14	46	41	52	13	10	21	29	42	6
CR	42	45	26	129	1481	41	201	100	5	205
LA	8	19	16	23	3	43	9	13	24	43
NB	12	27	18	11	7	8	6	7	12	7
ND	10	32	21	45	11	8	23	16	14	6
NI	25	52	34	61	426	68	70	69	5	105
V	346	347	287	285	240	409	197	213	5	375
ZN	86	131	134	119	74	116	77	102	53	83
ZR	113	209	153	215	48	81	110	132	75	55

TABLE 2: Continued.

INTRUSIVE ROCKS

A total of 18 intrusive rocks was analysed, most of which were intensely altered and carbonate replaced. Compositionally these rocks are diverse with no consistent geochemical signatures and unfortunately suggest no unequivocal tectonic environments.

Basic Intrusives

A suite of dark green, massive, discordant basic intrusive sheets is found intruding the Balloon, Matakia and Junction fault bounded blocks. The sheets are superficially similar in all blocks and may represent a single intrusive phase. They vary widely in alteration, some being up to 50% carbonate replaced and original mineralogy is often difficult to determine.

The sheets are medium grained and have a holocrystalline, subophitic texture. In fresh samples they comprise approximately 50-60 modal % plagioclase (An 0-5%), 15-30% calcic pyroxene (augite), 8-12% ilmenite/leucoxene. From bulk chemistry most are of basaltic composition, although some have more intermediate compositions. According to Streckeisen's petrographic classification system most samples are diorites. However, Na metasomatism is evident and original plagioclase composition may have been greater than An 50%, in which case the rocks were originally gabbros. In weathered sample up to 30-40% of a green alteration assemblage of chlorite + epidote + apatite + albite + quartz + sphene occurs after pyroxene.

The samples from all blocks have experienced metamorphism and contain a greenschist facies assemblage of epidote + chlorite + quartz + albite + sericite + sphene \pm tremolite \pm clinozoisite. No prehnite, pumpellyite or stilpnomelane, reported by Powell (1985) from this area, was identified.

The timing of intrusion is poorly constrained. Assuming one intrusive phase, emplacement must postdate juxtaposition of the three tectonic blocks. One sheet near Little Lake Sylvester (M26 794105) clearly cuts across foliation and is therefore intruded post imposition

of this fabric. Sheets do not show evidence for development of a penetrative fabric but in all belts have lower greenschist facies metamorphic assemblages. Greenschist facies metamorphism is inferred by Powell (1986) to be synkinematic with the regional extensional deformation. A localised passive greenschist to amphibolite facies metamorphism is also recorded by Powell (1986) north of the Anatoki River. This metamorphism affects the Permian strata at Parapara Peak and is thus a post Permian event. It has not been recorded as far south as Cobb. It is possible (?probable) that the metamorphic history is more complex than presently recognised.

Intrusive bodies (dykes) of similar mineralogy, texture and alteration have been described from other areas within the Eastern and Central Belts by Hickey (1985), Grindley (1980) and Coleman (1977,1981). Grindley (1980) places the intrusion of these dykes (attributed to a single event) as post Devonian, as they postdate cleavage formation in the Devonian Baton Formation. Coleman (1981) correlates the dykes with the Riwaka Complex and assigns them a Late Devonian to Early Carboniferous age.

Geochemistry

Analytical data for these intrusives is presented in Table 7.1, 23-33. The samples are heavily altered to carbonate and have LOI's of up to 10%. Na metasomatism is apparent from high Na concentrations and albitization of plagioclase. That major element concentrations have been altered is evident in the wide scatter of data. In general the sheets are high in Ti and Mg and have tholeiitic compositions, plotting in the Fe enrichment portion of the AFM diagram (figure 7.1). On the K_2O -silica diagram (figure 7.2) samples plot dominantly in the low K tholeiite field with more intermediate samples plotting as basaltic andesites. Samples scatter across the alkaline subalkaline boundary of the Alkali-Silica diagram (figure 7.3). Variation is probably due to Na metasomatism.

No unequivocal tectonic environment is indicated by trace element abundances but in general intrusives fall in the within plate basalt compositional fields. This can be clearly seen on the Cr-Y and Ti-Zr

plots (figures 7.4 and 7.6). On the Ti-Zr-Y ternary (figure 7.5) a number of the samples scatter in to the volcanic arc or MORB fields.

Other Intrusive Rocks

Minor thin (20-30 cm), very fine grained dykes with chilled margins are observed intruding all three of the major tectonic slices. Dyke intrusion postdates fabric development in all three belts. The dykes are composed of small, recrystallised, remnant feldspar laths crowded with abundant secondary chlorite, carbonate, albite, sericite and minor hematite. Larger (1mm) patches of coarser grained carbonate, chlorite and hematite probably represent altered phenocrysts. Two samples (20308 and 20473) were analysed. (Table 7.1. 35,36). The dykes have typical basaltic compositions with high Mg and Cr, and are olivine normative. The dykes may be related to the basic intrusions described above as they have similar major and trace element abundances. No firm conclusions can be drawn.

An outcrop of pale creamy white, very fine grained rock found at the junction of Deep and Heath Creeks is of probable igneous origin. It is composed of an equigranular mosaic of quartz, tiny (0.05-.1mm) laths of plagioclase and intergranular sericite, which is replaced by slightly larger rhombohedral carbonate crystals. No evidence of a sedimentary origin was observed. XRF analysis indicates the rock is compositionally a rhyolite.

The relationship of this lithology to surrounding rocks is not known.

The presence of a light grey igneous rock (U.C. 12605) in Bastite Creek (M27 787023), also of unknown relationship to surrounding rock is noted. The rock is composed of small laths of oligoclase, substantially replaced by carbonate and epidote, with intergranular skeletal ilmenite.

ANALYTICAL METHODS

A total of 17 andesite, 6 basalt and 18 assorted igneous rocks were analysed for major and trace element compositions. Analyses were carried

out on a Philips PW1400 XRF spectrometer, utilising a Cr tube for major elements and Au and Mo tubes for traces. Calibration was carried out by Dr S.D. Weaver and Arthur Alloway of the University of Canterbury using international standards. Samples for major element analysis were prepared as fused disks following the method of Norrish and Hutton (1969). Analysis for trace elements was carried out on pressed powder pellets bonded with a 7% PVA aqueous solution.

CHAPTER EIGHT

STRUCTURES COMMON TO ALL TECTONIC SLICES

INTRODUCTION

The fundamental structures of the field area are the fault bounded tectonic slices, introduced and described in the previous chapters. These slices have different lithologic assemblages and structures and markedly different structural histories prior to overprinting by a regional deformation.

The slices are separated by major N-S trending faults. Two of these bounding faults, the Balloon Fault and Cobb Thrust, were previously identified and named by Grindley(1980). Two new faults, the Matakiki and Junction Faults were recognized during the course of mapping (see Map 2). From west to east the faults are:

BOUNDING FAULTS

Balloon Fault

The Balloon Fault was first identified and named by Grindley(1980). He mapped it from the south of the area (Balloon Tablelands) north across the Cobb Valley to Lake Sylvester, where he mapped the fault terminating into the base of the overlying Lockett Conglomerate

My mapping has accurately determined the location of the Balloon Fault in the Balloon Tablelands area and north from Lake Sylvester to Diamond Lake Stream, Lake Lillie Stream and the crest of the Lockett Range. Lockett conglomerate is restricted to the area west of the Balloon Fault, and nowhere crosses the fault.

The Balloon Fault is exposed in four places : on Peel Ridge (M27 781067); in the Cobb River (M27 778086); at Lake Sylvester (M26 786109); and in Lake Lillie Stream (M26 778129).

At Peel Ridge the Balloon Fault dips steeply to the west and separates olistostromal conglomerate from bedded silt and sandstones (Tasman Formation of Grindley (1980)). It is marked by a 1m wide zone of structureless white material, probably carbonate/quartz recemented gouge. The fault is slightly discordant to the rocks to the west. Below the ridge line the fault passes just to the west of a large body of chert.

In the Cobb River a 20 m thick pod of talc magnesite outcrops on the fault plane. To the west this is separated from well bedded Tasman Formation (type Tasman) by a vertical 1-2m wide zone of intensely sheared fine grey material. The disrupted zone is narrow and does not significantly affect rocks to either side. A small north plunging anticlinal fold is developed in the Tasman siltstones and may or may not be related to development of the fault as a drag fold structure.

The fault again outcrops on the south shore of Lake Sylvester, here separating Lockett Conglomerate (type Lockett) from olistostromal conglomerate of the Balloon Formation. The fault plane is not exposed but can be placed in a zone <4m wide. An infaulted sliver of strongly foliated, sheared siltstone occurs within the conglomerate about 10m from the fault, and is of unknown affinity.

A new exposure of the fault was found in Lake Lillie Stream (see figure 8.1). Here the fault has an attitude of $175/50^{\circ}$ east and separates rounded conglomerates (? Lockett) from foliated sandstones. The fault plane is marked by 2-5 cm of soft grey plastic gouge within a highly sheared zone of 20cm. While shearing and quartz veining are found up to 0.5m either side of the fault, conglomerate pebbles can still be identified at this distance. The nearest bedding orientation ($045/45^{\circ}$ E) identified in the conglomerate, 150m away, is markedly different to the attitude of the fault.

The position of the Balloon Fault was also located with accuracy in the bluffs on the north side of Lake Lockett (M27 784146), but is not actually exposed. Here it is offset by at least two east-west trending cross faults.

The Balloon Fault is a major structure separating markedly different lithologies for a distance of at least 12 km.

Mataki Fault

The Mataki Fault is a newly recognized and named fault separating the Balloon Slice from the Mataki Slice. It is poorly exposed and is only observed to outcrop in Mataki Creek (M27 804042) and in a tributary of Balloon Creek (M27 803047).

In Mataki Creek the fault separates weathered hornblende andesites from very altered intrusive igneous rock and to the east of that basalt rich mass flow conglomerates. It is a heavily sheared zone 2-3 m wide, dipping steeply to the east. In the next creek to the north the fault again separates heavily altered andesite from basalts or basaltic conglomerate. In both creeks exposures occur within the zone of leaching underlying the peneplain surface and are intensely weathered.

The fault position is poorly constrained elsewhere. It is interpreted to terminate against the Junction Fault to the north of Heath Creek (see Map 2).

Junction Fault

Another major new fault, the Junction Fault, separating both Mataki and Balloon slices to the west from Junction slice to the east has been identified. It outcrops in Balloon (M27 826046), Mataki (M27 825049) and Deep (M27 822057) Creeks and in Diamond Lake Stream (M27 831132).

In Mataki and Balloon Creeks the fault is a narrow (<0.5m), vertical sheared zone separating Mataki Basalts from siltstones of the Junction Formation. Bedding is well preserved to within 0.5m of the fault plane.

In Deep Creek the fault is a complex 4-6m wide highly crushed and sheared zone (figure 8.2), within which minor (2cm) gouge zones are developed. Highly altered basic igneous rock within the fault zone is in faulted contact with both Mataki Basalt and Junction Formation, but later movements is interpreted to have occurred on the fault, as intrusion postdates juxtaposition of the structural slices.

In Diamond Lake Stream, the Junction Fault divides Junction Formation



Figure 8.1 Exposure of Balloon Fault, Lake Lillie Stream. Fault plane recognizable to within 0.5m of fault.



Figure 8.2 Exposure of Junction Fault, Deep Creek. Junction Formation sand on right, Mataki Basalt to left. Outcrop in middle foreground is altered basic intrusive. Width of view approximately 8m.

siltstones from strongly rodded nodular carbonate siltstones associated with the Battey Conglomerate.

Cobb Thrust

The Cobb Thrust is a major eastward dipping fault identified and named by Grindley (1980). The fault plane is beautifully exposed in Cobb river (M27 833128) where it dips eastward at 45° (figure 8.3), separating Cobb Ultramafic, on the hanging wall, from Junction Formation. The fault is a complex zone of cemented gouge 1-2m wide, within 4-6m of highly sheared material derived from both sides of the fault. Bedding becomes disrupted towards the fault but is recognisable to within 4-6m of the fault zone.

The Cobb Thrust is well located along most of its length (see S13 Cobb), but is not exposed at any other localities. It is obviously a major fault.

Overall these fault zones are characterised by their narrow widths. These features and the lack of cataclastic deformation indicate that faulting is likely to have occurred below the depth of cataclastic deformation (?10-13 km Sibson, 1986). However lack of development of mylonitic fabrics indicates deformation is likely to have occurred above the zone where steady state crystal plastic flow or grain boundary diffusion predominate (>13 km Sibson, 1986).

Narrow gouge zones are probably the product of Kaikoura reactivation.

It is likely that an examination of fault geometry and tectonite fabrics from the faults will prove fruitful in constraining their nature and relative motions.

OVERPRINTING DEFORMATION

The faults obviously postdate the youngest strata that they cut, in this case the Early Boomerangian Tasman Formation (Henderson and MacKinnon, 1980). The first recognised upper limit to the timing of movement is the imposition of a strong linear and planar fabric

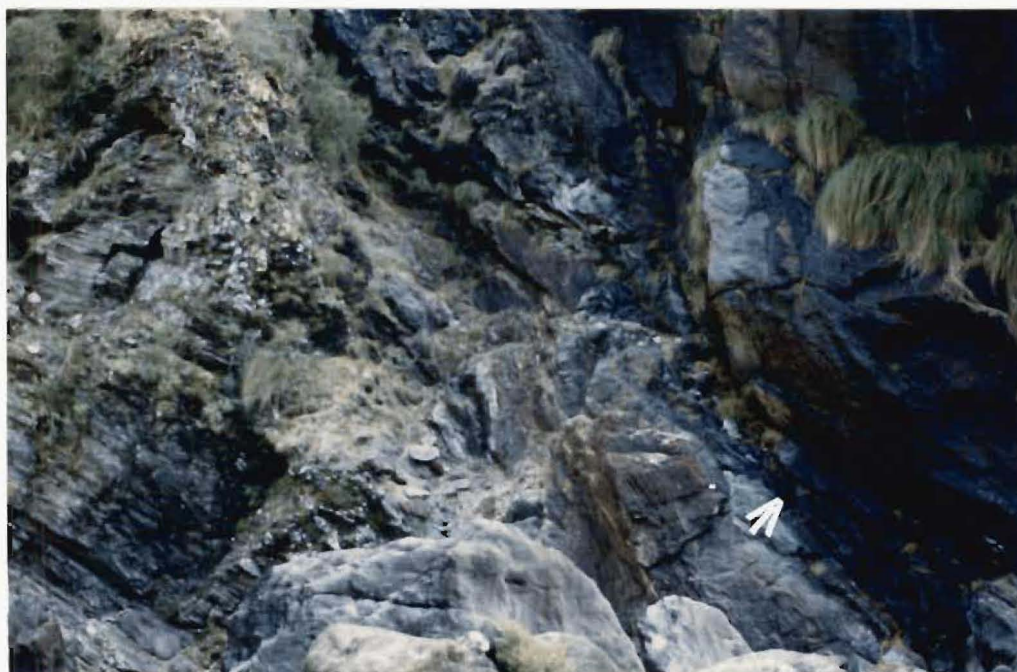


Figure 8.3 Exposure of Cobb Thrust, Cobb River below dam (fault plane arrowed). Cobb ultramafics on hanging wall, Junction Formation below. Scale bar approximately 2m.

overprinting all tectonic slices This fabric forms the dominant structural element visible in most outcrop.

The lineation is mesoscopically defined by: long axes of deformed conglomerate clasts,:long axes of sandstone inclusions in diamictite: rodding of carbonate siltstones: pencil structure in siltstones: mullion type structures on bedding planes and: a preferred breaking orientation of rock mass. It is most strongly developed in the east (Junction slice) and north (Battey Conglomerate).

Foliation is mesoscopically defined by: the flattening plane of deformed conglomerate clasts: the two longest dimension of inclusions in diamictite and: a preferred plane of breaking in sediments and volcanics. Microscopically it is defined by : a pervasive solution cleavage,: the average orientation of an anastomosing shear/solution fabric in block in matrix tectonites of the Balloon Formation and : a phyllosilicate preferred orientation fabric.

Geometry

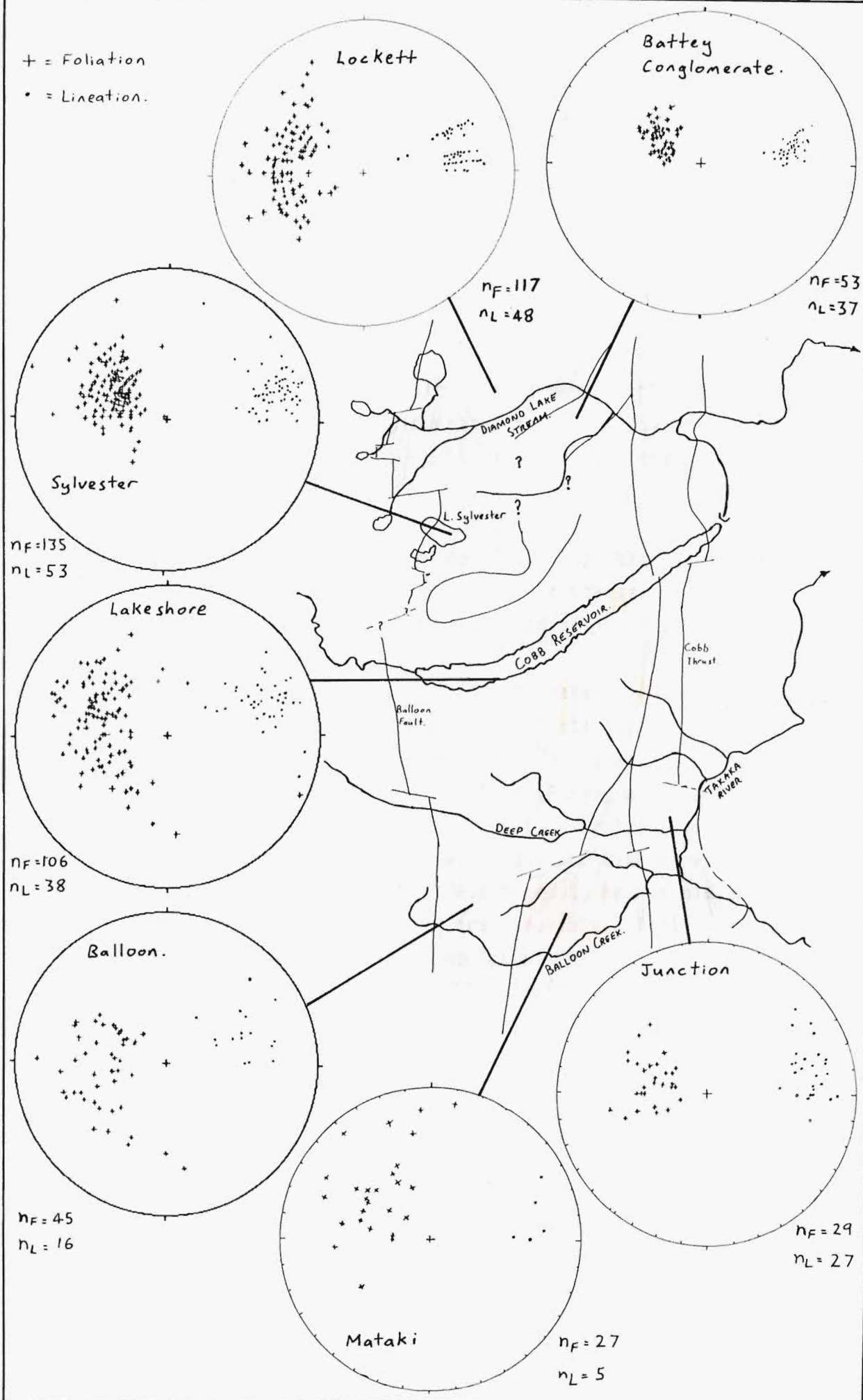
Lineation is remarkably consistent in orientation across the whole field area trending between 065° and 090° (average 075°) and plunging between 020° and 040° (average 031°) (Figure 8.4). No systematic or areal changes in lineation orientation were observed, only variation in intensity. Scattered observations of lineation recorded by Grindley(1980) on S13 Cobb indicate a similar orientation over the whole Central Belt.

The foliation is more variable than lineation, varying between approximately 150° and 045° strike and 20° and 50° dip (Figure 8.4). Within the Balloon Formation foliation is observed to anastomose around inclusions, varying in attitude between 30° and 50° perpendicular to the lineation. Two foliation orientations, the opposing faces to lemon pip shaped inclusions, are particularly common often creating the impression in the field that two intersecting fabrics are present. This is not the case. In no outcrop were intersecting or cross cutting fabric relationships observed and in polished outcrop on the lakeshore, fabric is observed to anastomose around inclusions (e.g figure 4.6).

Figure 8.4 Stereographic plots of foliation and lineation, plotted by domain (all plots lower hemisphere equal area projection).

+ = Foliation

• = Lineation.



Gross field variations in the measured foliation attitude are apparent, notably between the Lockett Range and Diamond Lake Stream, and east and west of M27 793081 on the shore of Cobb Reservoir (see Map 1). In these area gross changes in bedding orientation also parallel the changes in foliation and it is possible that post foliation macroscopic folding has occurred. However no structural domains of persistantly different orientation could be identified, and no folding of the bounding faults was recognised. Overall bedding attitude in the Balloon Formation resembles attitude of foliation.

Foliation in the Matakai slice is predominantly defined by a flattening plane in deformed conglomerates and fissility in siltstone and mudstone. Foliation attitude is quite variable, but the reason for this is unclear.

Foliation is strongly to weakly developed in the Junction slice, where it is defined by a plane of flattening in coarser grained sediments and a preferred parting plane in finer grained sediments.

Rough visual estimates from deformed marker lithologies (e.g. conglomerates) enable the character of finite strain to be estimated across the field area. Total finite strain varies from a general constriction (approaching uniaxial prolate (Ramsay and Huber 1984)), in the east to a general flattening in the west. Prolate deformation is strongest in the Battey Conglomerate/ Diamond Lake Stream area where conglomerate clasts have axial ratios estimated to be, at minimum, 3:1:1 (see figure 8.5). Higher strains are probable. Trilobites from the Junction Formation adjacent to the Cobb Thrust (M27 834113) have strain ellipse values of 6:1 in the plane of bedding (R.A. Cooper pers. comm.). Foliation in this area is either very weak (e.g figure 8.5) or absent. True constrictional deformation (i.e shortening in Y and Z) is indicated in thin sections (e.g U.C 12643) cut perpendicular to lineation, by short irregularly oriented solution veins developed on all sides of grains.

The strain path for rocks to the west is poorly understood as gross heterogeneity of strain has occurred and few passively deformed markers exist. As discussed in Chapter 4 large inclusions within Balloon Formation have behaved as rigid bodies during deformation and record low levels of strain. The Battey Conglomerate at its western most outcrop



Figure 8.5 Stretched Battey Conglomerate slabbed perpendicular and parallel to lineation. Note poorly developed foliation in face cut perpendicular to lineation.

(M27 790098) has a strong foliation and clast axis ratios of resistant pebbles are estimated to be approximately 1:2:3. Total finite strain may be considerably higher. These axial ratios are similar to ratios estimated for average sandstone inclusions within the Balloon Formation. However it is not known whether the disruption and formation of "block in matrix" texture is related to the overprinting deformation or to an earlier event. The strong parallelism of long axes of inclusions to foliation and lineation, and disruption of margins to intrusive andesites suggests that disruption is related to the overprinting deformation.

Powell(1984) has described foliated rocks with a strongly developed elongation lineation from the Waingaro Schist Zone, with measured strains as high as 500%, decreasing to the west. The foliation and lineation is accompanied by synkinematic lower greenschist facies metamorphism.

The fabric of the study area is considered likely to be related to that of the Waingaro Schist Zone. Elongation lineation is of similar morphology and magnitude, and in both areas is accompanied by a synkinematic greenschist facies metamorphism.

Powell (1984) contends that the Waingaro Schist Zone is a Tuhuan (Devonian or Silurian) feature. Assuming Powell's age and that the fabric of the study area is related to the Waingaro Schist Zone then the first recognised upper limit to timing of juxtaposition is Devonian or Silurian.

It is tempting to relate the gross structure described to an east dipping imbricate thrust system linked to the Anatoki Thrust as master thrust.

FAULTING

East west cross faults

The N-S trending faults are some of the few relatively easily recognisable and continuous planar features in the field area. Tracing of these faults in areas of good exposure, such as around Lake Sylvester,

has led to the recognition of an important set of ENE to ESE trending cross faults.

While these faults cannot be recognised in poorly exposed areas, their abundant development in areas of good exposure strongly suggests that they constitute an important structural element over the whole field area, and probably influence a more significant control on outcrop than is indicated by the map (see Maps 1 and 2).

The orientation of the cross faults is poorly constrained, but appears to fall roughly into two sets oriented ENE/WSW and ESE/WNW. No consistent sense of offset is apparent on either of these two sets, both exhibiting apparent sinistral and dextral senses of strike separation.

A fault plane exposed in Iron Lake Stream falls along strike from an offset of the Balloon Fault near Lake Lillie. The fault is a 6m wide zone of intense cataclasis and shearing, oriented 080/70°E, within which no single fault plane can be found. Another fault exposed in Mataki Creek (M27 827048) only accommodates minor strike offset of the Junction Fault. It is a 3m wide zone of cataclastic deformation. The brittle nature of this fault implies faulting at a high structural level (Sibson, 1986).

The age of these faults is not known. They are obviously younger than the N-S faults. They do not appear to offset the Early Tertiary peneplain surface.

Kink Bands/Crenulations

In places a weak, spaced kink banding (Ramsay and Huber, 1983) is developed in fine grained sediments. Kink bands are commonly .2 to 2 cm wide and strike approximately NS and dip variably but steeply west. They consistently have a west side up geometry.

Minor fracturing and deposition of quartz and carbonate along kink planes can be observed in thin section. No other evidence of any parallel fabric development is seen in the rock mass.

Kink bands are best developed to the eastern side of the map area. They are occasionally also observed developed in both conglomerates and Balloon Unit diamictite. In these lithologies the kink planes are further apart (up to 50cm).

CHAPTER NINE

CONCLUSIONS

The geology of the study area can be interpreted in terms of three fault bounded structural entities, from west to east, the Balloon, Matakī and Junction Fault Bounded Slices.

The Balloon Slice comprises two formations, the Balloon Formation and the Battey Conglomerate. The Balloon Formation is characterised by pervasive deformation and a "block in matrix" texture. It is considered that the texture is formed predominantly by tectonic disruption of a bedded sequence, not by soft sediment or olistostromal processes. Hornblende andesites of calc alkaline affinity are unique to the Balloon Slice and are probably intrusive sheets but may be in part flow deposits.

The Matakī slice contains three lithologic units, the M Creek Formation, the Salisbury Conglomerate and the Matakī Basalts. The relationships between these unit are poorly understood. The Salisbury Conglomerates are green to red, pebble to boulder volcanic and lithic rich conglomerates. The Matakī Basalts are high TiO₂ tholeiitic basalts of probable seamount origin.

Rocks of the Junction Fault Bounded Slice are included in the Junction Formation, a well bedded sandstone and siltstone sequence which has been folded into irregularly oriented but consistently east plunging folds.

A strong elongation lineation (and associated foliation) overprints all of the rocks of the field area, and is the first feature common to all slices. The lineation is thought to be related to development of the Waingaro Schist Zone and is of probable Silurian or Devonian age (Powell 1984).

The recognition of these fault bounded slices has important implications for those interpretations presented by Grindley (1980) in S13 "Cobb". Primarily the regional stratigraphy which Grindley (1971, 1980) has proposed for the Central Belt cannot be applied in the study area.

Stratigraphic contacts mapped by Grindley either can not be found or are actually faulted. Furthermore rocks assigned by Grindley to the same Formation are found not to be correlative. For instance, igneous rocks south of the Cobb, mapped by Grindley as Devil River Volcanics, actually comprise two sets of lithologically and geochemically distinct lavas; the Balloon Formation andesites and the Matakiki Basalts. Perhaps more perplexing is the mapping of well bedded rocks in the Flora/Takaka River area (now Junction Formation) as Balloon Formation. Lithologically identical rocks to these from the Diamond Lake Stream area are, however, mapped as Anatoki Formation.

The main problem with Grindleys stratigraphy lay in the insufficiently rigorous criteria by which formations were defined. No stratigraphic or measured sections, or detailed descriptions accompany his formation descriptions, and field mapping leads one to the conclusion that his formations are defined predominantly on the basis of gross lithology. Correlation (= recognition) of a formation implicitly requires that the unit was continuous at the time of deposition. Such an exact definition, especially in areas of faulting, consequently requires that correlation only be made if similarity is so strong that a reasonable degree of certainty can be demonstrated (Hedberg 1976).

Grindleys stratigraphy and map interpretation are based mainly on reconnaissance level mapping. Detailed mapping, and visiting of virtually all outcrops, has shown that the stratigraphy, and the range of lithologies present, is extremely varied. Indeed the structural complexity apparent in areas of adequate exposure is somewhat smaller scale than the resolution permitted by outcrop over most of the area.

Cooper (1986, in prep) has interpreted a similar set of fault bounded slices, recognised "largely on the distinctness of their stratigraphic successions". Cooper feels that "attempts to establish a uniform stratigraphy for the Central Sedimentary Belt are probably invalid and that each slice should be treated separately." So it appears that Grindleys stratigraphy is inapplicable over a large part of the Central Belt, including the type areas of three of the formations, Balloon, Tasman and Lockett.

In areas of poor to adequate exposure structural interpretations must be strongly based on stratigraphy. Many of the fold and thrust features (e.g. the Waingaro window) identified on S13 Cobb have obviously been interpreted on this basis. Consequently if the stratigraphy is too generalised or simply wrong these, the real structure may be completely different. As the main evidence for the Grindley tectonic model is the map and its structure this significantly weakens the overthrust Central Belt nappe model.

Identification of fault bounded slices begs the question as to whether these fragments of crust should be regarded as tectono-stratigraphic terranes. As was introduced in Chapter 3, the definition of terranes of Howell et al (1985) is that they be *fault bounded geological entities of regional extent that are characterised by a geological history different from that of neighbouring terranes*, a very broad definition. In attaching the name terrane to a structural entity, the definition requires that the entity be of regional extent.

Notwithstanding their small size, the Matakia and Balloon Slices contain igneous rocks of such different geotectonic character that they cannot have formed beside each other. While it is not felt that the term terrane is appropriate, the name attached to these slices is not really important. What is important is assuming no connection between rocks separated by faults unless one can be demonstrated. For now these entities have been informally named Fault Bounded Slices. It appears that the Takaka Terrane (Cooper, 1986) is comprised of juxtaposed fault slices and probably represents a dismembered island arc assemblage.

Suggestions for Future Work

1) One of the most valuable contributions for further work will be the continued detailed mapping of structural blocks and bounding faults. In particular the area east of the Cobb Thrust and west of the Waingaro Schist Zone need examination. Also the north and southward extension of mapping from the Cobb Valley. Undoubtedly the structure will turn out to be rather more complex than indicated to date.

2) A detailed study of the nature of the major faults of the area may prove useful in constraining movement history between blocks.

3) A geochemical study of volcanic rocks, carried out within the framework of the regional structure. Geochemical affinity of volcanics may be an effective way of demonstrating likeness or difference between slices.

4) A detailed structural analysis of deformation within the Junction Fault Bounded Slice.

ACKNOWLEDGEMENTS

I wish to express my gratitude to the staff from the Geology Department of the University of Canterbury who provided technical and logistical support, discussed ideas and reviewed drafts of the text. Thanks to Karen Holder for thin sections, Kerry Swanson for processing limestone samples and Arthur Alloway for teaching me the secrets of the XRF lab.

Dr Roger Cooper (N.Z.G.S.) Lower Hutt, provided invaluable discussions and encouragement and shared his extensive knowledge of N.W. Nelson Paleozoic geology with me.

My grateful thanks to the N.Z.F.S. for generously making available Cobb Hostel free of charge and especially to Hugh and Pam Mytton (of N.Z.F.S.) for their friendliness, hospitality and concern.

C.R.A. (N.Z.Ltd.) provided some helicopter time and food in return for a draft of the map.

Thanks to my supervisor, Dr John Bradshaw for suggesting this project, and for reading drafts of this text. Thanks also to Drs. Doug Lewis, Stephen Weaver and Dave Shelly who read and commented on various drafts also.

Indebtedness and bottles of wine to Tracy Robinson for the tribulations of printing.

Finally my eternal thanks and gratitude to the many friends, residents of Rugby St and classmates who kept me on the tracks and made life enjoyable. Special praise is due to Andrea for her invaluable help and amazing organisational skills at the end.

REFERENCES

- Bell, C.M., (1987) The origin of the Upper Paleozoic Chañaral Melange of N. Chile. J. Geol. Soc. London 144(4): 599-610.
- Bell, J.M., Webb, E.J.H., Clarke, E.C., (1907) The geology of the Parapara Subdivision, Karamea, Nelson. N.Z.G.S. Bulletin No. 3: 111p.
- Boles, J.R., Landis, C.A., (1984) Jurassic sedimentary melange and associated facies, Baja California, Mexico. B.G.S.A. Bull. 95: 513-521.
- Botsford, J., (1983) The Esk Head Melange in the Esk Head, Okuku area, North Canterbury. Unpublished M.Sc thesis, University of Canterbury Library, Christchurch, New Zealand.
- Bradshaw, J.D., (1972) Stratigraphy and structure of the Torlesse Supergroup (Triassic - Jurassic) in the foothills of the Southern Alps near Hawarden (S60-61) Canterbury. N.Z.J.G.G. 15: 71-87.
- Bradshaw, J.D., (1982) S13 Cobb. A review of the new map and the structural interpretation of the Central Belt rocks of S8 and S13. N.Z.J.G.G. 25: 371-375.
- Byrne, T., (1984) Early deformation in melange terranes of the Ghost Rocks Formation, Kodiak Islands, Alaska. in Raymond, L.A. (ed). Melanges: their nature, origin and significance. Geol. Soc. of America, Special Paper 198: 71-79.
- Cole, J.W., (1978) Andesites of the Tongariro Volcanic Centre, North Island, New Zealand. J. Volc. Geoth. Res. 3: 121-153.
- Cole, J.W., (1979) Chemical analyses of lavas and ignimbrites of the Taupo Volcanic Zone. Geology Department Publication No. 13. Victoria University of Wellington, 31p.
- Coleman, A.C., (1977) Structure and stratigraphy of the Mount Patriarch-Crow River area, N.W. Nelson. N.Z.J.G.G. 20(3): 401-424.
- Coleman, A.C., (1981) Part sheets S18, S19, S25, S26 Wangapeka. Geological Map of New Zealand 1:63360 Map (1 sheet) and Notes (48p.). Wellington D.S.I.R.
- Cooper, R.A., (1965) Lower Paleozoic Rocks between Upper Takaka and Riwaka, North-west Nelson. N.Z.J.G.G. 8: 49-61.
- Cooper, R.A., (1968) Lower and Middle Paleozoic Fossil Localities of North-west Nelson. Trans. Roy. Soc. N.Z., Geology. 6: 75-89.
- Cooper, R.A., (1971) New Middle and Upper Ordovician Graptolite localities, North-west Nelson, New Zealand. N.Z.J.G.G. 14: 242-248.

- Cooper, R.A., (1979) Lower Paleozoic rocks of New Zealand. Jour. Roy. Soc. N.Z. 9: 29-84.
- Cooper, R.A., (1984) Lower Paleozoic Terranes. Geol. Soc. N.Z. Misc. Publ. 31A.
- Cooper, R.A., (1986a) Central Belt structure: an alternative interpretation. Lower Paleozoic Workshop Abstracts. Geol. Soc. N.Z. Misc. Publ. 34: 11-13.
- Cooper, R.A., (1986b) A terrane interpretation of the early evolution of New Zealand. in Lower Paleozoic Workshop Abstracts. Geol. Soc. N.Z. Misc. Publ. 34: 14-16.
- Cooper, R.A., (1987) Are Terranes Real or Imaginery? Geol. Soc. N.Z. Newsletter No. 78. (Nov.): 44-53.
- Cooper, R.A. and Druce, E.C., (1975) Lower Ordovician sequence and conodonts, Mount Patriarch, North-west Nelson, New Zealand. N.Z.J.G.G. 18: 551-82.
- Cooper, R.A. and Wright, A.J., (1972) Silurian Rocks and Fossils at Hailes Knob, North-west Nelson, New Zealand. N.Z.J.G.G. 15: 318-335.
- Cowan, D.S., (1982) Deformation of partly dewatered and consolidated Franciscan sediments near Piedras Blancas Point, California. in Leggett, J.K. (ed). Trench Forearc Geology. Geol. Soc. London Special Publication 10: 439-457.
- Cowan, D.S., (1985) Structural styles in Mesozoic and Cenozoic melanges in the Western Cordillera of North America. G.S.A.Bull. 96(4): 451-462.
- Crittenden, M., Coney, P., Davis, G., (1980) Cordilleran Metamorphic Complexes. G.S.A. Memoir 153: 490p.
- Ewart, A., (1982) The mineralogy and petrology of Tertiary - Recent orogenic volcanic rocks: with special reference to the andesite - basaltic andesite compositional range. pp25-87.
- Flint, R.F., et al., (1960A) Symmictite: A new name for non-sorted terrigenous sedimentary rocks that contain a wide range of particle sizes. Bull. G.S.A. 71: 507-509.
- Flint, R.F., et al., (1960B) Diamictite: A substitute term for symmictite. Bull. G.S.A. 71: 1809.
- Folk, R.L., Andrews, P.B., Lewis, D.W., (1970) Detrital rock classification and nomenclature for use in New Zealand. N.Z.J.G.G. 13: 937-968.
- Graham, I.J., Hackett, W.R., (1987) Petrology of calc-alkaline lavas from the Ruapehu Volcano and related vents, Taupo Volcanic Zone, New Zealand. J. Pet.

- Grindley, G.W., (1961) Sheet S13 Golden Bay (1st Ed.) "Geological Map of New Zealand 1:250,000" D.S.I.R. Wellington, New Zealand.
- Grindley, G.W., (1971) Sheet S8 Takaka (1st Edition) "Geological Map of New Zealand" 1:63,360 D.S.I.R. Wellington, New Zealand.
- Grindley, G.W., (1980) Sheet S13 Cobb (1st Edition) "Geological Map of New Zealand" 1:63,360 D.S.I.R. Wellington, New Zealand.
- Grindley, G.W., (1982) S13 Cobb. A review of the new map and the structural interpretation of the Central Belt rocks of S8 and S13: reply, (see Bradshaw 1982) N.Z.J.G.G. , 25: 375-379.
- Grindley, G.W., (1986) Paleozoic tectonic history, N.W. Nelson. in Lower Paleozoic Workshop Abstracts. Geol. Soc. N.Z. Misc. Publication 34: 20-23.
- Gucwa, P.R., (1975) Middle to Late Cretaceous Sedimentary Melange, Franciscan Complex, northern California. Geology 3: 105-108.
- Henderson, J., (1923) Notes to accompany a Geological sketch map of the Mount Arthur District. N.Z.J.Sci.Tech. 6(3): 174-190.
- Henderson, J., McPherson, E.O., Grange, L.I., (1959) The geology of Motueka Subdivision. N.Z. Geol. Survey Bulletin 35.
- Hickey, K.A., (1986) Geology of the Paleozoic and Tertiary rocks between Upper Takaka and the Waingaro River, north west Nelson. unpublished M.Sc. thesis, University of Auckland Library, Auckland, New Zealand.
- Irvine, T.N., Barager W.R.A., (1971) A guide to the chemical classification of the common volcanics rocks. Can. J. Earth Sci. 8: 523-548.
- Keble, R.A., Benson, W.N., (1929) Ordovician graptolites of N. W. Nelson. Trans. N.Z. Inst. 59(4): 840-863.
- Lundberg, N., Moore, J., (1981) Structural Features of the Middle America Trench Slope off Southern Mexico. Leg 66 DSDP: Initial reports of the Deep Sea Drilling Project. V.66 Washington (U.S. Government Printing Office).
- McKay, A., (1879) Reports on the Baton River and Wangapeka Districts and Mount Arthur Range. in N.Z.G.S Reports on Geological Explorations during 1878 - 79.
- Page, B.M., Suppe, J., (1981) The Pliocene Lichi Melange of Taiwan: Its plate tectonic and olistostromal origin. Amer. J. Sci. 281: 193-227.
- Park, J., (1890) On the geology of Collingwood County, Nelson. N.Z.G.S. Report on Geological Explorations 20: 1888-89.

- Pearce, J.A., (1982) Trace element characteristics of lavas from destructive plate boundaries. in Thorpe R.S. (ed) *Andesites*, John Wiley and Son, New York. 1982, pp552-548.
- Pearce, J.A., Cann, J.R., (1973) Tectonic setting of basic volcanic rocks determined using trace element analyses. Earth and Plan. Sci. Letters 19: 290-30.
- Raymond, L.A., (1984) Classification of melanges. in Raymond, L.A. (ed). *Melanges: their nature, origin and significance*. Geol. Soc. of America, Special Paper 198: 7-20.
- Ramsay, J.G., (1967) *Folding and Fracturing of Rocks*. McGraw-Hill, Inc. 568p.
- Ramsey, J.G., Huber, M.I., (1984) The techniques of modern structural geology. Volume 1 Strain Analysis. Academic Press Inc. London: 307p.
- Ramsey, J.G., Huber, M.I., (1987) The techniques of modern structural geology. Volume 2 Folding and Fracturing. Academic Press Inc. London: 391p.
- Robin, C., (1982) Mexico. in Thorpe R.S, (ed) *Andesites*. John Wiley and Son, New York. 1982, 137-148.
- Shelley, D., (1975) *Manual of Optical Mineralogy*. Elsevier, Amsterdam: 239pp.
- Sibson, R.H., (1986) Earthquakes and Rock Deformation in Crustal Fault Zones. Ann. Rev. Earth Planet. Sci. 14: 149-175.
- Stewart, M., (1986) The Balloon Formation. in Lower Paleozoic Workshop Abstracts. Geol. Soc. N.Z. Misc. Publication 34: 40-42.
- Ward, C.M., (1986a) The Fanny and Goodyear Terranes of Southern Fiordland and their relationships with N.W. Nelson. in Lower Paleozoic Workshop Abstracts. Geol. Soc. N.Z. Misc. Publication 34: 46-47.
- Ward, C.M., (1986b) Speculations on the provenance of the Lockett Conglomerate (Nelson) and False Edgecumbe Conglomerate (Fiordland) in Lower Paleozoic Workshop Abstracts. Geol. Soc. N.Z. Misc. Publication 34: 48-50.

APPENDIX 1

SAMPLE IDENTIFICATION

<u>Identification</u>		<u>Locality</u>		<u>Identification</u>		<u>Locality</u>	
U of C Number	Field Number	NZMS 260 Sheet No.	Grid Reference	U of C Number	Field Number	NZMS 260 Sheet No.	Grid Reference
<hr/>							
12579	205	M27	807 048	12607	363	"	826 097
12580	339	"	790 086	12609	381	"	828 048
12581	337	"	777 086	12610	382	"	823 050
12582	350	"	777 084	12611	391	"	866 052
12583	239	"	802 040	12612	458	M26	794 106
12584	252	"	805 055	12613	501	"	791 141
12585	253	"	810 514	12614	510	"	793 144
12586	256	"	813 057	12615	512	"	794 146
12587	257	"	816 056	12616	516	"	791 130
12588	258	"	816 055	12617	522	"	799 148
12589	259	"	825 057	12618	523	"	796 132
12590	260	"	822 057	12619	363	M27	826 097
12591	169	"	806 042	12620	387	"	804 042
12592	225	"	813 058	12621	402	"	826 039
12593	228	"	805 055	12622	409	"	840 045
12594	230	"	819 055	12623	426	M26	106 811
12595	234	"	823 057	12624	137A	M27	786 058
12596	235	"	828 057	12625	137B	"	786 058
12597	261	"	828 057	12626	152A	"	791 037
12599	313	"	808 087	12627	152B	"	791 037
12600	314	"	809 088	12628	155	"	794 037
12601	317	"	814 093	12629	159	"	795 038
12602	319	"	816 094	12630	178	"	797 034
12603	320	"	817 095	12631	189	"	781 082
12604	340	"	814 098	12632	193	"	794 074
12605	343	"	783 073	12633	268	"	805 084
12606	359	"	779 064	12634	327	"	808 083
12640	259	"	825 056	12635	325	"	807 085
12641	250	"	832 055	12636	215	"	815 088
12642	428	M26	832 123	12637	181	"	803 030
12643	424	"	813 101	12638	176	"	820 049
				12639	168	"	805 042

APPENDIX TWO.

FOSSIL AGE CONTROL.

A) Four fossil localities are known from within the study area. Fossils are strongly distorted. Identifications are by Dr. R.A Cooper, NZGS Lower Hutt, and samples are lodged in NZGS collections.

Locality	F ref.#	Grid Ref.	Taxa	Age
Heath Ck.	M27 f181	M27 805067	<u>Peronopsis</u> cf. <u>longinqua</u> Opik <u>P. cf fallax</u> (Linnarsson) <u>Kootenia</u> sp <u>Follicept</u> sp	Floran " " "
By gate on Sylvester Rd.	M26 f194	M26 833112	Dolichometopidae gen et sp indet. Agnostida gen et sp indet.	Mid. Camb.
T.R trib. Deep Ck.	M27 f198	M27 807048	<u>Hypagnostus</u> sp ptychagnostids indet. polymerids-3 sp indet.	Mid. Camb.
Nth shore of Cobb reservoir.	M27 f192	M27 789086	Dolichometopidae <u>?Hypagnostus</u> lge polymerid tail indet.	Mid. Camb.

B) A total of 10 limestone samples were processed for fossils. Samples were processed by Kerry Swanson of the University of Canterbury Geology Department by treatment in glacial acetic acid for 2-8 days. Residues were washed and size sorted then hand picked by the author. No fossils were identified from these samples.